



Calhoun: The NPS Institutional Archive
DSpace Repository

Theses and Dissertations

1. Thesis and Dissertation Collection, all items

1983

Characteristics of a four nozzle, slotted mixing
stack with slanted shroud, gas eductor system.

Pritchard, Nolie Delton.

Monterey, California. Naval Postgraduate School

<http://hdl.handle.net/10945/19666>

Downloaded from NPS Archive: Calhoun



Calhoun is the Naval Postgraduate School's public access digital repository for research materials and institutional publications created by the NPS community. Calhoun is named for Professor of Mathematics Guy K. Calhoun, NPS's first appointed -- and published -- scholarly author.

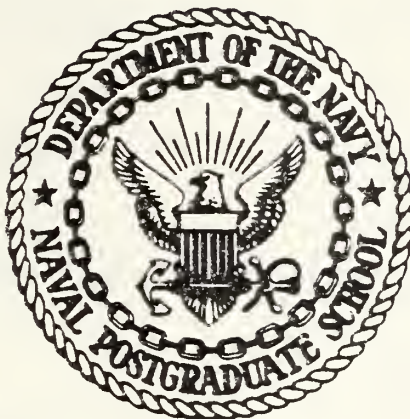
Dudley Knox Library / Naval Postgraduate School
411 Dyer Road / 1 University Circle
Monterey, California USA 93943

<http://www.nps.edu/library>

Dudley Knox Library, NPS
Monterey, CA 93943

NAVAL POSTGRADUATE SCHOOL

Monterey, California



THESIS

CHARACTERISTICS OF A FOUR NOZZLE,
SLOTTED MIXING STACK WITH
SLANTED SHROUD, GAS
EDUCTOR SYSTEM

by

Nolie Delton Pritchard, Jr.

September 1983

Thesis Advisor:

P. F. Pucci

Approved for public release; distribution unlimited

T210149

REPORT DOCUMENTATION PAGE

**READ INSTRUCTIONS
BEFORE COMPLETING FORM**

DD FORM 1 JAN 73 1473 EDITION OF 1 NOV 65 IS OBSOLETE
S/N 0102-LF-014-6601

1 SECURITY CLASSIFICATION OF THIS PAGE (When Data Entered)

20. Abstract (contd)

mixing stack pressure distributions were used to evaluate the slant shrouded mixing stacks.

The pumping performance of the four straight nozzle shrouded system was found to be comparable to previously tested unshrouded models, showing no specific advantages. The pumping performance of the tilted nozzles and slanted shroud showed an improvement over the straight shroud model, with a noticeable increase in the tertiary pumping.

Approved for public release; distribution unlimited

Characteristics of a Four Nozzle, Slotted
Mixing Stack with Slanted Shroud,
Gas Eductor System

by

Nolie Delton Pritchard, Jr.
Lieutenant Commander, United States Navy
B.A., Arkansas College, 1974

Submitted in partial fulfillment of the
requirements for the degree of

MASTER OF SCIENCE IN MECHANICAL ENGINEERING

from the

NAVAL POSTGRADUATE SCHOOL
September 1983

These

p 944165

c. 1

ABSTRACT

Cold flow tests were conducted on a four nozzle gas eductor system to evaluate the system's performance utilizing a slotted mixing stack with slanted shroud and diffuser rings. The stack length-to-diameter ratios, L/D , evaluated were 1.5 and 2.25. The nozzles were constructed with a ratio of total area of primary flow to area of mixing stack of 2.5. One set of straight nozzles, and another set tilted at 15° were used. Secondary and tertiary pumping coefficients, and mixing stack pressure distributions were used to evaluate the slant shrouded mixing stacks.

The pumping performance of the four straight nozzle shrouded system was found to be comparable to previously tested unshrouded models, showing no specific advantages. The pumping performance of the tilted nozzles and slanted shroud showed an improvement over the straight shroud model, with a noticeable increase in the tertiary pumping.

TABLE OF CONTENTS

I.	INTRODUCTION	15
II.	THEORY AND ANALYSIS	20
	A. MODELING TECHNIQUE	21
	B. ONE-DIMENSIONAL ANALYSIS OF A SIMPLE EDUCTOR . .	21
	C. NON-DIMENSIONAL FORM OF THE SIMPLE EDUCTOR EQUATION	29
	D. EXPERIMENTAL CORRELATION	32
III.	MODEL GEOMETRIES	33
	A. MIXING STACK CONFIGURATIONS AND SHROUDS	33
	B. ANGLED PRIMARY NOZZLE AND BASE PLATE CONFIGURATION AND GEOMETRIES	35
IV.	EXPERIMENTAL APPARATUS	38
	A. PRIMARY AIR SYSTEM	38
	B. SECONDARY AIR PLENUM	40
	C. TERTIARY AIR PLENUM	42
	D. INSTRUMENTATION	42
	E. ALIGNMENT	44
V.	EXPERIMENTAL METHOD	45
	A. PUMPING COEFFICIENT	45
	B. INDUCED AIR FLOW	47
	C. PRESSURE DISTRIBUTION IN THE MIXING STACK	47
	D. MIXING STACK ROTATION ANGLE	48
VI.	DISCUSSION OF EXPERIMENTAL RESULTS	49

A. L/D = 1.5 STRAIGHT NOZZLES, 15-20 NOZZLES . . .	50
B. L/D = 2.25 STRAIGHT NOZZLES, 15-20 NOZZLES . . .	51
VII. CONCLUSIONS	53
VIII. RECOMMENDATIONS	54
APPENDIX A: FORMULAE	114
APPENDIX B: UNCERTAINTY ANALYSIS	117
LIST OF REFERENCES	119
INITIAL DISTRIBUTION LIST	121

LIST OF TABLES

1.	Shrouded Stack L/D = 1.5: Straight Nozzles	92
2.	Shrouded Stack L/D = 1.5: 15-20 Nozzles	97
3.	Shrouded Stack L/D = 2.25: Straight Nozzles . . .	102
4.	Shrouded Stack L/D = 2.25: 15-20 Nozzles	107
5.	Secondary Pumping Coefficient Comparison (Open to Environment)	112
6.	Tertiary Pumping Coefficient Comparison (Open to Environment)	113

LIST OF FIGURES

1.	Eductor Model Testing Facility	55
2.	Test Facility with Secondary and Tertiary Plenums . .	56
3.	Dimensions of Slotted Mixing Stack	57
4.	Schematic of L/D 1.5 - Shroud & Diffuser Rings	58
5.	Schematic of L/D 2.25 - Shroud & Diffuser Rings . . .	59
6.	Simple Single Nozzle Eductor System	60
7.	Schematic of Shrouded Mixing Stack Gas Eductor with Angled Nozzles	61
8.	Isometric View of Slotted Mixing Stack	62
9.	Mixing Stack and Diffuser Rings	63
10.	Shroud and Diffuser Rings	64
11.	Dimensions of Primary Nozzles	65
12.	Angled Primary Nozzles and Base Plate	66
13.	Base Plate and Nozzle Rotation Angles	67
14.	Dimensions of the Four Nozzle Rotatable Base Plate . .	68
15.	Exterior of Secondary and Tertiary Plenums	69
16.	Instrumentation	70
17.	Schematic of Instrumentation	71
18.	Schematic of Instrumentation for Primary Air Flow Measurement	72
19.	Mixing Stack with Pressure Taps and Air Seal	73
20.	Sample Pumping Coefficient Plot	74
21.	Sample Mixing Stack Pressure Distribution Plot	75
22.	Performance Plots for L/D = 1.5 Straight Nozzles, PCD (Secondary)	76

23.	Performance Plots for $L/D = 1.5$ Straight Nozzles, PCD (Tertiary)	77
24.	Performance Plots for $L/D = 1.5$ Straight Nozzles, MSD	78
25.	Performance Plots for $L/D = 1.5$ 15/20 Nozzles, PCD (Secondary)	79
26.	Performance Plots for $L/D = 1.5$ 15/20 Nozzles, PCD (Tertiary)	80
27.	Performance Plots for $L/D = 1.5$ 15/20 Nozzles, MSD	81
28.	Performance Plot Comparison $L/D = 1.5$, 15/20 Nozzles, PCD (Secondary)	82
29.	Performance Plot Comparison $L/D = 1.5$, 15/20 Nozzles, PCD (Tertiary).	83
30.	Performance Plots for $L/D = 2.25$, Straight Nozzles, PCD (Secondary)	84
31.	Performance Plots for $L/D = 2.25$ Straight Nozzles, PCD (Tertiary)	85
32.	Performance Plots for $L/D = 2.25$ Straight Nozzles, MSD	86
33.	Performance Plot Comparison $L/D = 2.5$, Straight Nozzles, PCD (Secondary)	87
34.	Performance Plot Comparison $L/D = 2.5$, Straight Nozzles, PCD (Tertiary)	88
35.	Performance Plots for $L/D = 2.25$ 15/20 Nozzles, PCD (Secondary)	89

36.	Performance Plots for L/D = 2.25 15/20 Nozzles,	
	PCD (Tertiary)	90
37.	Performance Plots for L/D = 2.25 15/20 Nozzles,	
	MSD	91

NOMENCLATURE

English Letter Symbols

A	Area (in.^2)
c	Sonic velocity (ft/sec)
C	Coefficient of discharge
D	Diameter (in.)
F_a	Thermal expansion factor
F_{fr}	Wall skin-friction force (lbf)
g_c	Proportionality factor in Newton's Second Law ($g_c = 32.174 \text{ lbm-ft/lbf-sec}^2$)
h	Enthalpy (Btu/lbm)
k	Ratio of specific heats
L	Length (in.c)
P	Pressure (in. H_2O)
P_a	Atmospheric pressure (in. Hg)
P_v	Velocity head (in. H_2O)
PMS	Static pressure along the length of the mixing stack (in. H_2O)
R	Gas constant for air ($R = 53.34 \text{ ft-lbf/lbm-R}$)
s	Entropy (Btu/lbm-R)
S	Distance from primary nozzle exit plane to mixing stack entrance plane (in.)
T	Absolute temperature (R)

u	Internal energy (Btu/lbm)
U	Velocity (ft/sec)
v	Specific volume (ft ³ /lbm)
W	Mass flow rate (lbm/sec)
Y	Expansion factor

Dimensionless Groupings

A*	Ratio of secondary flow area to primary flow area
AR	Area ratio
f	Friction factor
K	Flow coefficient
K _e	Kinetic energy correction factor
K _m	Momentum correction factor at the mixing stack exit
K _p	Momentum correction factor at the primary nozzle exit
L/D	Ratio of mixing stack length to mixing stack diameter
M	Mach number
P*	Pressure coefficient
PMS*	Mixing stack pressure coefficient
Re	Reynolds number
S/D	Standoff; ratio of distance from primary nozzle exit plane to entrance plane of the mixing stack (S) to the diameter of the mixing stack (D)
T*	Absolute temperature ratio of the secondary flow to primary flow
T _t *, TT*	Absolute temperature of the tertiary flow to primary flow

W_s^*, W^* Secondary mass flow rate to primary mass flow rate ratio
 W_t^*, W_t^* Tertiary mass flow to primary mass flow rate ratio
 ρ^* Induced flow density to primary flow density ratio

Greek Letter Symbols

μ Absolute viscosity (lbf-sec/ft²)
 ρ Density (lbm/ft³)
 θ Primary nozzle tilt angle
 ϕ Primary nozzle rotation angle
 ψ Nozzle base plate rotation angle
 β Ratio of ASME long radius metering nozzle throat diameter to inlet diameter

Subscripts

0 Section within secondary air plenum
 1 Section at primary nozzle exit
 2 Section at mixing stack exit
 f Film or wall cooling
 m Mixed flow or mixing stack
 or Orifice
 p Primary
 s Secondary
 t Tertiary (Cooling)
 u Uptake
 w Mixing stack inside wall

Computer Tabulated Data

DPOR	Pressure differential across the orifice (in. H ₂ O)
POR	Static pressure at the orifice (in. H ₂ O)
PSEC	Static pressure at the mixing stack entrance (in. H ₂ O)
PTER	Static pressure in the tertiary air plenum (in. H ₂ O)
PUPT	Static pressure in the uptake (in. H ₂ O)
TAMB	Ambient air temperature (°F)
TOR	Air temperature at the orifice (°F)
TUPT	Temperature of air in the uptake (°F)
UM	Average velocity in the mixing stack (ft/sec)
UP	Primary flow velocity at primary nozzle
UUPT	Primary flow velocity in uptake (ft/sec)
UPT MACH	Uptake Mach number
UE	Average velocity at the mixing stack exit (ft/sec)
WM	Mass flow rate from mixing stack (lbm/sec)
WP	Mass flow from primary nozzles (lbm/sec)
WS	Secondary mass flow rate (lbm/sec)
WT	Tertiary mass flow rate (lbm/sec)

I. INTRODUCTION

The current shipbuilding trend of today's Navy is leading to a large inventory of gas-turbine powered ships. Their lower manning requirements, high horsepower to specific weight, and competitive specific fuel consumption have made the gas-turbine power plant extremely attractive for present and future naval ship propulsion applications. Gas turbines require large amounts of cooling air in addition to that required for combustion. As a result, air-fuel ratios of four to five times those of conventional power plants are required. Large quantities of hot exhaust gases are therefore generated. The exhaust gas temperatures often run as high as twice those for conventional plants. These exhaust gases contribute to greater thermal and corrosive damages to the mast, superstructure and electronics equipment mounted thereon. Also, the hot plume can cause aircraft control problems for helicopter operations, and generate a high infrared signature from both the gases and the external surfaces of the stack.

The temperature and volume of the exhaust gases is set by the gas turbine operating conditions. Therefore some method must be employed to cool the gases and counter the problems associated with the exhaust. Several methods have been employed to recover waste heat from gas turbines such as the

waste heat boiler and the RACER (Rankine Cycle Energy Recovery) system. A by-product of these systems is a reduction in exhaust gas temperatures.

A simple, effective method of reducing the exhaust gas temperature is to employ the use of a gas eductor. This system can produce the desired effects with no external system connections and has no moving parts. The gas eductor system, properly dimensioned, produces turbulent mixing of the exhaust gases and secondary or ambient air, thereby reducing the overall exit temperature of the exhaust gases. The gas eductor system is presently in use on several naval vessels. A positive feature of gas eductor systems is that they can be used in conjunction with waste heat recovery systems, such as the RACER system, with minor modifications.

This thesis is a further extension of research conducted by Ellin {Ref. 1}, Moss {Ref. 2}, Lemke and Staehli {Ref. 3}, Shaw {Ref. 4}, Ryan {Ref. 5}, Davis {Ref. 6}, Drucker {Ref. 7}, and Boykin {Ref. 8} on the cold flow eductor model testing facility.

The eductor model testing facility constructed by Ellin consists of an intake, centrifugal compressor, primary flow nozzles, mixing stack, and a means to control and measure the primary and secondary air flows. Figures 1 and 2 show the general test model layout and terminology used in the model.

The primary air flow in the testing facility represents a gas turbine's hot exhaust gas. The secondary air flow is ambient air induced into the mixing stack entrance by the primary air flow utilizing the gas eductor concept. From Ellin's study of multiple vice single nozzle flow systems, it was determined that four primary flow nozzles were preferable to either three or five nozzle systems. Ellin also determined that the nozzle length had little if any effect on the overall performance of the gas eductor system. He then verified the independence of the one-dimensional gas eductor modeling correlation parameters used on the primary flow rate or uptake Mach number. His research showed that the one-dimensional analysis provided good correlation of data for Mach numbers from 50 to 145 percent of the design Mach number of 0.062.

Moss investigated the effects of the stand-off distance (the distance between the exit plane of the primary flow nozzles and the entrance plane of the mixing stack). For non-dimensional analysis, the stand-off distance, S , is divided by the mixing stack diameter, D , to give the S/D ratio. Moss determined that the optimum S/D ratio was 0.5, which maximizes eductor pumping. He also explored the effects of adding a conical transition piece at the mixing stack entrance. His experiments showed that the transition piece produced a slightly degraded system performance.

Lemke and Staehli conducted research utilizing various mixing stack geometric configurations and area ratios of primary nozzles. The area ratio for nozzles is defined as the cross-sectional area of the mixing stack divided by the total cross-sectional area of the primary nozzles. The results of their research showed that decreasing the nozzle area ratio from 3.0 to 2.5 decreased back pressure but also decreased the eductor's pumping ability. They investigated the effects of adding a solid diffuser, a two-ring diffuser, and a three-ring diffuser to the exit region of the mixing stack. They utilized mixing stack length-to-diameter ratios of 2.5 and 3.0. They demonstrated with these various geometries that the pumping can be improved without an increase in back pressure and that sufficient tertiary air flow can be produced to provide the potential for stack cooling and additional mixing air.

Davis conducted research to study the effects of tilting and rotating the primary nozzles on the eductor pumping ability and stack turbulent mixing. He conducted tests on various tilt and rotation combinations with the optimum combination being a 15 degree tilt angle and a 20 degree rotation angle. He maintained the nozzle area ratio at 2.5 and the stand-off ratio (S/D) at 0.5. Davis then tested the effects of shortening the mixing stack length using L/D ratios of 1.75, 1.5, and 1.25. His research indicated that the same overall performance as a straight nozzle eductor could be realized using a much reduced L/D with tilted and angled nozzles.

Drucker continued the research begun by Davis on the tilted-angled nozzles and short mixing stacks by using a slotted mixing stack and adding a shroud and diffuser rings for cooling potential.

The object of this thesis is to investigate the effects of a slanted shroud and diffuser arrangement when placed on a slotted mixing stack. The mixing stack, shroud and diffuser rings combined provided L/D ratios of 1.5 and 2.25. The stack, shroud and diffuser are dimensionally shown in Figures 3, 4, and 5. The shroud and diffuser ring arrangement was tested to determine the effects on pumping capability, both secondary and tertiary. Two different sets of primary nozzles were used. The first was maintained at a 15 degree tilt angle and a 20 degree rotation angle, a result from Davis' and Druckers' research. The second set tested were straight nozzles (no tilt, no rotation). The standoff ratio (S/D) was maintained at 0.5.

II. THEORY AND ANALYSIS

This thesis is a further extension of the work conducted by Ellin, Moss, Lemke and Staehli, Ryan, Davis, Drucker and Boykin {Ref. 1,2,3,4,5,6,7 and 8} and uses the same one-dimensional analysis of a simple eductor system. The geometries tested and the data acquired in this investigation are similar to that of Ellin, and the error analysis performed by him is applicable for this investigation as well. The dimensionless parameters controlling the flow phenomena used previously were also used in the present research along with the basic means of data analysis and presentation. Dynamic similarity was maintained by using uptake Mach number similarity to establish the gas eductor model's primary flow rate.

The analysis presented here is for an eductor model with primary, secondary and tertiary air flows. Systems with tertiary flow for film or wall cooling air have been non-dimensionalized with the same base parameters as the secondary air flow and have been calculated using the same one-dimensional analysis. This allows a simple comparison of tabulated and graphical results. Parameters pertaining to the secondary systems are subscripted with an "s" and those relating to the tertiary are subscripted with a "t".

A. MODELING TECHNIQUE

Dynamic similarity between the models tested and an actual prototype was maintained by using the same primary air flow uptake Mach number. For the primary air flow uptake Mach number used, (0.062), based on the average flow properties within the uptake and the hydraulic diameter of the uptake, the flow is turbulent ($Re > 10^5$). As a consequence of this, momentum exchange is predominant over shear interaction, and the kinetic and internal energy terms are more influential on the flow than are viscous forces. It can also be shown that the Mach number represents the ratio of kinetic energy of a flow to its internal energy and is, therefore, a more significant parameter than the Reynolds number in describing the primary flow through the uptakes.

B. ONE-DIMENSIONAL ANALYSIS OF A SIMPLE EDUCTOR

The theoretical analysis of an eductor may be approached in two ways. One method attempts to analyze the details of the mixing process of the primary and secondary air streams as it takes place inside the mixing stack. This requires an interpretation of the mixing phenomenon which, when applied to a multiple nozzle system, becomes extremely complex. The other method, which was chosen here, analyzes the overall performance of the eductor system. Since details of the mixing process are not considered in this method, an analysis of the simple single nozzle eductor system shown in Figure 6

leads to a determination of the dimensionless groupings governing the flow. To avoid repetition with previous reports, only the main parameters and assumptions will be presented here. A complete derivation of the analysis used can be found in References {1} and {9}.

The driving or primary fluid, flowing at a rate W_p and at a velocity U_p , discharges into the throat of the mixing stack, inducing a secondary flow rate of W_s at velocity U_s . The primary and secondary flows are mixed and leave the mixing stack at a flow rate of W_m and a bulk-average velocity of U_m .

The one-dimensional flow analysis of the simple eductor system described depends on the simultaneous solution of the continuity, momentum and energy equations coupled with the equation of state, all compatible with specific boundary conditions.

The idealizations made for simplifying the analysis are as follows:

1. The flow is steady state and incompressible.
2. Adiabatic flow exists throughout the eductor with isentropic flow of the secondary stream from the plenum (at Section 0) to the throat or entrance of the mixing stack (at Section 1) and irreversible adiabatic mixing of the primary and secondary streams occurs in the mixing stack (between Sections 1 and 2).
3. Isentropic flow of the tertiary flow exists from the tertiary plenum to the minimum area at Section 2, with irreversible adiabatic mixing of the flows between section 2 and 3.

4. The static pressure across the flow at the entrance and exit planes of the mixing-stack (at Sections 1, 2 and 3) is uniform.

5. At the mixing-stack entrance (Section 1) the primary flow velocity U_p and temperature T_p are uniform across the primary stream, and the secondary flow velocity U_s and temperature T_s are uniform across the secondary stream, but U_p does not equal U_s , and T_p does not equal T_s .

6. At Section 2, the mixing primary-secondary air has an average velocity, U_2 , and an average temperature, T_2 .

7. Incomplete mixing of the primary, secondary and tertiary streams in the mixing stack is accounted for by the use of a non-dimensional momentum correction factor K_m which relates the actual momentum rate to the pseudo-rate based on the bulk-average velocity and density, and by the use of a non-dimensional kinetic energy correction factor K_e which relates the actual kinetic energy rate to the pseudo-rate based on the bulk-average velocity and density.

8. Both gas flows behave as perfect gases.

9. Changes in gravitational potential energy are negligible.

10. Pressure changes P_{os} to P_1 , P_{ot} to P_2 , P_1 to P_2 and P_2 to P_3 ($=P_a$) are small relative to the static pressure so that the gas density is essentially dependent upon temperature and atmospheric pressure.

11. Wall friction in the mixing stack is accounted for with the conventional pipe friction factor term based on the bulk-average flow velocity and the mixing stack wall area A_w .

The following parameters, defined here for clarify, will be used in the following development.

$\frac{A_p}{A_m}$ area ratio or primary flow area to mixing stack cross sectional area

$\frac{A_w}{A_m}$ area ratio of wall friction area to mixing stack cross sectional area

K_p momentum correction factor for primary flow

K_m momentum correction factor for mixed flow

f wall friction factor

Based on the continuity equation, the conservation of the mass principle for steady flow yields

$$W_m = W_p + W_s + W_t \quad (1)$$

where

$$W_p = \rho_p U_p A_p \quad (1a)$$

$$W_s = \rho_s U_s A_s$$

$$W_t = \rho_t U_t A_t$$

$$W_m = \rho_m U_m A_m$$

All of the above velocity and density terms, with the exception of ρ_m and U_m , are defined without ambiguity by the virtue of idealizations (3) and (4) above. Combining equations (1) and (1a) above, the bulk average velocity at the exit plane of the mixing stack becomes

$$U_m = \frac{W_s + W_t + W_p}{\rho_m A_m} \quad (1b)$$

where A_m is fixed by the geometric configuration and

$$\rho_m = \frac{P_a}{RT_m} \quad (2)$$

where T_m is calculated as the bulk average temperature from the energy equation (9) below. The momentum equation stems from Newton's second and third laws of motion and is the conventional force and momentum-rate balance in fluid mechanics.

$$K_p \left(\frac{W_p U_p}{g_c} \right) + \left(\frac{W_s U_s}{g_c} \right) + \left(\frac{W_t U_t}{g_c} \right) + P_1 A_1 = K_m \left(\frac{W_m U_m}{g_c} \right) + P_2 A_2 + F_{fr} \quad (3)$$

Note the introduction of idealizations (3) and (5). To account for possible non-uniform velocity profiles across the primary nozzle exit, the momentum correction factor K_p is introduced here. It is defined in a manner similar to that of K_m and by idealization (4), and supported by work conducted by Moss, K_p is set equal to unity. K_p is carried through this analysis only to illustrate its effect on the final result. The momentum correction factor for the mixing stack exit is defined by the relation.

$$K_m = \frac{1}{W_m U_m} \int_0^{A_m} U_2^2 \rho_2 dA \quad (4)$$

where U_m is evaluated as the bulk-average velocity from equation (1b). The wall skin friction factor F_{fr} can be related to the flow stream velocity by

$$F_{fr} = f A_w \left(\frac{U_m^2 \rho_m}{2 g_c} \right) \quad (5)$$

using idealization (9). As a reasonably good approximation for turbulent flow, the friction factor may be calculated from the Reynolds number

$$f = 0.046 (Re_m)^{-0.2}. \quad (6)$$

Applying the conservation of energy principle to the steady flow system in the mixing stack between the entrance and exit planes,

$$\begin{aligned}
 W_p \left(h_p + \frac{U_p^2}{2g_c} \right) + W_s \left(h_s + \frac{U_s^2}{2g_c} \right) + W_t \left(h_t + \frac{U_t^2}{2g_c} \right) \\
 = W_m \left(h_m + K_e \frac{U_m^2}{2g_c} \right)
 \end{aligned} \tag{7}$$

neglecting potential energy of position changes (idealization 7). Note the introduction of the kinetic energy correction factor K_e , which is defined by the relation

$$K_e = \frac{1}{W_m U_m^2} \int_0^{A_m} U^3 \rho_2 dA \tag{8}$$

It may be demonstrated that for the purpose of evaluating the mixed mean flow temperature T_m , the kinetic energy terms may be neglected to yield

$$h_m = \frac{W_p}{W_m} h_p + \frac{W_s}{W_m} h_s + \frac{W_t}{W_m} h_t \tag{9}$$

where $T = \theta(h_m)$ only, with the idealization (6).

The energy equation for the isentropic flow of the secondary air from the plenum to the entrance of the mixing stack may be shown to reduce to

$$\frac{P_{os} - P_s}{\rho_s} = \frac{U_s^2}{2g_c} \tag{10}$$

similarly, the energy equation for the tertiary flow reduces to

$$\frac{P_o - P_t}{\rho_t} = \frac{U_t^2}{2g_c}$$

The previous equations may be combined to yield the vacuum produced by the eductor action in either the secondary or tertiary air plenums. Letting

$$K_3 = K_m, \rho_3 = \rho_m, W_3 = W_m, P_3 = P_a$$

and making the additional assumptions that $A_3 = A_2$, $A_2 \approx A_1$, and that the friction ($F_{fr2,3}$) is negligible, the vacuum produced for the secondary air plenum is

$$P_a - P_{os} = \frac{1}{g_c A_m} \left(K_p \frac{W_p^2}{A_p \rho_p} + \frac{W_s^2}{A_s \rho_s} \left(1 - \frac{1}{2} \frac{A_m}{A_s} \right) - \frac{W_m^2}{A_m \rho_m} \left(K_m + \frac{f}{2} \frac{A_w}{A_m} \right) \right). \quad (11)$$

It is understood that A_p and ρ_p apply to the primary flow at the entrance to the mixing stack, A_s and ρ_s apply to the secondary flow at the same section, and A_m and ρ_m apply to the mixed flow at the exit of the mixing stack system. P_a is atmospheric pressure, and is equal to the pressure at the exit of the mixing stack. A_w is the wall area of the inside of the mixing stack.

For the tertiary air plenum, making the same approximations as used in equation (11), the vacuum produced is

$$P_a - P_{ot} = \frac{1}{g_c A_m} \left\{ K_2 \frac{(W_p + W_s)^2}{\rho_2 A_m} + \frac{W_t^2}{\rho_t A_t} \left(1 - \frac{1}{2} \frac{A_m}{A_t} \right) - K_m \frac{W_m^2}{\rho_m A_m} \right\} \quad (11a)$$

where K_2 is the momentum correction factor at section 2.

C. NON-DIMENSIONAL FORM OF THE SIMPLE EDUCTOR EQUATION

In order to provide the criteria of similarity of flows with geometric similarity, the non-dimensional parameters which govern the flow must be determined. The means chosen for determining these parameters was to normalize equations (11) and (11a) with the following dimensionless groupings.

$$P^* = \frac{\frac{P_a - P_{os}}{\rho_s}}{\frac{U_p^2}{2g_c}}$$

a pressure coefficient which compares the pumped head $P_a - P_{os}$ for the secondary flow to the driving head $\frac{U_p^2}{2g_c}$ of the primary flow

$$PT^* = \frac{\frac{P_a - P_{ot}}{\rho_t}}{\frac{U_p^2}{2g_c}}$$

a pressure coefficient which compares the pumped head $P_a - P_{os}$ for the tertiary flow to the driving head $\frac{U_p^2}{2g_c}$ of the primary flow

$$W^* = \frac{W_s}{W_p}$$

a flow rate ratio, secondary to primary mass flow rate

$$WT^* = \frac{W_t}{W_p}$$

a flow rate ratio, tertiary to primary mass flow rate

$$T^* = \frac{T_s}{T_p}$$

an absolute temperature ratio, secondary to primary

$$TT^* = \frac{T_t}{T_p}$$

an absolute temperature ratio, tertiary to primary

$$\rho_s^* = \frac{\rho_s}{\rho_p}$$

a flow density ratio of the secondary to primary flows. (Note $P_s \approx P_p$ and $P_t \approx P_p$ also since the fluids are considered perfect gases,

$$\rho_s^* = \frac{T_p}{T_s} = \frac{1}{T_s^*} \quad)$$

$$\rho_t^* = \frac{\rho_t}{\rho_p}$$

a flow density ratio of the tertiary or film cooling flow to primary flows. (Note that since the fluids are considered perfect gases,

$$\rho_t^* = \frac{T_p}{T_t} = \frac{1}{T_t^*} \quad)$$

$$A_s^* = \frac{A_s}{A_p}$$

an area ratio of secondary flow area to primary flow area

$$A_t^* = \frac{A_t}{A_p}$$

an area ratio of tertiary flow area to primary flow area

With these non-dimensional groupings, equations (11) and (11a) can be rewritten in dimensionless form. Since both equations follow the same format, only the results for the secondary air plenum will be presented here.

$$\begin{aligned} \frac{P^*}{T^*} = & 2 \frac{A_p}{A_m} \left(\left(K_p - \frac{A_p}{A_m} \beta \right) - W^* (K_p + T^*) \frac{A_p}{A_m} \beta \right. \\ & \left. + W^{*2} T^* \left(\frac{1}{A^*} \left(K_p - \frac{A_m}{2A^* A_p} \right) - \frac{A_p}{A_m} \beta \right) \right) \end{aligned} \quad (12)$$

where

$$\beta = K_m + \frac{f}{2} \frac{A_w}{A_m} \quad .$$

This may be rewritten as

$$\frac{P^*}{T^*} = C_1 + C_2 W^*(T + 1) + C_3 W^{*2} T^* \quad (13)$$

where

$$C_1 = 2 \frac{A_p}{A_m} (K_p - \frac{A_p}{A_m} \beta),$$

$$C_2 = - \left(\frac{A_p}{A_m} \right)^2 \beta, \text{ and}$$

$$C_3 = 2 \frac{A_p}{A_m} \left(\frac{1}{A^*} - \frac{A_m}{2A^* A_p} \beta - \frac{A_p}{A_m} \beta \right).$$

As can be seen from equation (13),

$$P^* = F(W^*, T^*).$$

The additional dimensionless quantities listed below were used to correlate the static pressure distribution down the length of the mixing stack.

$$PMS^* = \frac{\frac{PMS}{\rho_s}}{\frac{U_p^2}{2g_c}}$$

a pressure coefficient which compares the pumping head $\frac{PMS}{\rho_s}$ for the secondary flow to the driving head $\frac{U_p^2}{2g_c}$ of the primary flow,

where PMS = static pressure along the mixing stack length

$$\frac{X}{D}$$

ratio of the axial distance from the mixing stack entrance to the diameter of the mixing stack.

D. EXPERIMENTAL CORRELATION

For the geometries and flow rates investigated, it was confirmed by Ellin and Moss {Ref. 1,2} that a satisfactory correlation of the variables P^* , T^* , and W^* takes the form

$$\frac{P^*}{T^*} = f(W^*T^{*n}) \quad (1)$$

where the exponent 'n' was determined to be equal to 0.44. The details of the determination of $n = 0.44$ as the correlating exponent for the geometric parameters of the gas eductor model being tested is given in Reference {1}. To obtain a gas eductor model's pumping characteristic curve, the experimental data is correlated and analyzed by using equation (1), that is, P^*/T^* is plotted as a function of $W^*T^{*0.44}$. Variations in the model's geometry will change the pumping ability, which is evaluated by the plot of equation (1). For ease of discussion, $W^*T^{*0.44}$ will be referred to as the pumping coefficient in this report. Similarly, $WT^{**}TT^{0.44}$ will be referred to as the film cooling or tertiary pumping coefficient.

III. MODEL GEOMETRIES

The gas eductor system in this report made use of a single primary flow uptake with a cluster of four primary nozzles, one set of straight nozzles, and another set tilted at 15 degrees, within a rotatable base plate. Slotted, cylindrical mixing stacks of two lengths were used, with slanted (conical) shrouds and diffuser rings.

A. MIXING STACK CONFIGURATIONS AND SHROUDS

The main body of this research was to study the effects of mixing stacks with slanted shrouds and diffuser rings, Figure 7. Initial investigations utilized mixing stacks with straight (concentric-cylindrical) mixing stacks and shrouds. The latest geometry tested by Drucker {7}, had an L/D ratio of 1.5 using tilted and angled nozzles.

The mixing stack used along with the shroud and diffuser rings was manufactured from nominally 12 inch O.D. and 11.7 inch I.D. PVC agriculture water irrigation pipe. The stack was slotted with rectangular shaped slots which repeated every forty-five degrees as seen in Figures 8 and 9. Exact stack dimensions are given in Figure 3. Two shroud lengths were tested to evaluate film cooling much like the type evaluated by Lemke and Staehli {Ref. 3}. Unlike the Lemke and Staehli shroud, the diffuser rings were attached to the shroud and not the stack. The first shroud-diffuser ring

combination was manufactured from 1/16 inch steel, cut and rolled to the desired diameters. Spacing between the shroud and stack at the top portion of the stack is .266 inch, the shroud is angled away from the stack at 10° to a maximum distance of 1.04 inch and then angled toward the stack at an angle of 10° to a distance of .523 inch. This configuration is repeated for the length of the stack. (12.125 inches for the L/D 1.5 stack/shroud combination and 20.5 inches for the L/D 2.25 stack/shroud combination) The five concentric diffuser rings are positioned to give an effective diffuser angle of 10° . The diffuser angle is measured from the inside diameter edge of the stack to the inside edge of the fifth diffuser ring. The individual rings are slanted outward at an angle of 10° from the vertical giving the appearance of the base of inverted cone on the top of the mixing stack. A detailed drawing of the stack and shroud can be seen in Figures 4 and 5. A photograph of the shroud and diffuser rings can be seen in Figure 10.

Pressure taps were installed at 0.25 X/D increments (2.93 inch spacing) to provide data points for evaluating the stack pressure distribution. Small tubing (one-sixteenth of an inch I.D.) was fitted into the stack presenting very little resistance to the flow under the shroud.

B. ANGLED PRIMARY NOZZLE AND BASE PLATE CONFIGURATION AND GEOMETRIES

The angled nozzle concept was first tested by Davis {Ref. 8}, and from his data the 15 degree tilt angle and 20 degree rotation angle were chosen as the optimum nozzle configuration for this research. The nozzles have a constant cross section while having the ability to be inclined and rotated about their centerline axis. The nozzle tilt angle, θ , is the cant angle measured from the centerline of the straight nozzle to the centerline of the cant portion of the nozzle. Nozzle rotation, θ , is a measure of the angle through which the nozzle is rotated inward toward the mixing stack centerline from a perpendicular to a radial line from the base plate center to the center of the nozzle. Figures 11 and 12 may provide a clearer vizualization of the nozzle configuration. The slanted nozzles were manufactured from clear, cast acrylic pipe with nominal 4.0 inch O.D. and 3.625 inch I.D. which was machined to 3.7 inch I.D. for a nozzle area ratio of 2.5 for the four nozzle groups. The straight nozzles were manufactured from aluminum with the same characteristics as above. The angled nozzles were dimensioned so that the distance measured from the base to the centerline at the exit plane was euqual to that of the straight nozzle. (See Figure 11) This allowed alignment of the nozzles and mixing stack and setting the S/D ratio with the straight nozzles and not having to completely realign the system when the

angled nozzles are inserted. Similar materials were used in the construction of the nozzles and base plate so that with the use of tight tolerances and friction the nozzles were held in place even when the base plate was rotated. The angled nozzles and base plate are shown in Figures 13 and 14.

The nozzle base plate was constructed from acrylic plexiglass flat stock. Four recess holes were machined to accept the nozzles, and they were in turn machined to a 0.5 inch radius on the underside to present a smooth flow entrance region for the nozzles. The outer edge of the base plate was machined so that the whole base plate fit inside a matching aluminum base ring. The construction was such that the base plate could be rotated within the ring, primary flow pressure kept the two concentric surfaces mated which eliminated seals, and the base plate could not be ejected from the uptake by the considerable dynamic pressures associated with the high velocity primary air flow. Four symmetrically located locking cams allowed the base plate and installed nozzles to be locked in place. This was required for alignment procedures and to prevent rotation during initial start-up. Once the system was warmed up to operating conditions, the difference between thermal expansion factors for the ring and base plate allowed sufficient expansion to make the use of the locking cams unnecessary. In fact, rotation of the base plate could be difficult when the system was fully warmed up, and a dry teflon lubricant was used to help overcome this problem.

A third parameter was used for describing the base plate rotation. The base plate rotation angle, ψ , is defined as the angle of base plate rotation measured from the 90 degree point on the uptake transition piece as depicted in Figure 13. This parameter serves to give a general indication of the flow directions within the mixing stack due to the angled nozzles. The base plate's geometry and dimensions are given in Figure 14, and a photograph can be seen in Figure 12.

IV. EXPERIMENTAL APPARATUS

Air is supplied to the primary nozzles by means of a centrifugal compressor and associated ducting schematically illustrated in Figure 1. The mixing stack configuration being tested is placed inside an air plenum containing an airtight partition so that two separate air flows, secondary and tertiary, may be measured. The air plenum facilitates the accurate measurement of secondary and tertiary air flows by using ASME long radius flow nozzles.

A. PRIMARY AIR SYSTEM

The circled numbers found in this section refer to circled locations on Figure 1. The primary air ducting is constructed of 16-guage steel with 0.635 cm (0.25 in.) thick steel flanges. The ducting sections were assembled using 0.635 cm (0.25 in) bolts with air drying silicone rubber seals between the flanges of adjacent sections. Entrance to the inlet ducting (1) is from the exterior of the building through a 91.44 cm (3.0 ft) square to a 30.48 cm (1.0 ft) square reducer, each side of which has the curvature of a quarter ellipse. A transition section (2) then changes the 30.48 cm (1.0 ft) square section to a 35.31 cm (13.90 in) diameter circular section (3). This circular section runs approximately 9.14 m (30 ft) to the centrifugal compressor inlet.

A standard ASME square edged orifice (4) is located 15 diameters downstream of the entrance reducer and 11 diameters upstream of the centrifugal compressor inlet, thus insuring stability of flow at both the orifice and compressor inlet. Piezometer rings (5) are located one diameter upstream and one-half diameter downstream of the orifice. The duct section also contains a thermocouple just downstream of the orifice. Primary flow is measured by means of the standard ASME square edged orifice designed to the specifications given in the ASME power test code {Ref. 9}. The 17.55 cm (6.902 in) diameter orifice used was constructed out of 304 stainless steel 0.635 cm (0.25 in) thick. The inside diameter of the duct at the orifice is 35.31 cm (13.90 in) which yields a beta ($\beta = d/D$) of 0.497. The orifice diameter was chosen to give the best performance in regard to pressure drop and pressure loss across the orifice for the primary air flow rate used (1.71 kd/sec (3.77 lbm/sec)).

The centrifugal compressor (7) used to provide primary air to the system is a Spencer Turbo Compressor, catalogue number 25100-H, rated at 6000 cfm at 2.5 psi back pressure. The compressor is driven by a three phase, 440 volt, 100 horsepower motor.

A manually operated sliding plate variable orifice (6) was designed to constrict the flow symmetrically and facilitate fine control of the primary air flow. During operation, the

butterfly valve (8) , located at the compressor's discharge, provided adequate regulation of primary air flow, eliminating the necessity of using the sliding plate valve. The sliding plate valve was positioned in the wide-open position for all data runs.

On the compressor discharge side, immediately downstream of the butterfly valve, is a round to square transition (9) followed by a 90 degree elbow (10) and a straight section duct (11) . All ducting to this point is considered part of the fixed primary air supply system. A transition section (12) is fitted to this last square section which reduces the duct cross section to a circular section 29.72 cm (11.17 in) in diameter. This circular ducting tapers down to a diameter of 26.30 cm (11.5 in) to provide the primary air inlet to the eductor system being tested. For the single nozzle testing an additional transition piece was inserted, further reducing the diameter of the duct to 14.60 cm (5.75 in). The transition is located far enough upstream of the model to insure that the flow reaching the model is fully developed.

B. SECONDARY AIR PLENUM

The secondary air plenum, shown in Figures 1, 2, and 15, is constructed of 1.905 cm (0.75 in) plywood and measures 1.22 m by 1.22 m by 1.88 m (4.6 ft by 4.0 ft by 6.17 ft). It serves as an enclosure that can contain all or only part of the eductor model and still allow the exit plane of the

mixing stack to protrude. The purpose of the secondary air plenum is to serve as a boundary through which secondary air for the eductor system must flow. Long radius ASME nozzles, designed in accordance with ASME power test codes {Ref. 9} and constructed of fiberglass, penetrate the secondary air plenum, thereby providing the sole means for metering the secondary air reaching the eductor as shown in Figures 1, 2 6 and 15. Appendix D of Reference {1} outlines the design and construction of the secondary air flow nozzles. By measuring the temperature of the air entering and the pressure differential across the ASME flow nozzles, the mass flow rate of secondary air can be determined. Flexibility is provided in measurement for the mass flow rate of secondary air by employing flow nozzles with three different throat diameters: 20.32 cm (8 in), 19.16 cm (4 in), and 5.08 cm (2 in). By using a combination of flow nozzles, a wide variety of secondary cross sectional areas can be obtained.

A secondary air flow straightener, shown in Figures 1 and 2, consisting of a double screen is installed 1.22 m (4 ft) from the open end of the secondary air plenum, between the ASME long radius nozzles and the primary air flow nozzles. The purpose of the straightener is to reduce any swirl in the secondary flow.

C. TERTIARY AIR PLENUM

The tertiary air plenum, shown in Figures 1, 2, 17 and 16, is constructed of 1.90 cm (0.75 in) plywood and measures 1.22 m by 1.22 m by 1.22 m (4.0 ft by 4.0 ft by 4.0 ft). It serves as an enclosure that completely surrounds the mixing stack and allows the exit and entrance regions to protrude. An airtight rubber diaphragm type seal, schematically illustrated in Figure 2, is located at the entrance to the tertiary plenum (seal between secondary and tertiary plenums). The seal slides over the mixing stack with a nominal 1/8 inch clearance and a bead of silicone rubber is used to make the final seal. The interior of the tertiary air plenum is pictured in Figure 19. The stand which holds the mixing stack can be seen mounted inside the plenum.

D. INSTRUMENTATION

Pressure taps for measuring static pressures are located inside the primary air uptake just prior to the primary nozzles, inside the secondary air plenum, inside the tertiary air plenum, and at various points on the model. A variety of manometers, pictured in Figure 16, were used to indicate the pressure differentials. A schematic representation of the pressure measuring instrumentation is illustrated in Figures 17 and 18. Monitoring of each of the various pressures was facilitated by the use of a scanivalve and a multiple valve manifold. The scanivalve was used to select the

pressure tap to be read, while the multiple valve manifold allowed selection of the optimum manometer for the pressure being recorded. A vent was included in the multiple valve manifold which provided a means of venting the manometers between pressure readings. The valve manifold provided a selection of 15.24 cm (6.0 in) inclined water manometer, and a 5.08 cm (2.0 in) inclined water manometer. In addition, the following dedicated manometers were used in the system: a 50.80 cm (20.0 in) single column water manometer connected to the primary air flow just prior to the primary nozzles, a 1.27 m (50.0 in) U-tube water manometer with each leg connected to the piezometric ring on either side of the orifice plate in the air inlet duct, and a 2.55 cm (1.0 in) inclined water manometer connected to the upstream piezometric ring.

Primary air temperatures, measured at the orifice outlet and just prior to the primary nozzles, are measured with copper-constantan thermocouples. The thermocouples are in assemblies manufactured by Honeywell under the trade name Megapak. Polyvinyl covered 20 gauge copper-constantan extension wire is used to connect the thermocouples to an Omega Digital Thermometer, Model Number 2176A, which provided temperatures in degrees Fahrenheit or Celsius. A copper-constantan thermocouple was used to measure secondary/tertiary ambient air temperature.

E. ALIGNMENT

The alignment of the mixing stack with the primary flow nozzles is accomplished by using two round alignment plugs, a nozzle alignment plate and a 0.75 inch O.D. steel alignment bar. The two circular alignment plugs are inserted into opposite ends of the mixing stack, and the nozzle alignment plate is then carefully inserted over the straight nozzles. The steel alignment bar is then inserted through the centerline holes in the alignment plugs and brought up to the centerline hole in the nozzle alignment plate. The three axis mounting stand, pictured in Figure 19, is adjusted until the alignment bar can be fully inserted into the nozzle alignment plate and recess in the nozzle base plate without difficulty.

V. EXPERIMENTAL METHOD

Evaluation of the eductor model requires the experimental determination of pressure differentials across the ASME long radius flow nozzles, temperatures of primary and induced air flows, internal mixing stack pressure distributions, and mixing stack exit velocity profiles from pitot tube pressure readings. In addition, base plate rotations angles are used to get a general understanding of the flow patterns within the mixing stack. These experimentally determined quantities are then reduced with the aid of a computer to obtain pumping coefficients, induced air flow rates and pressure distributions in the mixing stack.

The following sections address the individual performance criteria used to evaluate the eductor. Circled numbers refer to regions located on the representative plots used in the evaluation process.

A. PUMPING COEFFICIENT

The secondary pumping coefficient and the tertiary pumping coefficient provide a basis for analyzing the eductor's pumping capability. Changes in stack geometries such as L/D ratio's, slotting, shrouding, diffuser rings, and spacing between stack and shroud and between shroud and diffuser rings will alter the eductor's pumping performance and the pumping coefficient. The pumping coefficients for the model should

correspond to the coefficients for the shipboard eductor system. At the shipboard operating point, the eductor is exposed to no restrictions in the secondary or tertiary air flows. In the model, this is simulated by completely opening the air plenums which provides an open to the environment simulation.

Unfortunately, at this condition the secondary and/or tertiary air flow rates cannot be measured. The eductor model's characteristics are first established over the measurable flow range and then extrapolated to the desired operating point.

The data for this extrapolation is established by varying the associated induced air flow rate, either secondary or tertiary, from zero to its maximum measurable rate. These rates are determined by sequentially opening the ASME flow nozzles mounted to the appropriate plenum and recording the pressure drop across the nozzles. Values for nozzle cross sectional areas, pressure drops, induced flow air temperatures, and barometric pressures are then used to calculate the dimensionless parameters P^*/T^* , $W*T^{0.44}$, $P T^*/T T^*$ and $W T^* T T^{0.44}$. The dimensionless parameters are then plotted as illustrated in Figure 20. Data point (1) is the maximum vacuum which is produced by the eductor with no secondary flow, obtained by closing all ASME flow nozzles. Data points in region (2) correspond to opening most of the ASME flow nozzles and the final point corresponds to opening all flow nozzles. Although the data point in region (2) appear to be zero or nearly so,

they do have a small finite value. The uncertainty associated with these points is relative high. The data points in region (3) provide the most consistent and accurate data. Extrapolation of the pumping characteristic curve to intersect the zero P^*/T^* or PT^*/TT^* abscissa locates the appropriate operating point for the eductor model configuration.

B. INDUCED AIR FLOWS

Secondary and tertiary air flows are induced flows. The secondary air flow is the amount of air induced by the primary nozzles which is mixed within the mixing stack with primary air to reduce the exhaust gas temperature. Tertiary or film cooling air flow is the amount of air induced by the low pressure areas along the mixing stack and diffuser.

C. PRESSURE DISTRIBUTION IN THE MIXING STACK

The axial pressure distribution in the mixing stack is obtained by taking static pressure readings from pressure taps attached to the stack in two rows. In the cold flow test facility, the mixing stack is located horizontally in the tertiary plenum. The first row is located on the top of the mixing stack, and the second row is offset 45 degrees from the first row as shown in Figures 3, 9 and 10. The pressure taps were located 0.25 mixing stack diameters apart. The dimensionless mixing stack pressure term, PMS^* , as derived in Section II is calculated from this static pressure data. PMS^* is plotted versus X/D pressure tap locations to obtain the mixing stack pressure distribution. A sample distribution

is shown in Figure 21. Region (1) is located at the entrance of the mixing stack, and it has the greatest negative pressure readings. Pressures near region (2), located toward the end of the mixing stack, although they show a lesser potential for inducing tertiary air compared with region (1), still represents a significant pumping capability. Pressure taps are located in the shrouded stack area only and are not located in the diffuser rings, therefore no pressure distribution data for this region is available.

D. MIXING STACK ROTATION ANGLE

The nozzles produce a symmetric flow consisting of high and low pressure areas along the axis of the mixing stack. Pressure taps at position 'A' were used to record the peaks while the position 'B' taps were used to record the lower pressure regions. A rotatable base plate was used to scan the entire circumference of the mixing stack at each L/D position and thereby obtain a record of the varying axial pressure distribution. This allowed the peaks and troughs to be rotated to the stationary pressure taps for data acquisition. The base plate rotation angle, ψ , is recorded for each pressure tap position, and when plotted, provides a rough indication of the flow pattern variations.

Tests were conducted early in Davis' research to determine the sensitivity of the rotation angles. Results showed that changes as small as one degree of rotation could cause large pressure changes while at other times, the base plate could be rotated 30 degrees without any pressure changes.

VI. DISCUSSION OF EXPERIMENTAL RESULTS

The discussion of this investigation will be confined mainly to the amount of induced air flows within the mixing stack, both secondary and tertiary (the amount of film cooling air available to cool the exterior of the eductor system); and mixing stack mixing of primary, secondary and tertiary air. Back pressure in the uptake caused by the eductor system is primarily fixed by the nozzle area ratio which was tested and confirmed by Davis {Ref. 8} and Lemke and Staehli {Ref. 3}. This is not a major area of discussion here since the nozzle area ratio was maintained at 2.5 and the back pressure remained relatively constant at 6.15 inches of water.

Throughout the entire investigation the standoff ratio (S/D) was maintained at 0.5. The nozzles utilized were the 15 degree tilt angle nozzles tested by Drucker and the straight nozzles used by Davis. During the discussion the nozzles used by Drucker will be referred to by their degree of tilt and their degree of rotation (i.e., 15/20 nozzles will mean 15 degree tilt and 20 degree rotation). Also when reference is made to the shrouded stack, it should be clear that the five diffuser rings are attached to the shroud, and that the shroud with the diffuser rings are a separate unit from the stack. Another term which will be used will be

the effective diffuser angle which was maintained at 10 degrees by design.

The tabulated data is presented in the same format as Davis and Drucker. During the discussion of this data the following abbreviations will be used; PCD for pumping coefficient, MSD for mixing stack pressure distribution. Along with the tabular data is a series of mini-plots which can prove to be helpful when reviewing the data.

Initial data was taken utilizing the slant shrouded mixing stack, $L/D = 1.5$ and 15/20 nozzles. This data was taken to develop a data baseline for comparison with the data reported by Drucker. Drucker had tested this stack/nozzle combination for pumping coefficient, mixing stack pressure distribution and tertiary pumping coefficient.

A. $L/D = 1.5$ STRAIGHT NOZZLES, 15-20 NOZZLES

The L/D ratio of 1.5 mixing stack was installed, aligned and tested. The results of the straight nozzles are shown in Figures 22, 23 and 24 and in Table 1. The evaluated data showed the secondary pumping coefficient to be .43 and the tertiary pumping coefficient to be .17 with the straight nozzles. Earlier studies by Davis showed the secondary pumping coefficient to be .51 for a non-shrouded mixing stack with the same overall L/D of 1.5. The present model had an inner mixing stack of one diameter in length with considerable mixing occurring in the half diameter length of

diffuser rings. This led to a significant tertiary flow. The total pumping (secondary and tertiary) exceeded that of Davis.

The 15-20 nozzles provided much better correlation with the data taken by Drucker. The results of the 15-20 nozzles are shown in Figures 25, 26 and 27 and in Table 2. The results obtained by Drucker showed the pumping coefficient to equal .59 for his shrouded two diffuser ring stack. The results obtained from the slant shroud stack showed a pumping coefficient of .58. A plot of the comparison of data can be seen in Figure 28. The added feature of the shrouded stack is the film cooling or tertiary air flow. In this case a tertiary pumping coefficient of .185 provided a significant increase over the flow through the version of Drucker. A plot of this comparison can be seen in Figure 29. The mixing stack pressure distribution of the slant shroud stack was similar to the straight shroud model tested by Drucker.

B. $L/D = 2.25$ STRAIGHT NOZZLES, 15-20 NOZZLES

The L/D ratio of 2.25 slant-shrouded stack was installed, aligned and tested. A direct correlation of data is not possible, however when compared to the L/D 2.5 shrouded stack used by Lemke and Staehli no significant deviations were noted in the pumping coefficient. A significant improvement in the tertiary pumping coefficient was observed. The results of the straight nozzles are shown in Figures 30, 31 and in Table 3. The mixing stack pressure distribution

was similar to the results obtained by Lemke and Staehli and can be seen in Figure 32. A comparison of the slant shroud stack with the straight shroud stack tested by Lemke can be seen in Figures 33 and 34 respectively.

As was expected from the previous data by Davis the 15-20 nozzles provided a significant increase in secondary pumping and tertiary flow when compared to the straight nozzles. This data is shown in Figures 34, 35 and 36. Table 4 shows the actual data taken.

Comparison of the secondary pumping coefficients and the tertiary pumping coefficients for the slant-shroud stack with the results obtained by Davis, Drucker, and Lemke can be found in Table 5 and 6. This comparison shows no significant difference in secondary pumping. The tertiary pumping coefficient was significantly higher for the slant shroud stack which shows a marked increase in the potential for stack cooling.

VII. CONCLUSIONS

This research investigated the effects on the eductor system's overall performance of using a slanted shroud and diffuser ring combination. The conclusions from this investigation are as follows:

1. An improvement in secondary pumping was obtained by the use of canted 15-20 nozzles vice straight nozzles for the same stack geometry.
2. In comparing the performance of the use of the slanted shroud and diffuser rings with the straight shroud and diffuser ring geometries:
 - a. no significant difference was observed in secondary pumping
 - b. a significant increase in tertiary flow was observed for the slanted shroud and diffuser ring geometry.

VIII. RECOMMENDATIONS

Based on the findings of this investigation the following recommendations for future research are presented.

1. Test the same two mixing stacks, shrouds, and diffuser ring arrangements using hot gas for the primary air flow.

2. Investigate to find the optimum angle for the shroud and diffuser ring to obtain the maximum tertiary pumping coefficient.

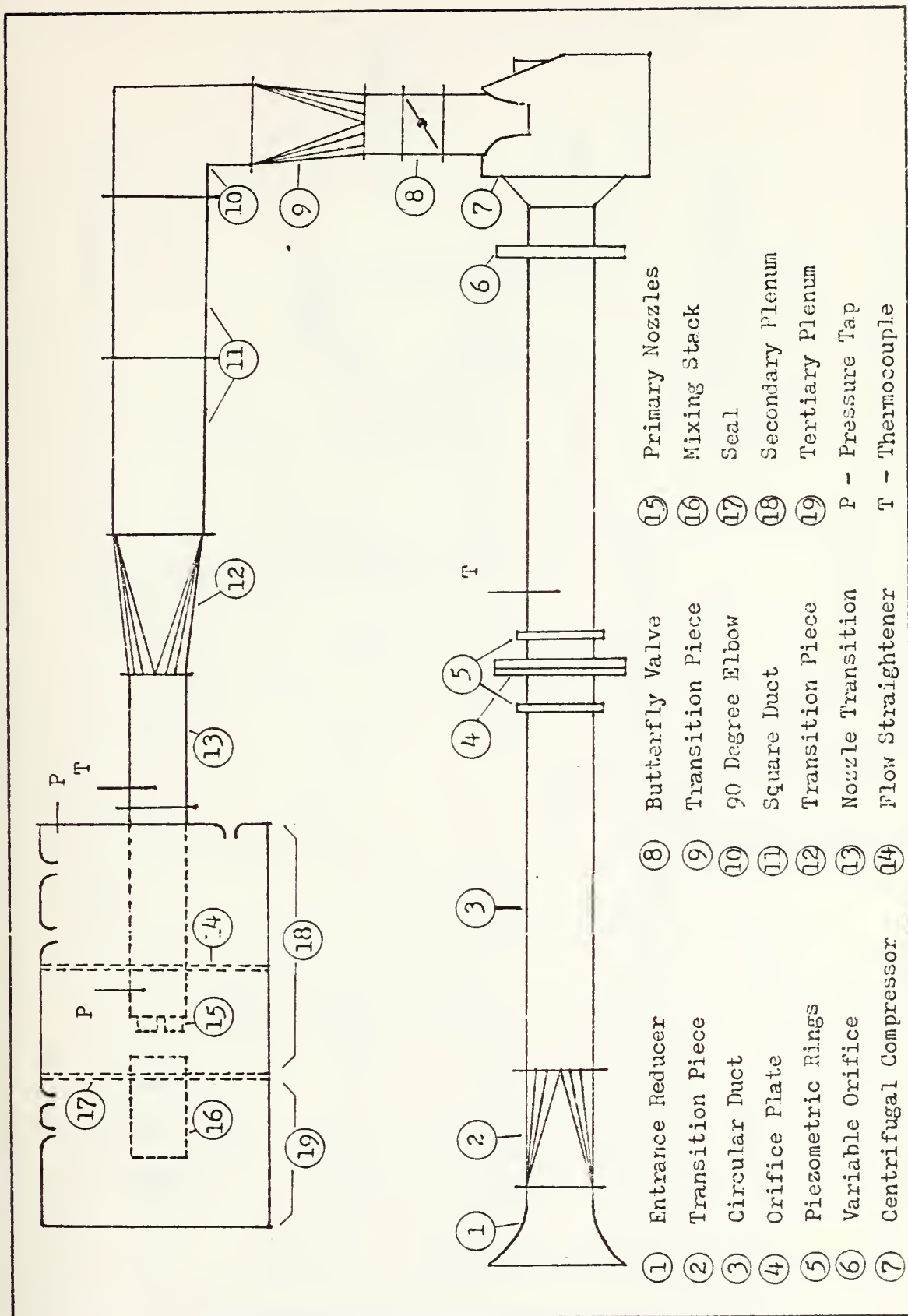


Figure 1. Eductor Model Testing Facility

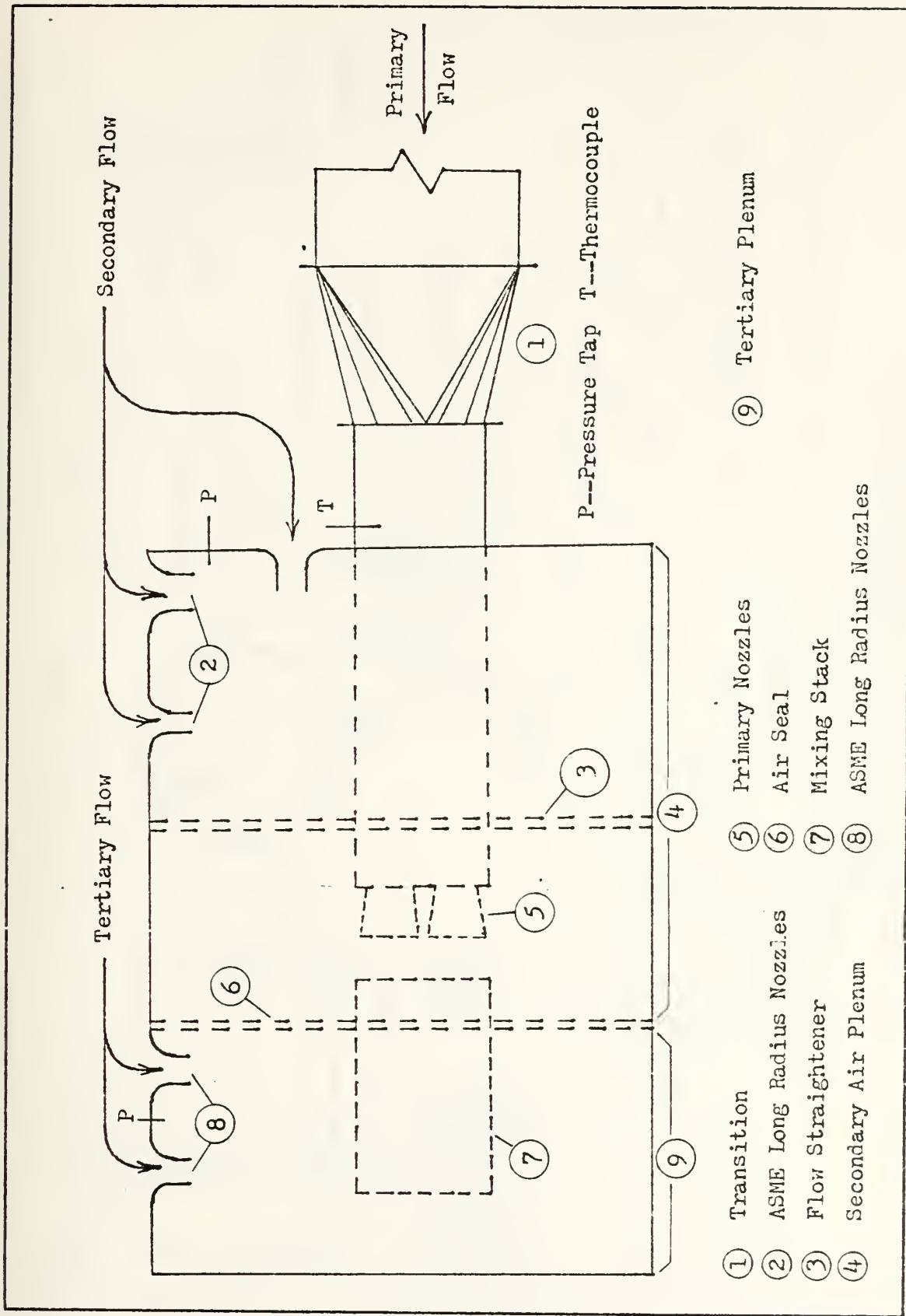


Figure 2. Test Facility with Secondary and Tertiary Plenums



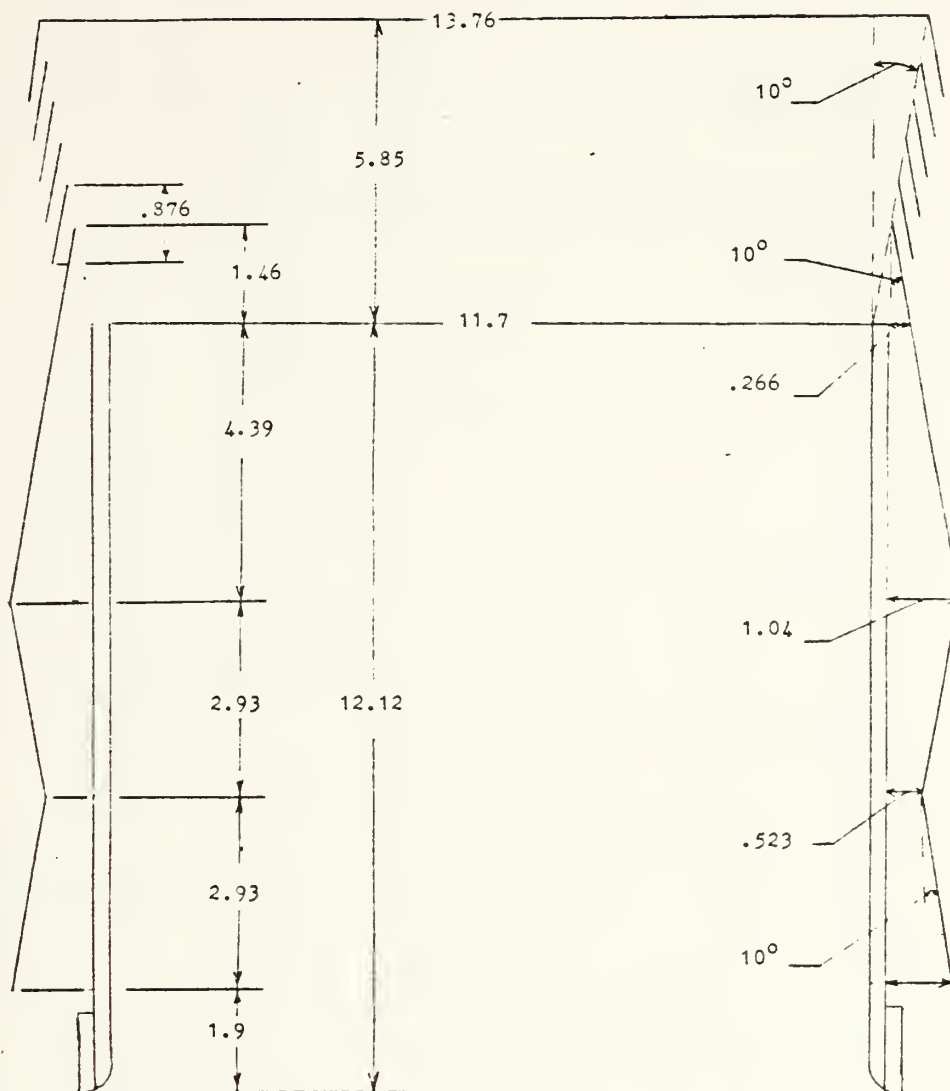
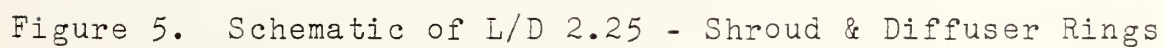


Figure 4. Schematic of L/D 1.5 - Shroud & Diffuser Rings



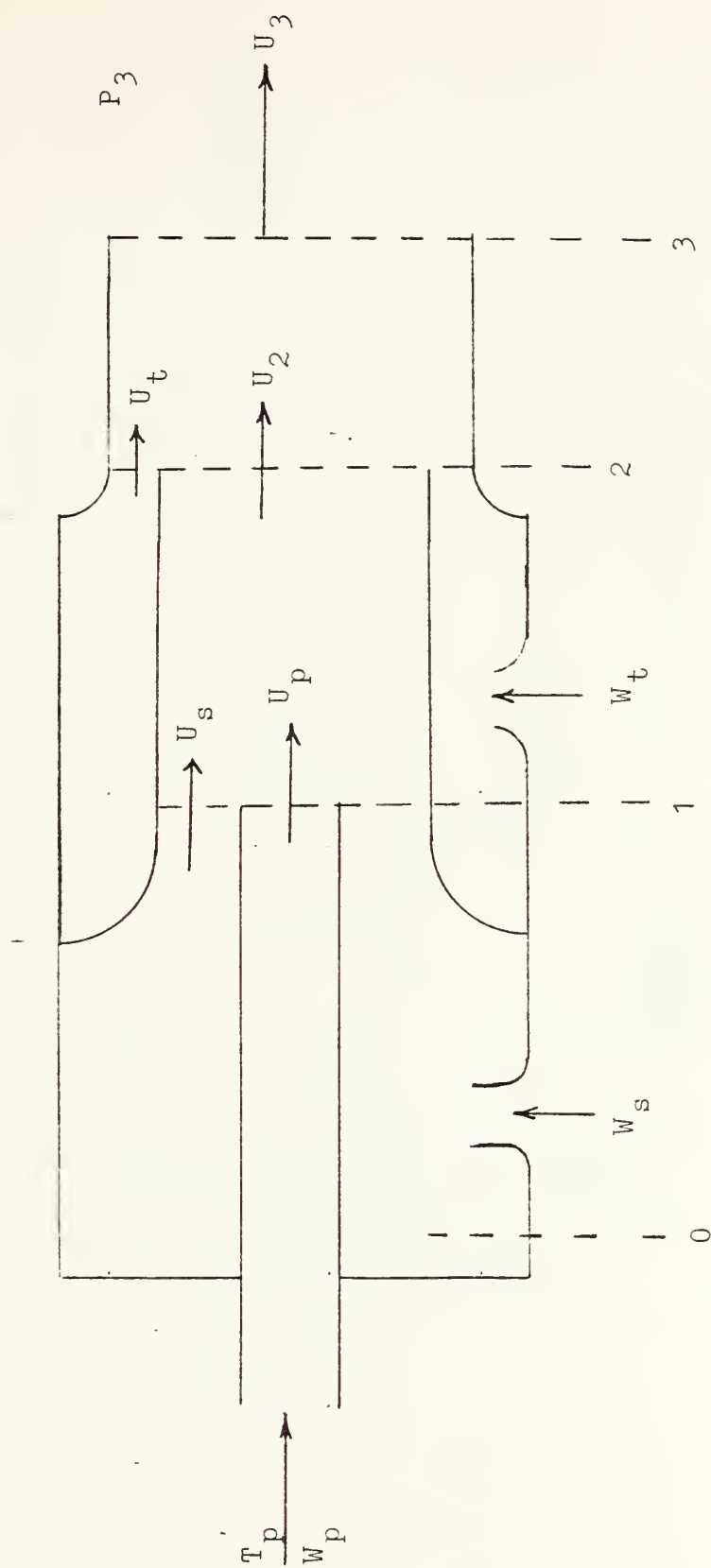


Figure 6. Simple Single Nozzle Ejector System.

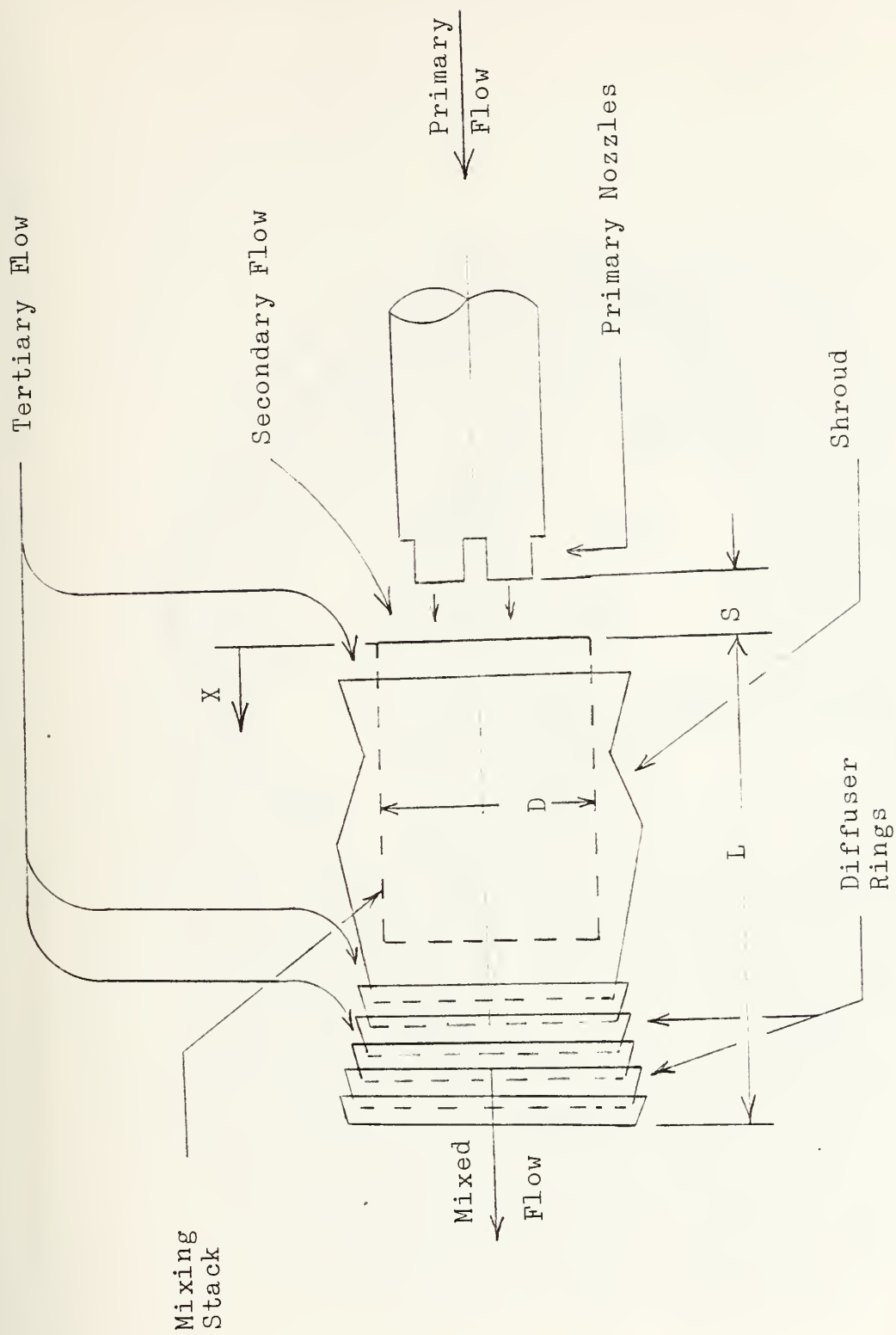


Figure 7. Schematic of Shrouded Mixing Stack Gas Educator with Angled Nozzles

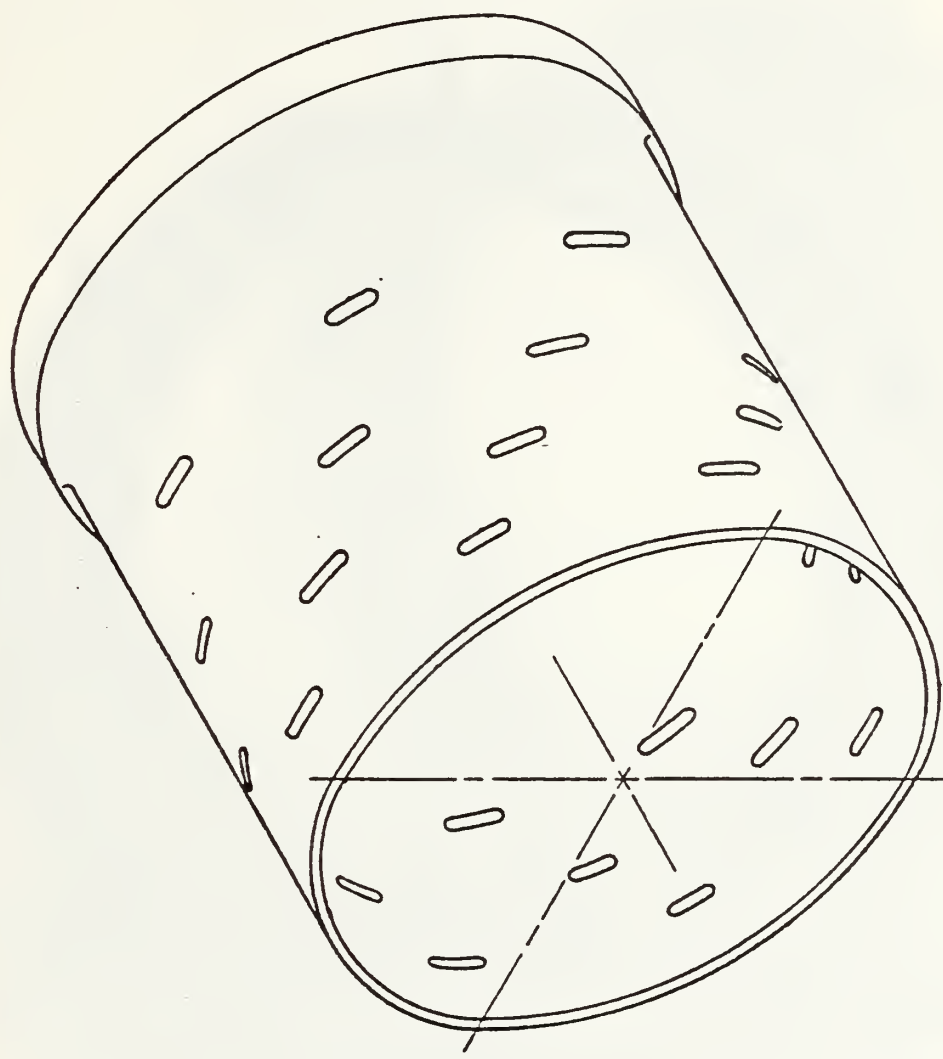


Figure 8. Isometric View of Slotted Mixing Stack

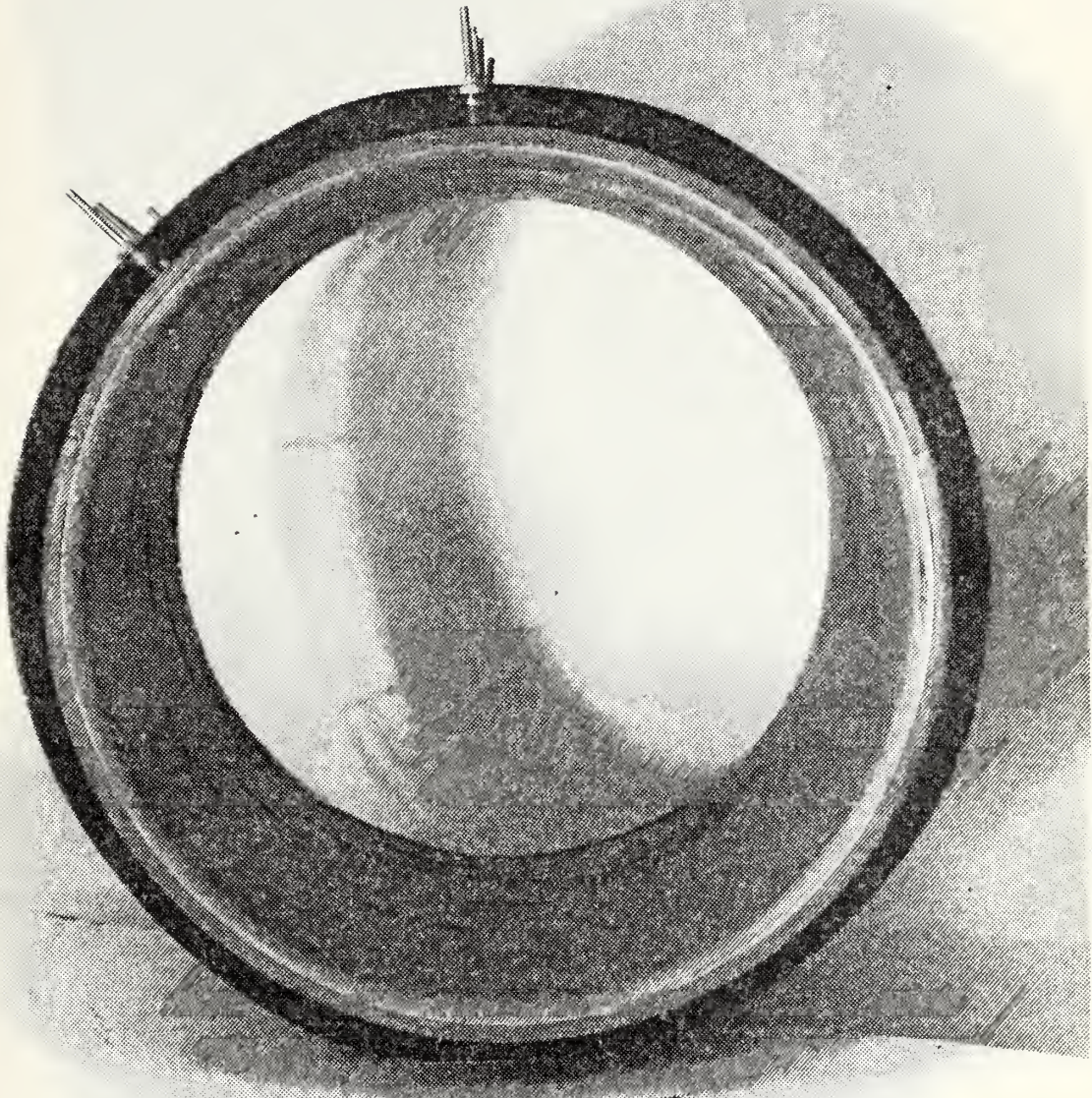


FIGURE 9. - MIXING STACK AND DIFFUSER RINGS

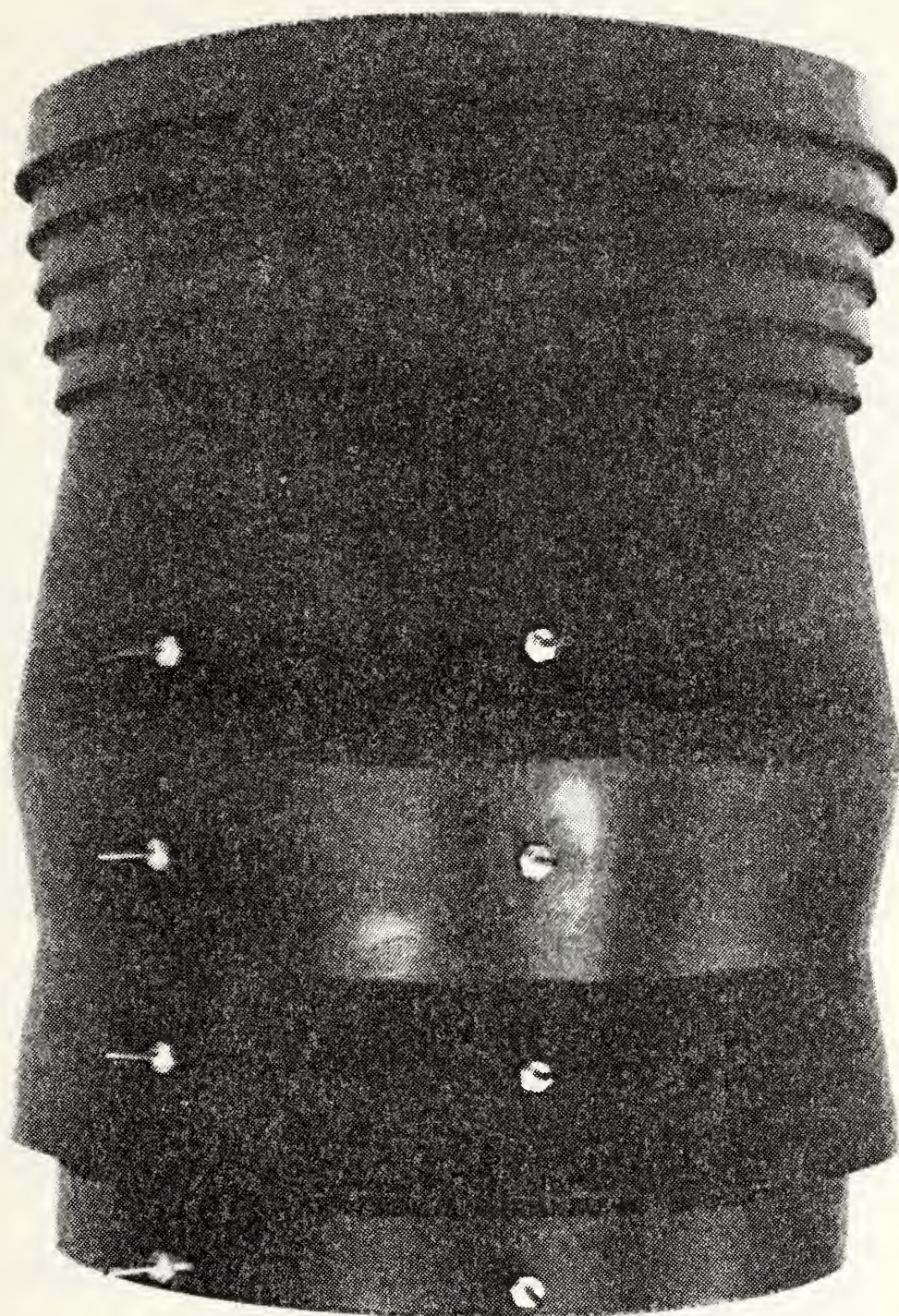
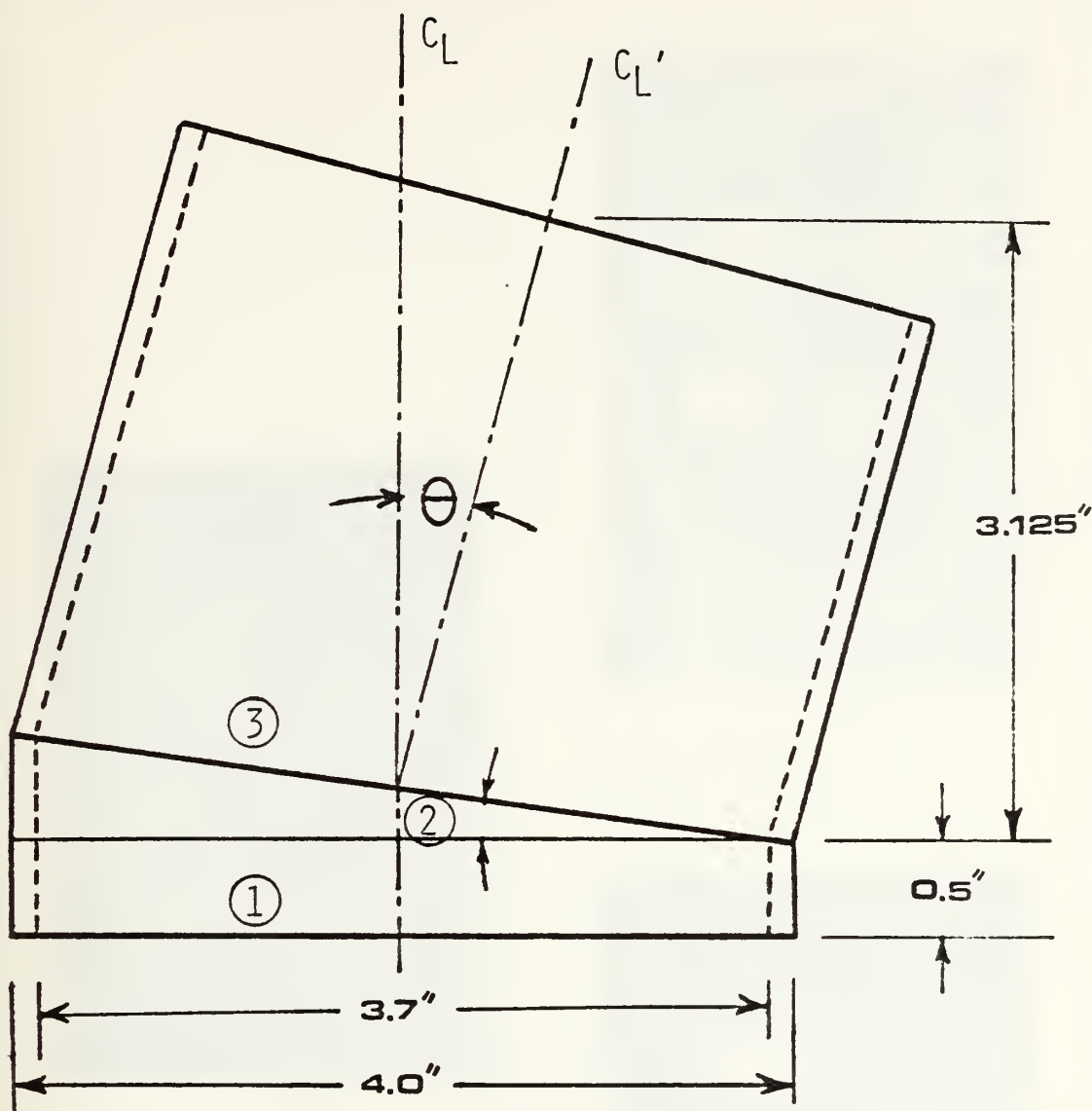


FIGURE 10. - SHROUD AND DIFFUSER RINGS



- ① 0.5 INCH MACHINED SURFACE TO FIT THE
NOZZLE BASE PLATE RECESSES
- ② MITER ANGLE-ONE -HALF OF THE TILT ANGLE
- ③ CUT AND JUNCTURE LINE

NOZZLE TILT ANGLE(Θ)= 15 DEGREES

Figure 11. Dimensions of Primary Nozzles

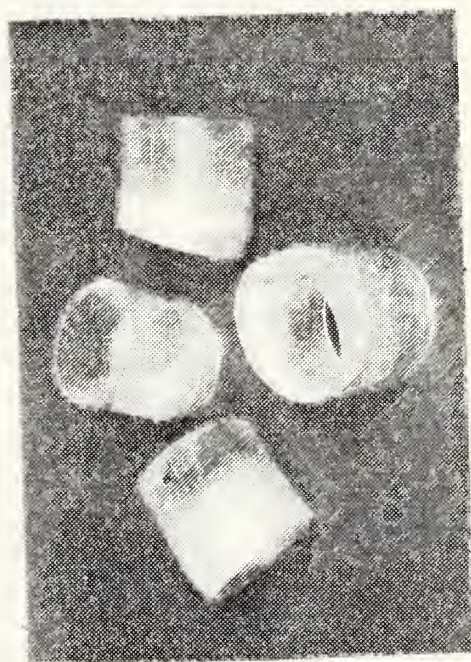
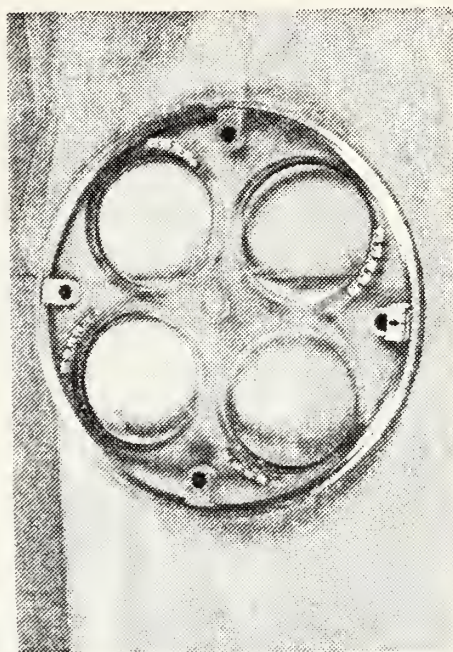
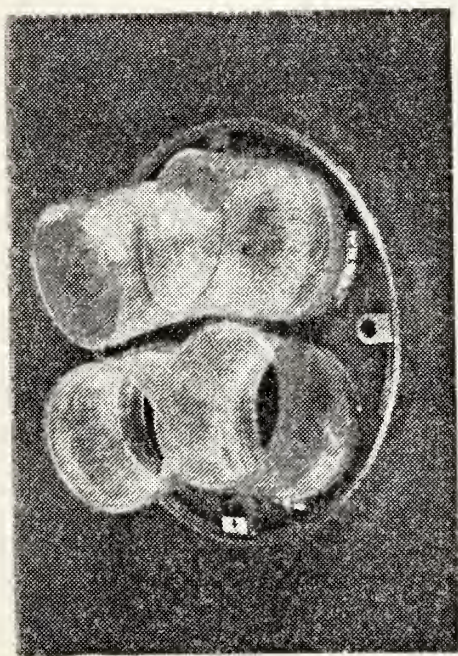
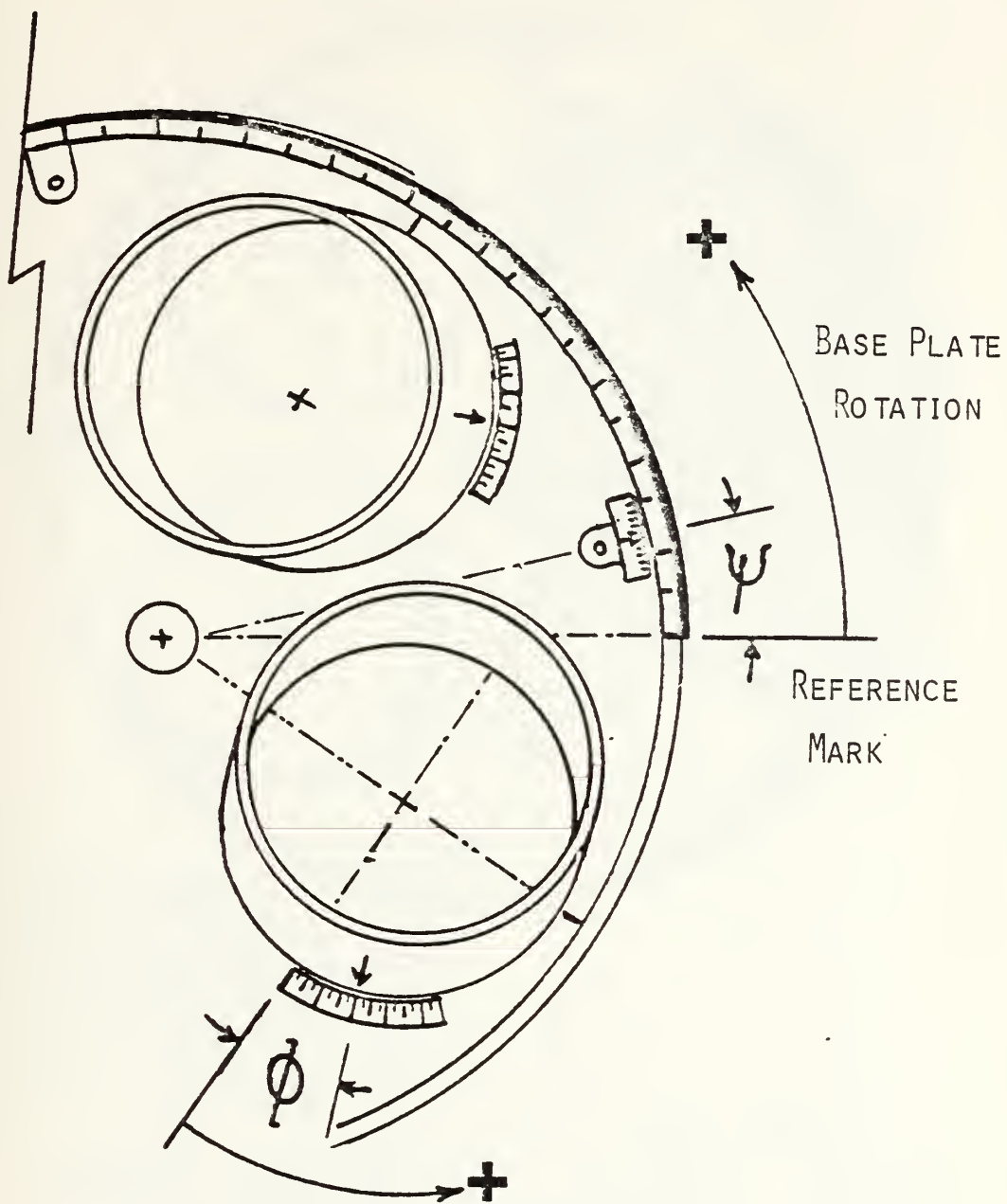
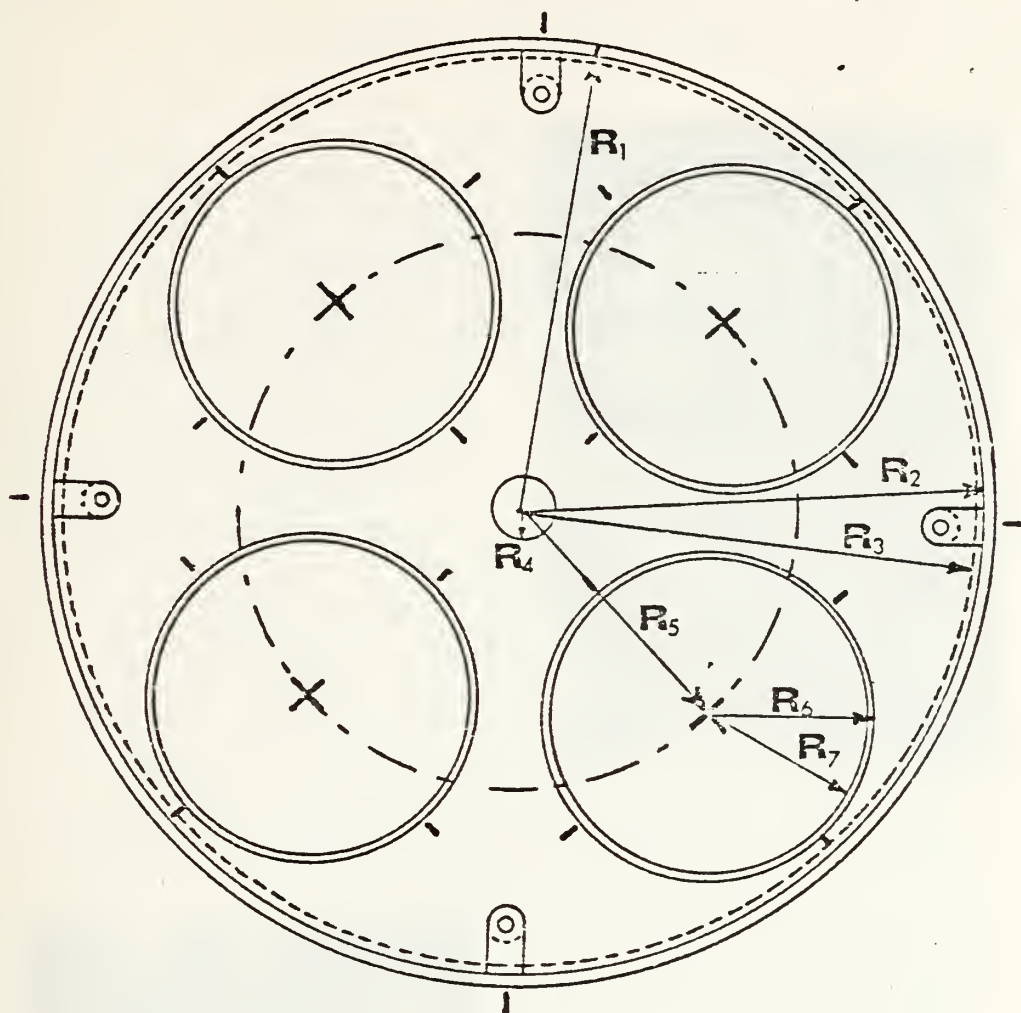


Figure 12. Angled Primary Nozzles and Base Plate



NOZZLES SHOWN HAVE A 15 DEGREE TILT ANGLE
 NOZZLE ROTATION(ϕ) IS 20 DEGREES
 BASE PLATE ROTATION(ψ) IS 13 DEGREES

Figure 13. Base Plate and Nozzle Rotation Angles



	Radii (Inches)	
1 Fixed Outer Ring	$R_1 = 5.750$	$R_6 = 2.000$
2 Rotating Base Plate	$R_2 = 5.600$	$R_7 = 1.850$
3 Recesses for Angled Nozzles	$R_3 = 5.400$	
4 Locking Cams	$R_4 = 0.375$	
	$R_5 = 3.200$	

Figure 14. Dimensions of the Four Nozzle Rotatable Base Plate

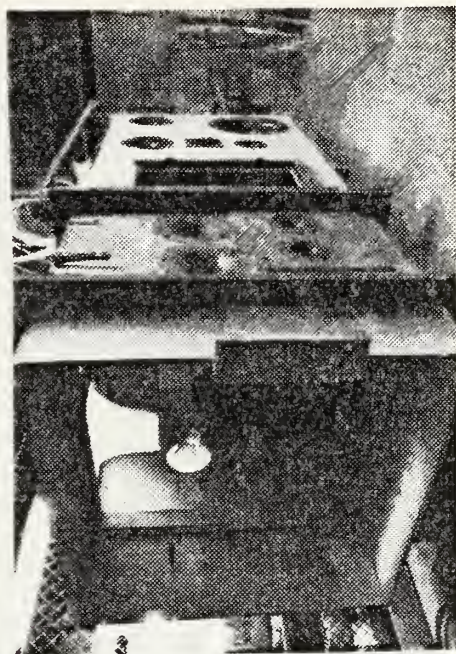
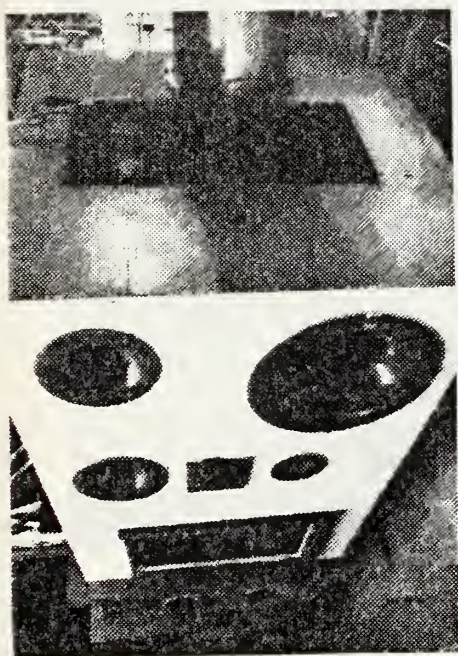


Figure 15. Exterior of Secondary and Tertiary Plenums

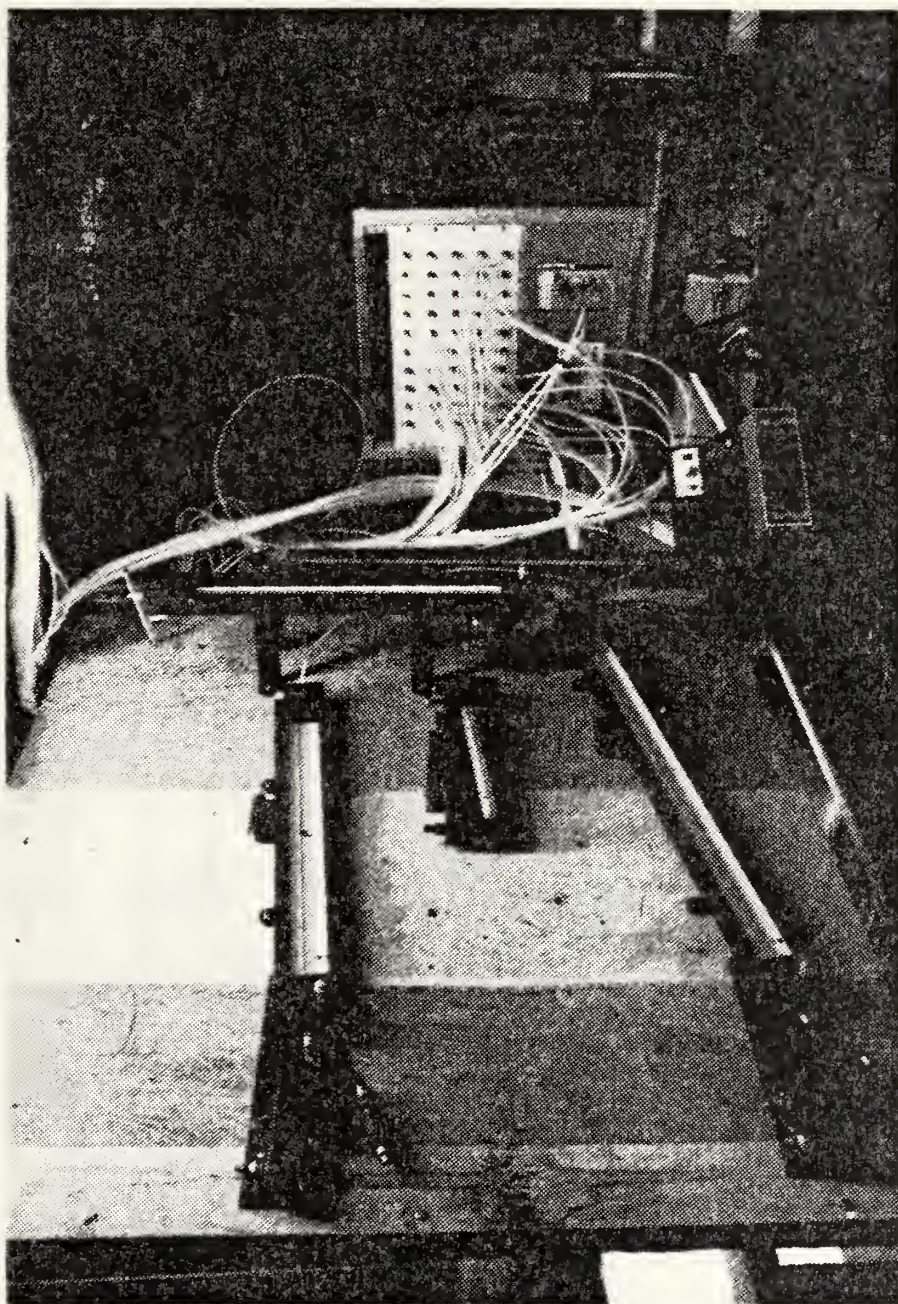


Figure 16. Instrumentation

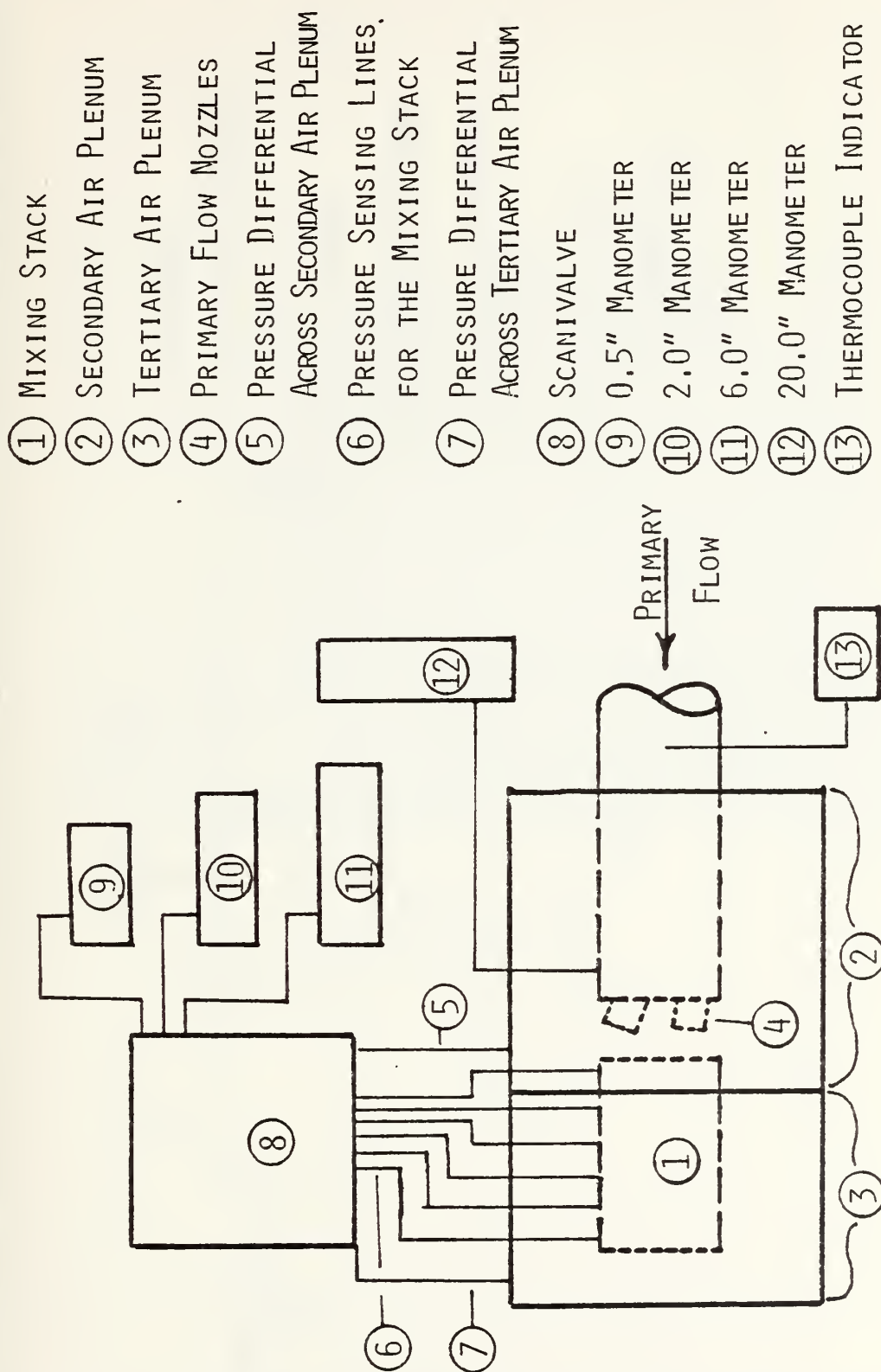


Figure 17. Schematic of Instrumentation

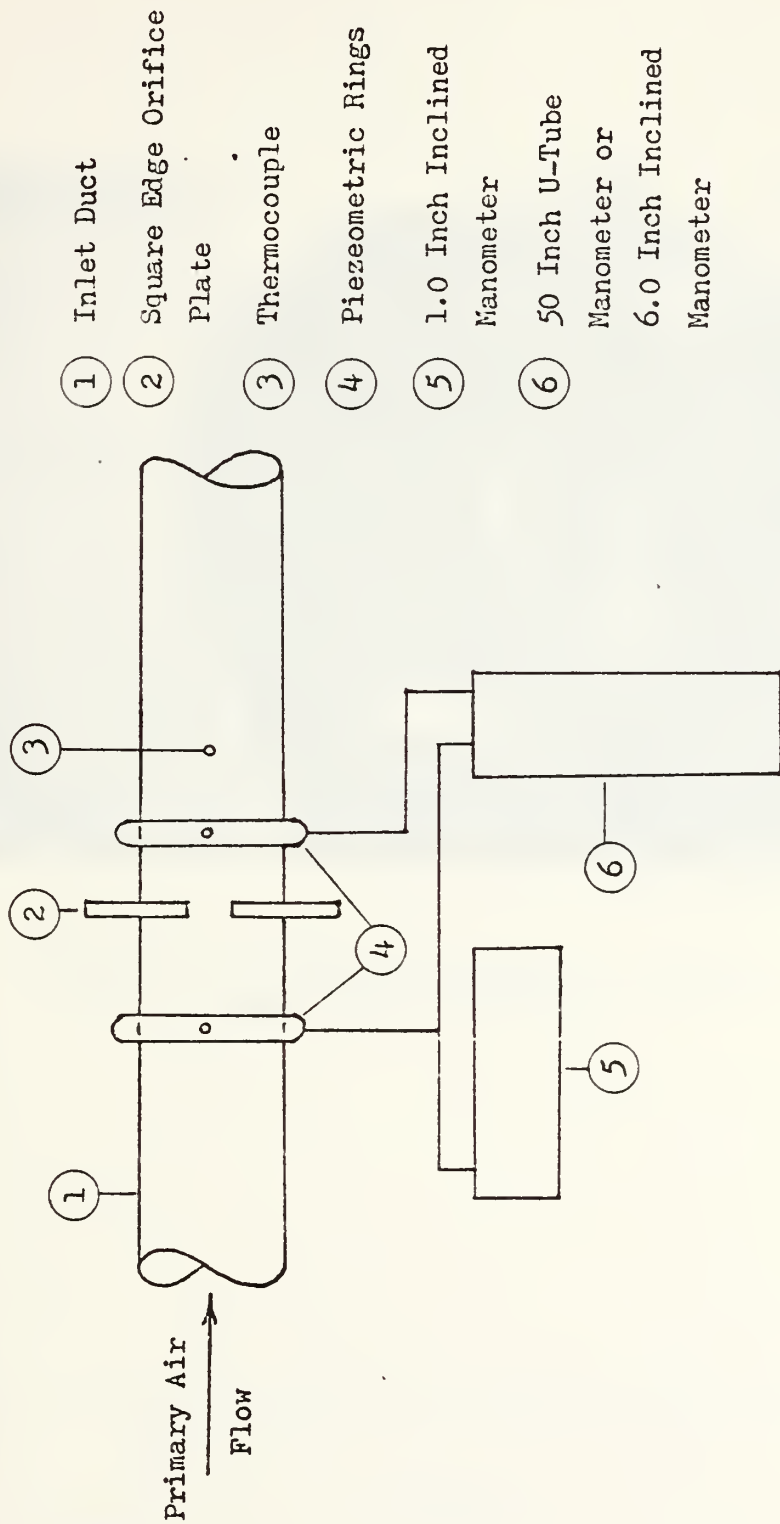


Figure 18. Schematic of Instrumentation for Primary Air Flow Measurement

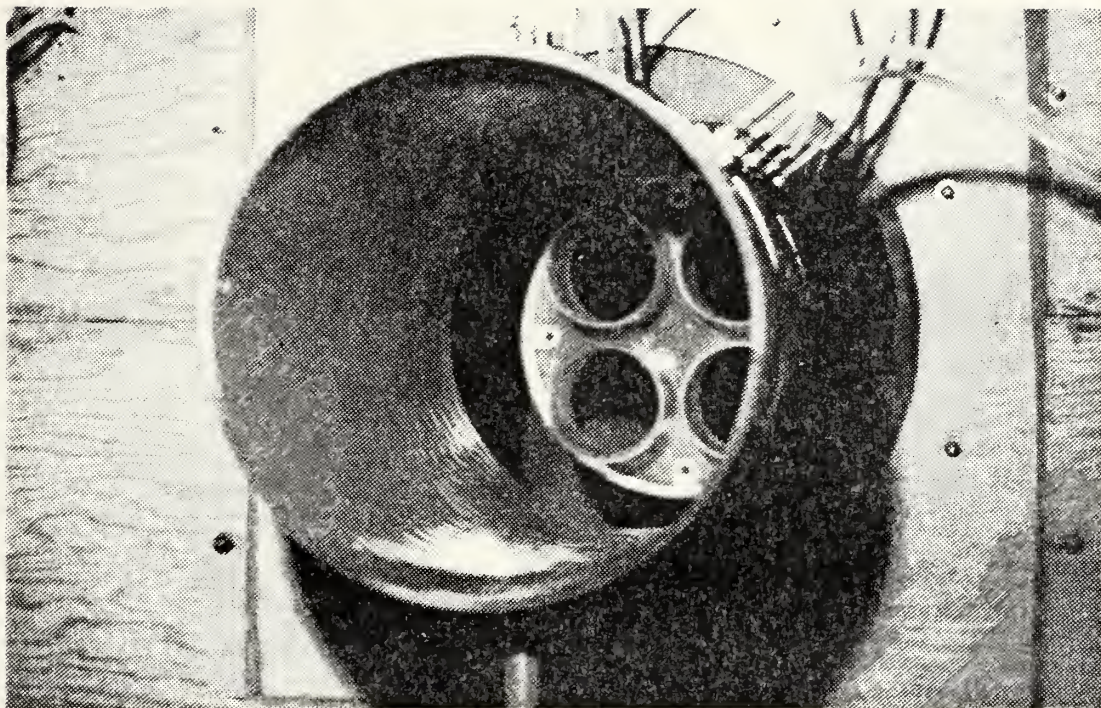


Figure 19. Mixing Stack with Pressure
Taps and Air Seal

EXPERIMENTAL PUMPING COEFFICIENT COMPARISON

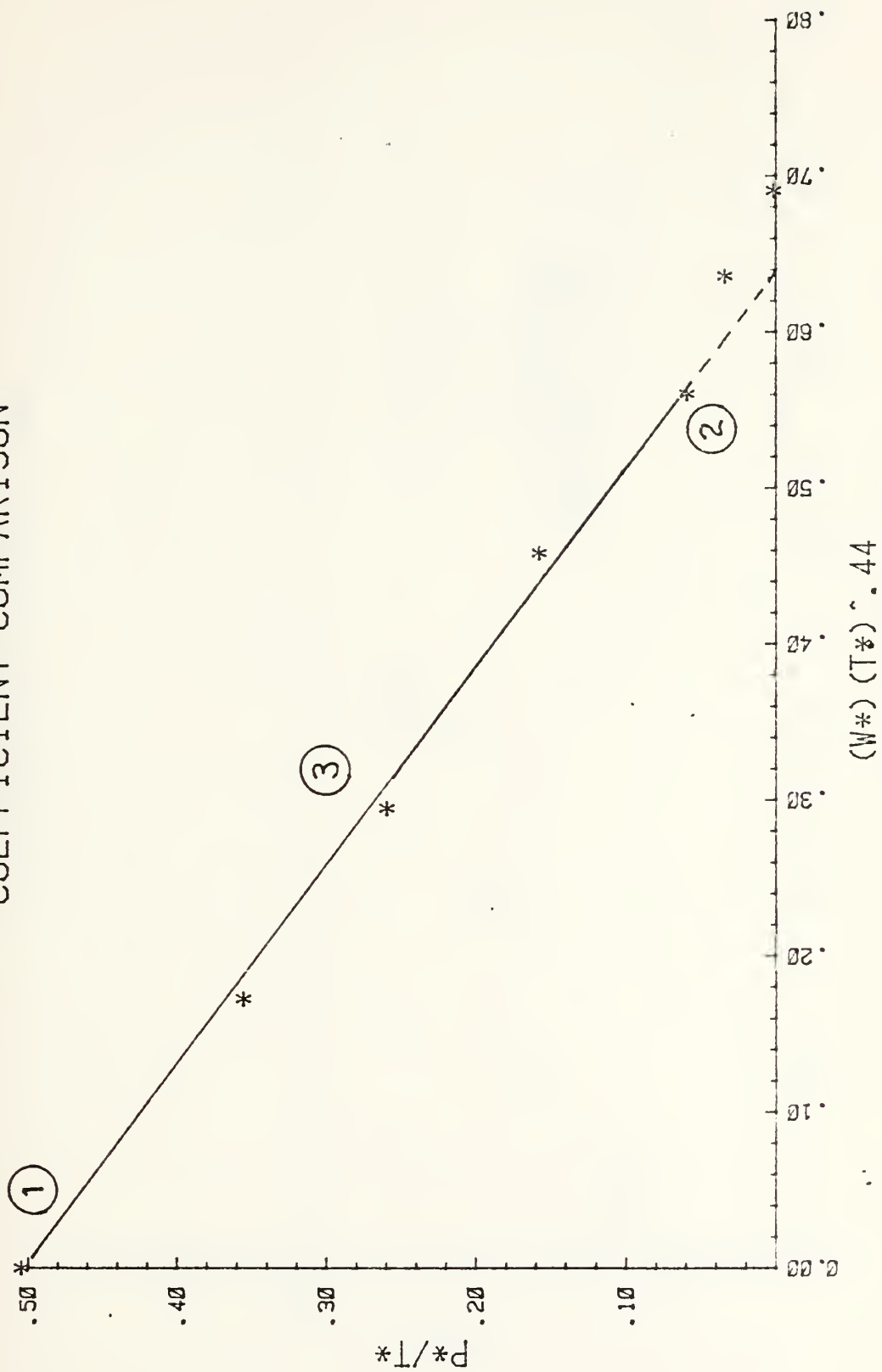


Figure 20. Sample Pumping Coefficient Plot

AXIAL PRESSURE DISTRIBUTION COMPARISON

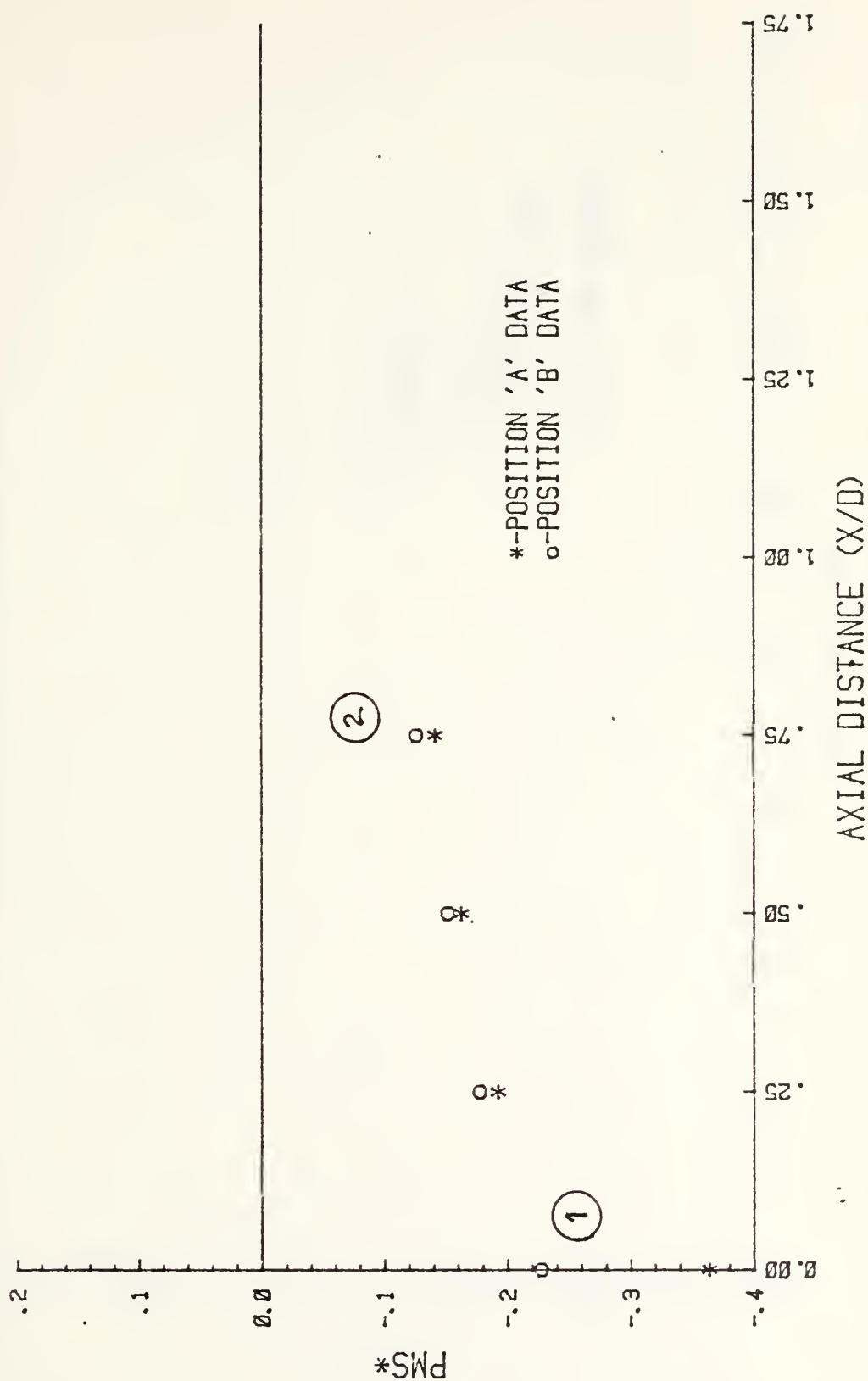


Figure 21. Sample Mixing Stack Pressure Distribution Plot

EXPERIMENTAL PUMPING COEFFICIENT COMPARISON

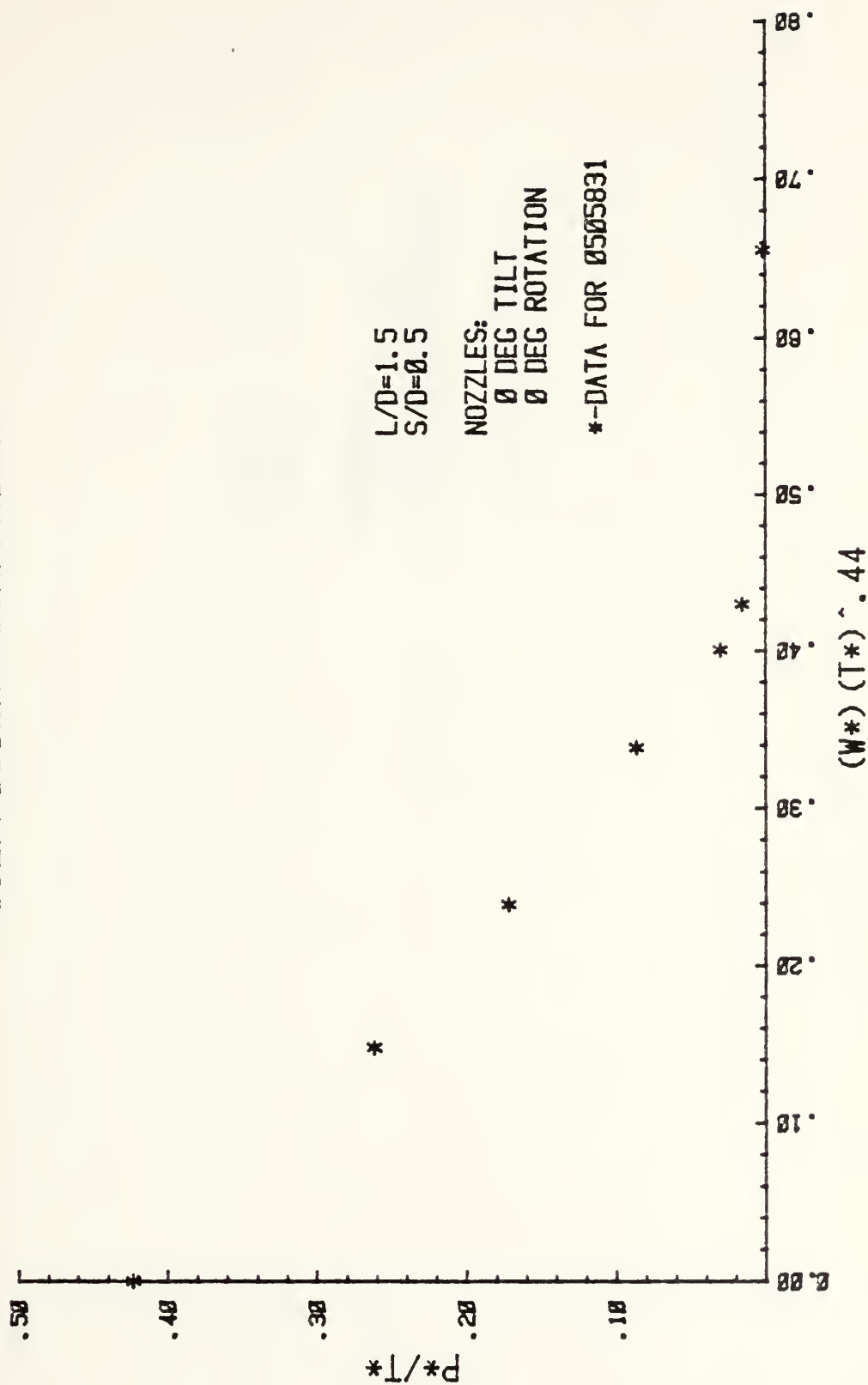


FIGURE 22 - PERFORMANCE PLOTS FOR $L/D = 1.5$ STRAIGHT NOZZLES, PCD (SECONDARY)

EXPERIMENTAL PUMPING COEFFICIENT COMPARISON

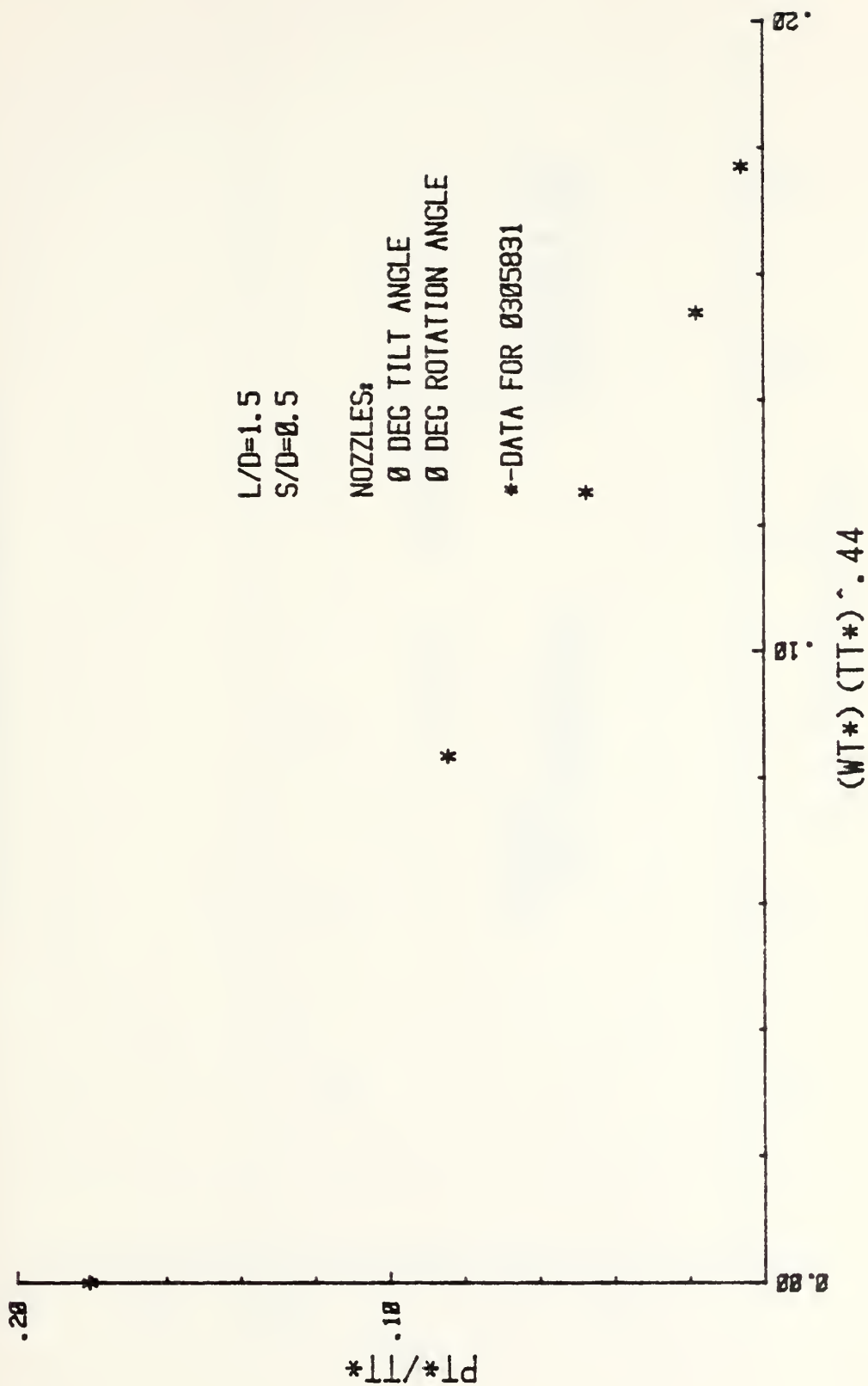


FIGURE 23 - PERFORMANCE PLOTS FOR L/D = 1.5 STRAIGHT NOZZLES, PCD (TERTIARY)

AXIAL PRESSURE DISTRIBUTION COMPARISON

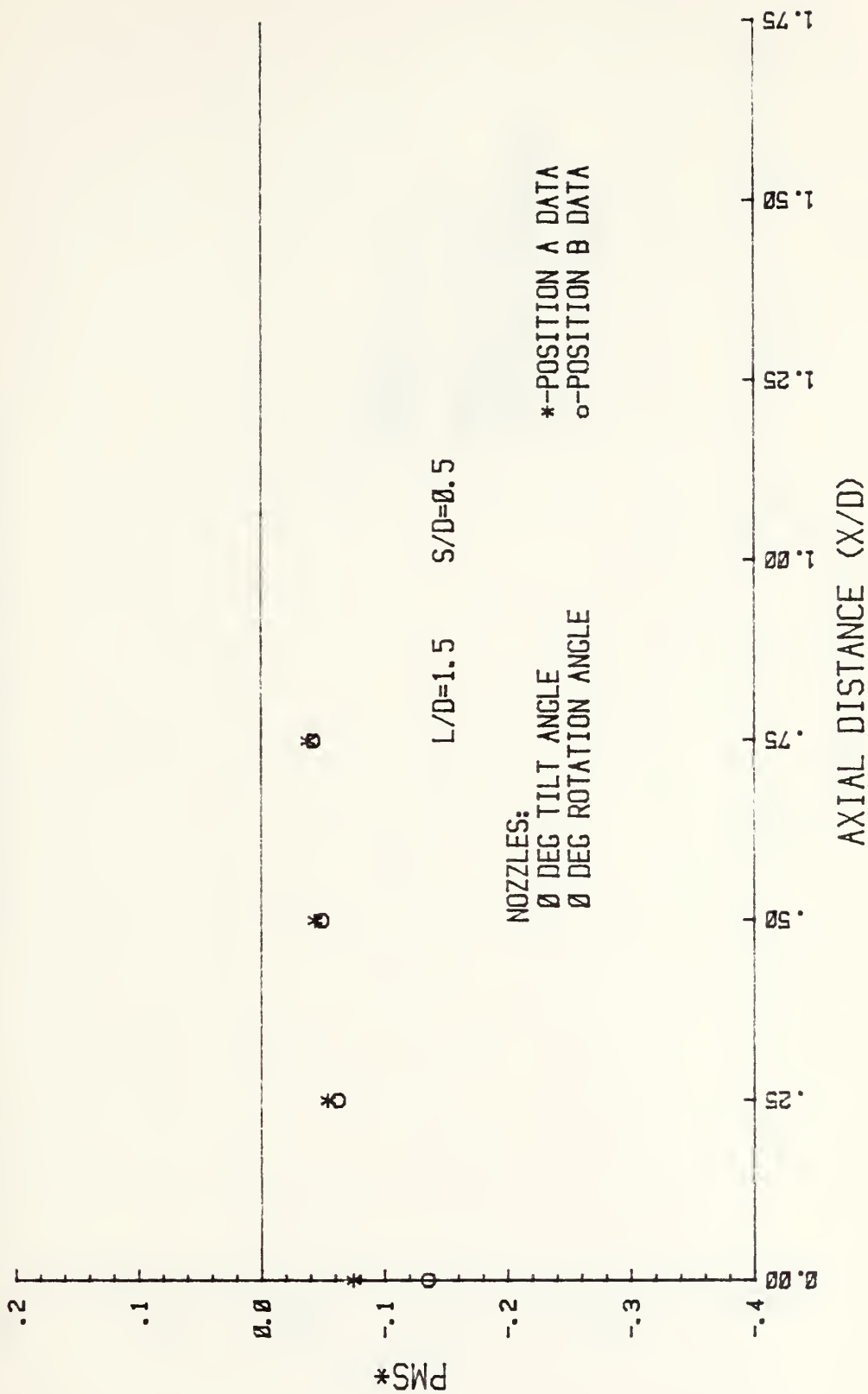


FIGURE 24 - PERFORMANCE PLOTS FOR L/D = 1.5 STRAIGHT NOZZLES, MSD

EXPERIMENTAL PUMPING COEFFICIENT COMPARISON

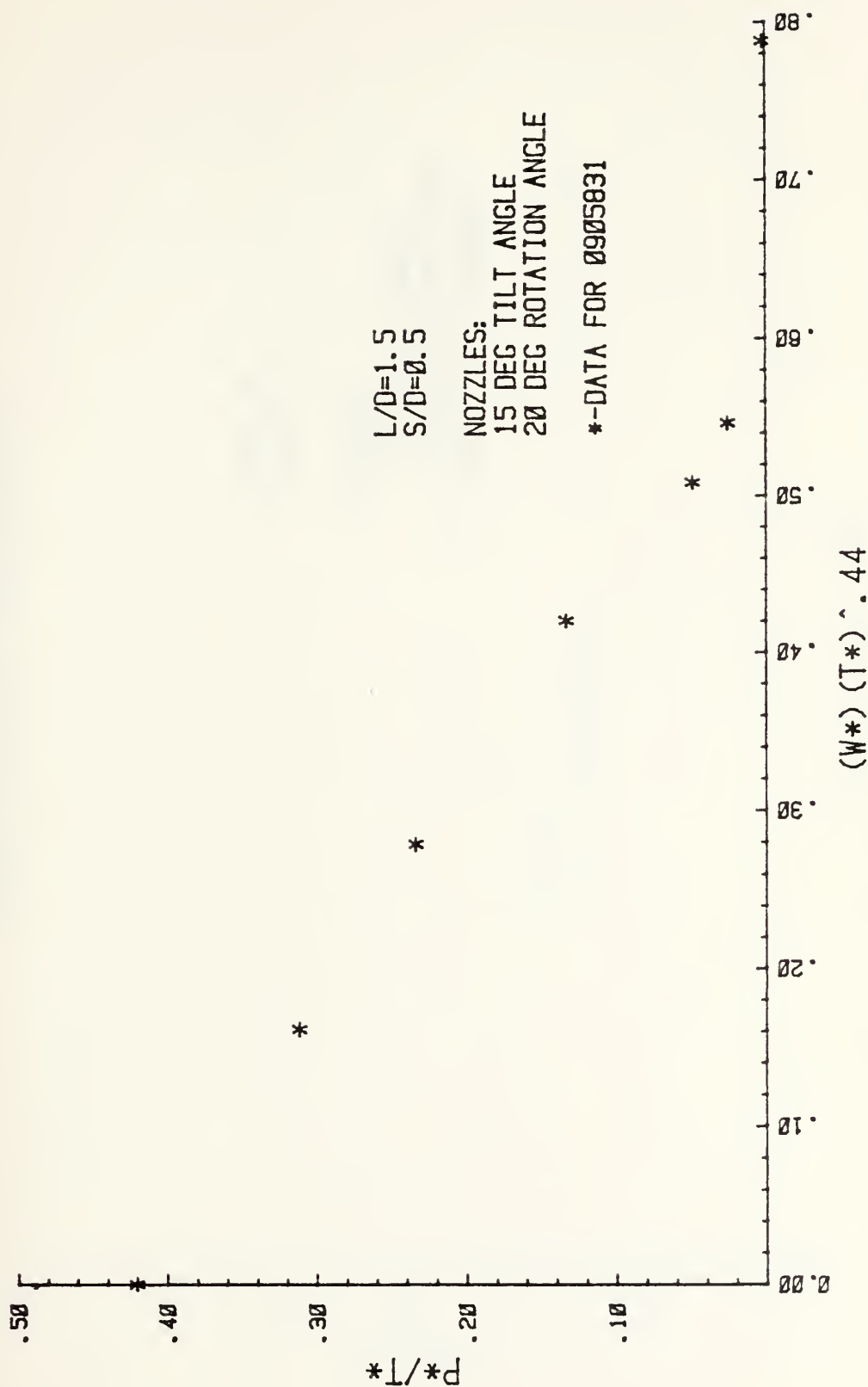


FIGURE 25 - PERFORMANCE PLOTS FOR $L/D = 1.5$ 15/20 NOZZLES, PCD (SECONDARY)

EXPERIMENTAL PUMPING COEFFICIENT COMPARISON

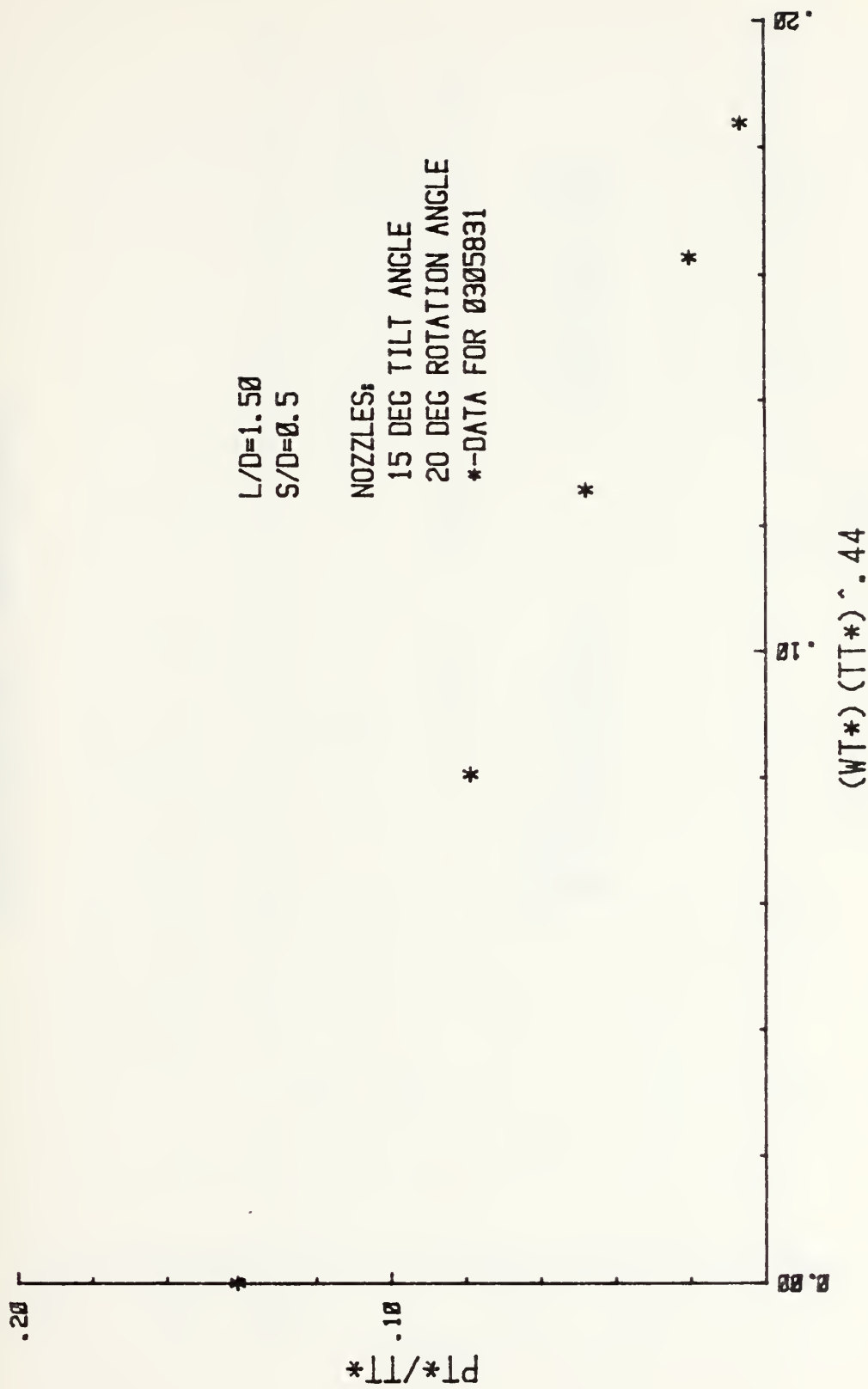


FIGURE 26 - PERFORMANCE PLOTS FOR $L/D = 1.5$ 15/20 NOZZLES, PCD (TERTIARY)

AXIAL PRESSURE DISTRIBUTION COMPARISON

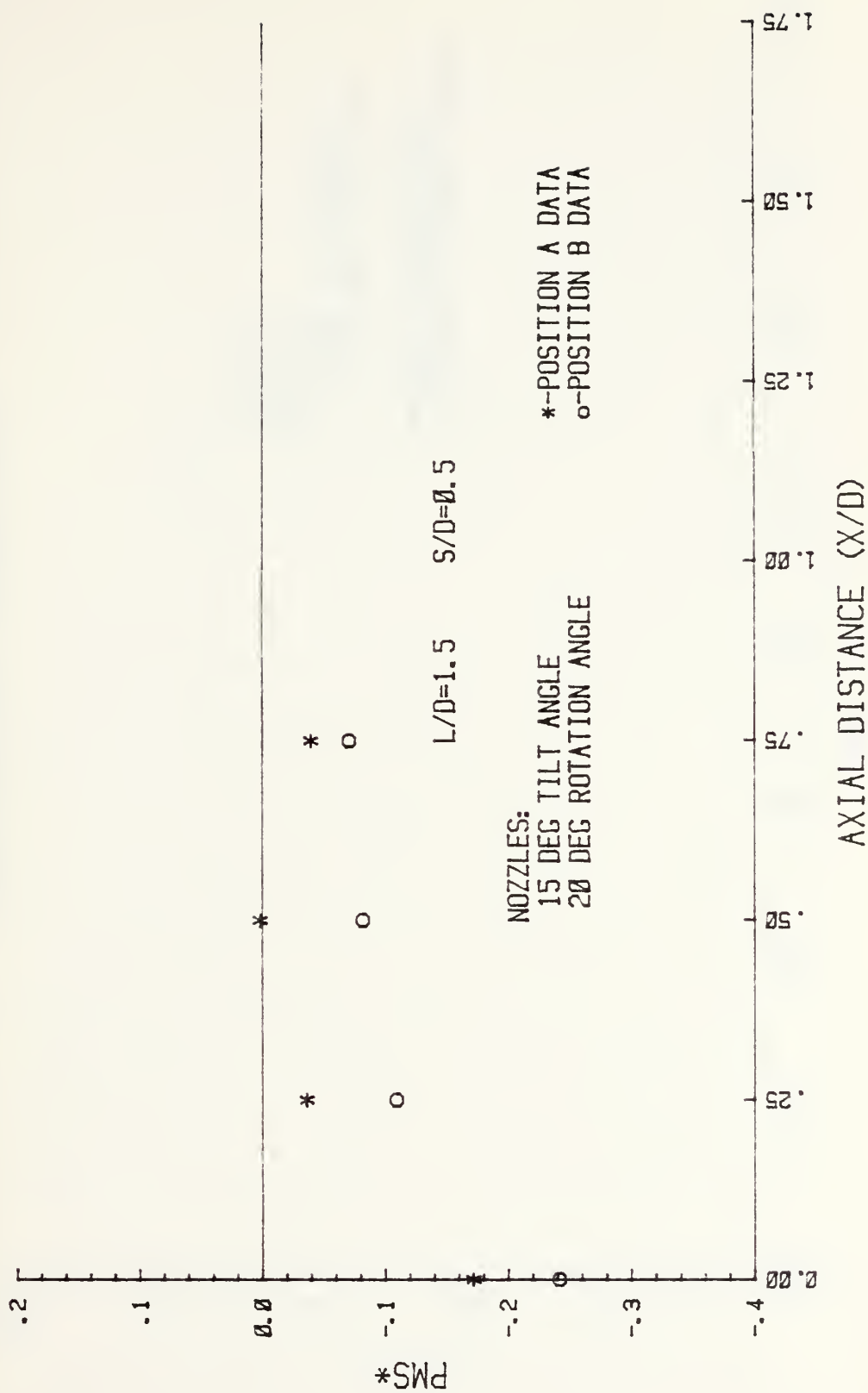


FIGURE 27 - PERFORMANCE PLOTS FOR L/D = 1.5 15/20 NOZZLES, MSD

EXPERIMENTAL PUMPING COEFFICIENT COMPARISON

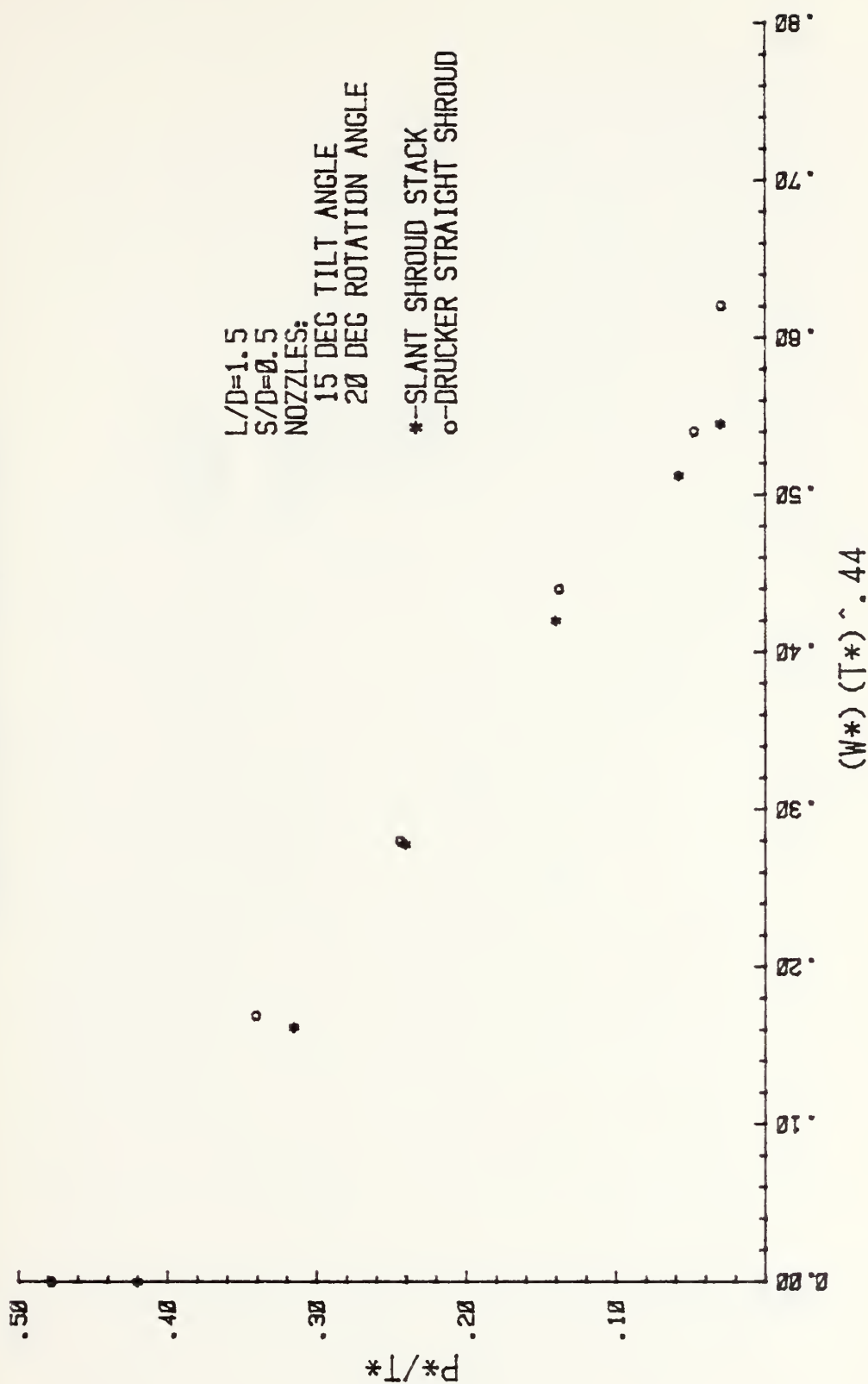


Figure 28. Performance Plot Comparison $L/D = 1.5$,
15/20 Nozzles, PCD (Secondary)

EXPERIMENTAL PUMPING COEFFICIENT COMPARISON

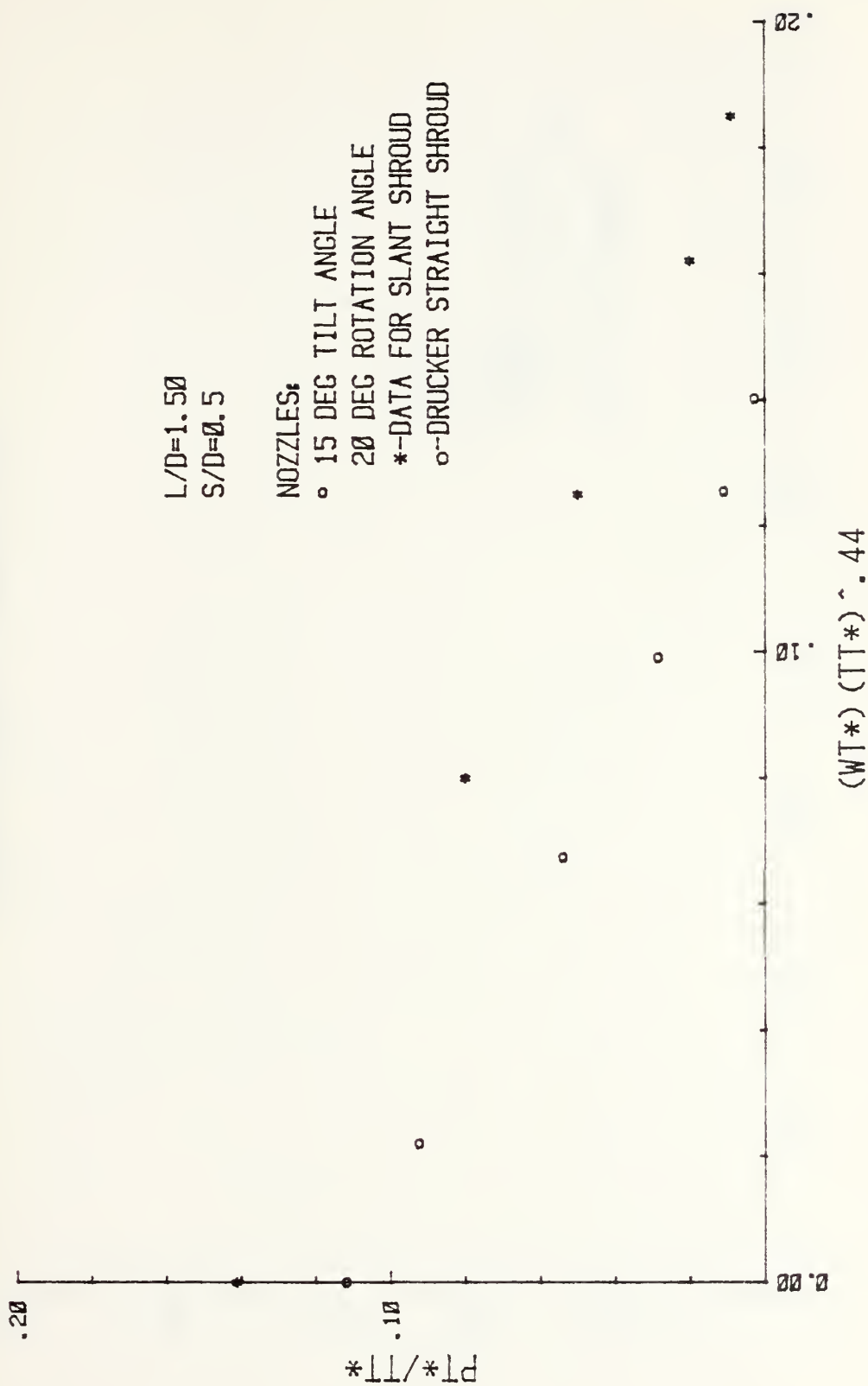


Figure 29. Performance Plot Comparison $L/D = 1.5$,
15/20 Nozzles, PCD (Tertiary)

EXPERIMENTAL PUMPING COEFFICIENT COMPARISON

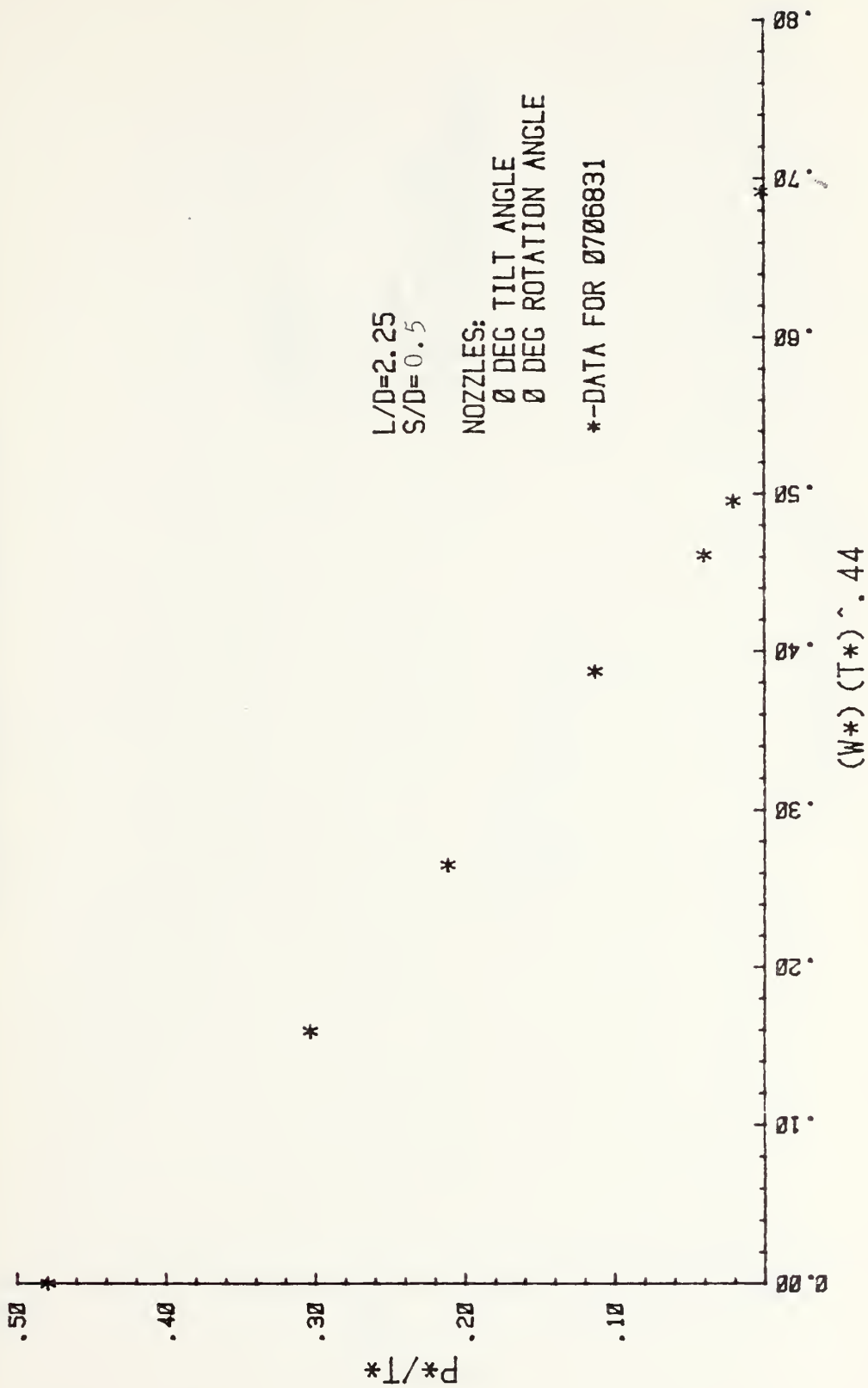


FIGURE 30. - PERFORMANCE PLOTS FOR $L/D = 2.25$, STRAIGHT NOZZLES, PCD (SECONDARY)

EXPERIMENTAL PUMPING COEFFICIENT COMPARISON

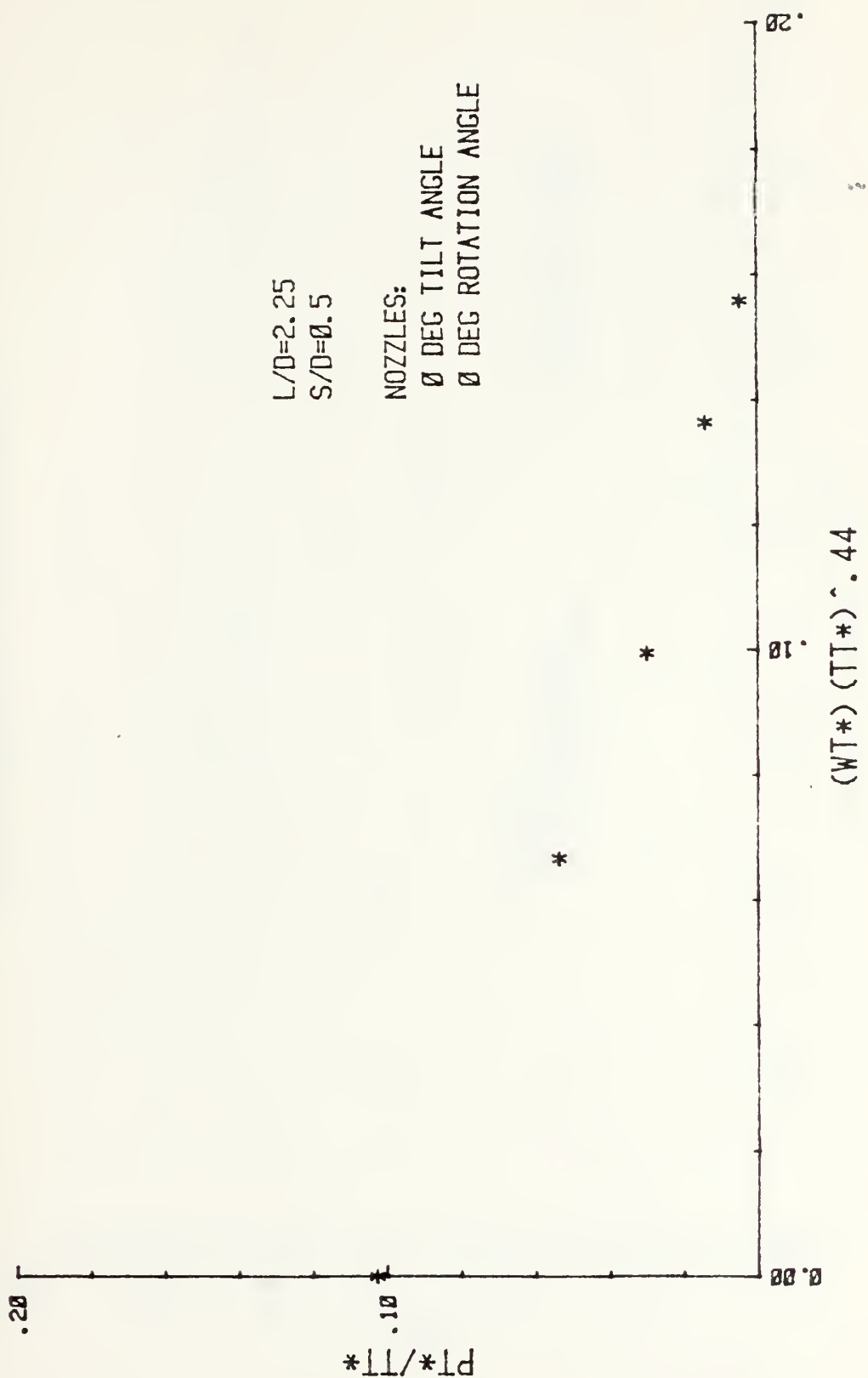


FIGURE 31 - PERFORMANCE PLOTS FOR $L/D = 2.25$ STRAIGHT NOZZLES, PCD (TERTIARY)

AXIAL PRESSURE DISTRIBUTION COMPARISON

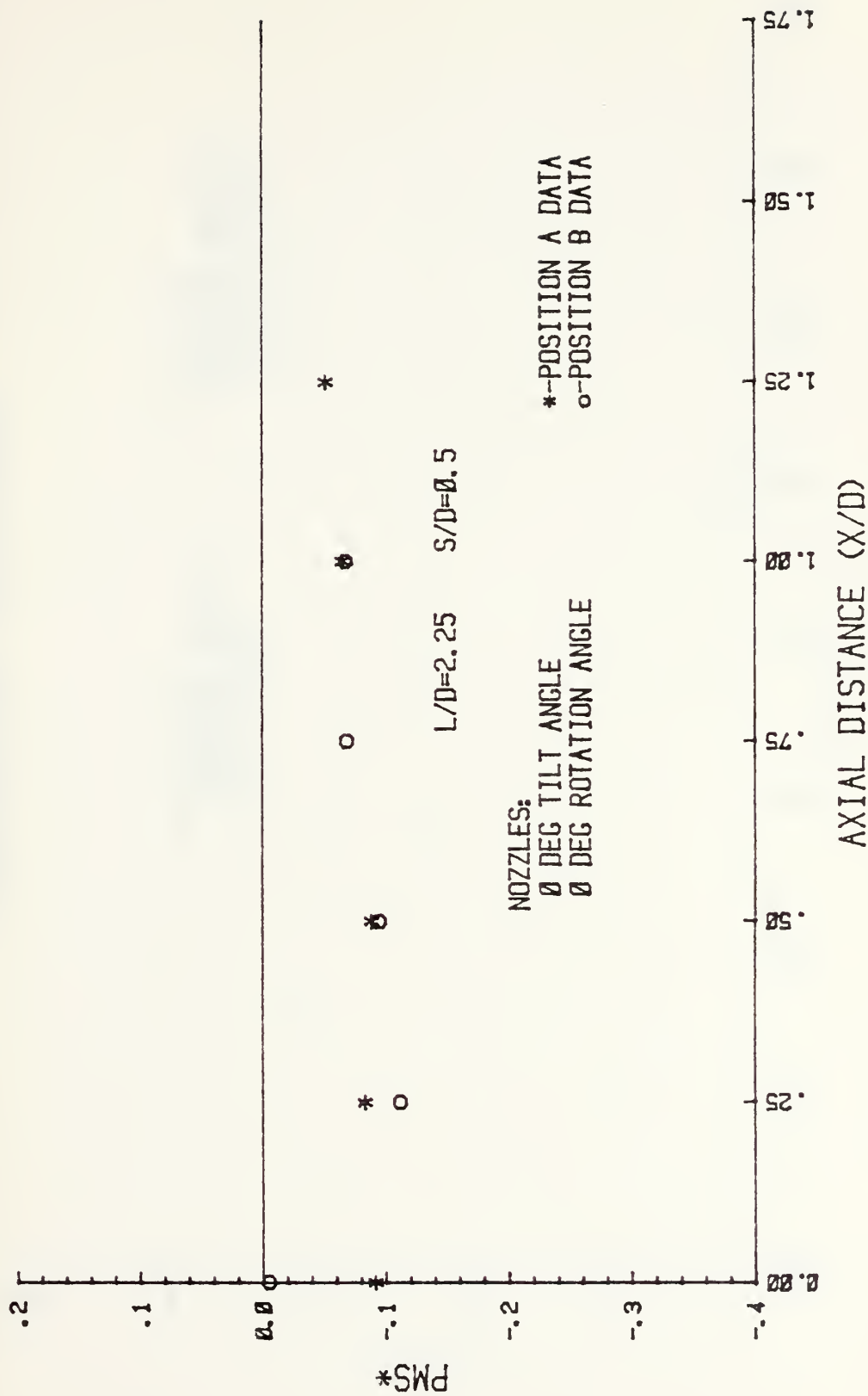


FIGURE 32 - PERFORMANCE PLOTS FOR L/D = 2.25 STRAIGHT NOZZLES, MSD

EXPERIMENTAL PUMPING COEFFICIENT COMPARISON

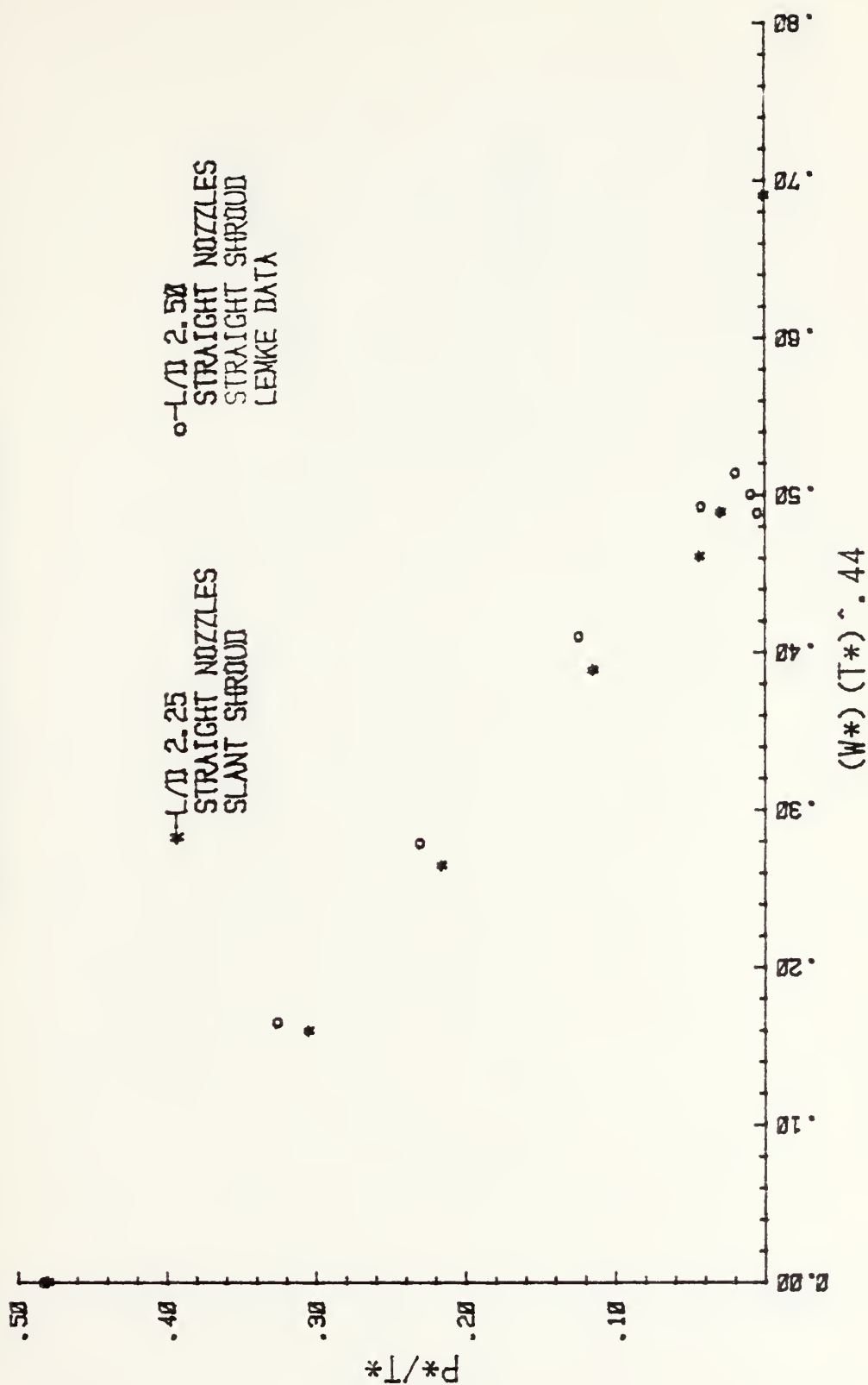


Figure 33. Performance Plot Comparison L/D = 2.5,
Straight Nozzles, PCD (Secondary)

EXPERIMENTAL PUMPING COEFFICIENT COMPARISON

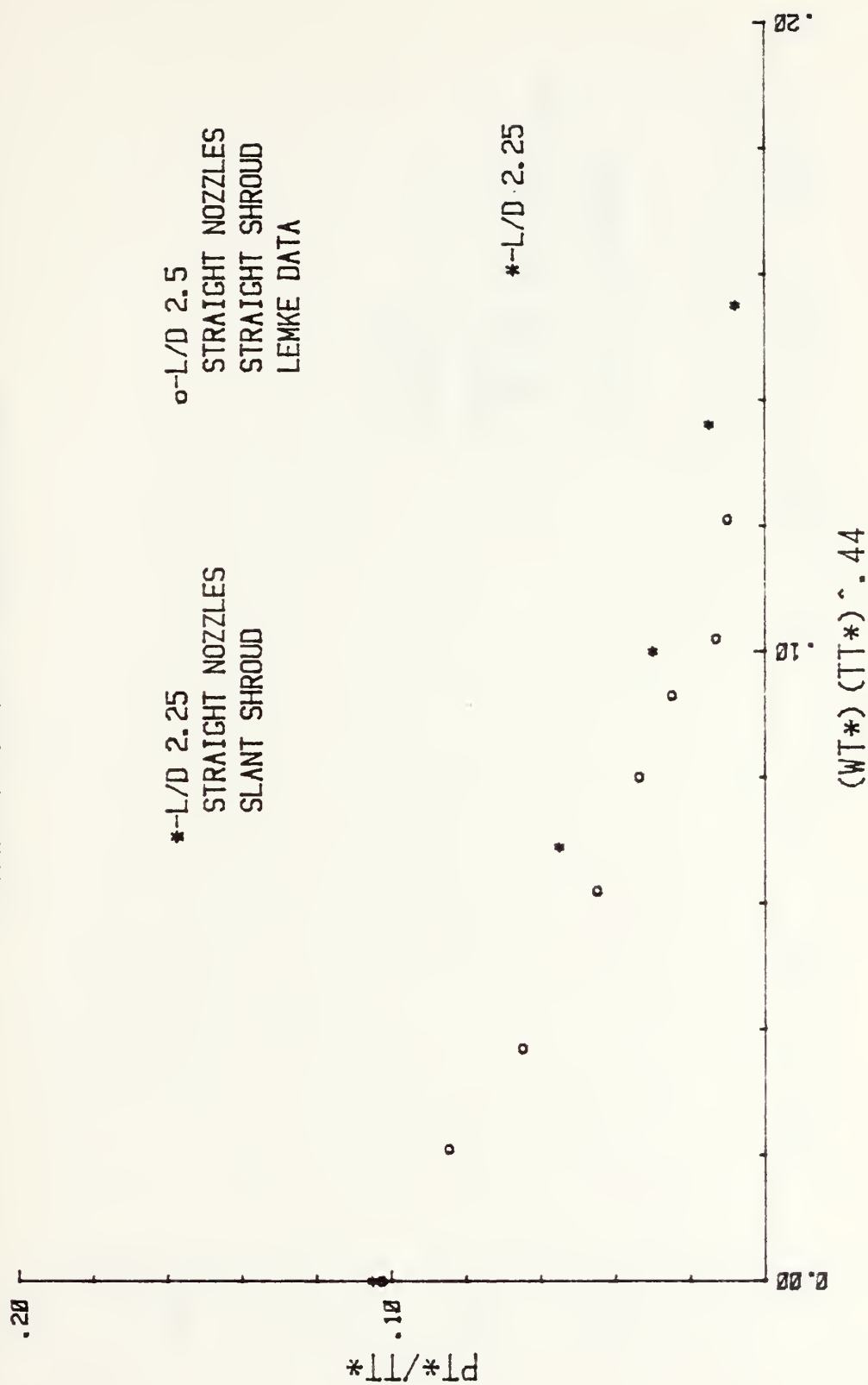


Figure 34. Performance Plot Comparison L/D = 2.5,
Straight Nozzles, PCD (Tertiary)

EXPERIMENTAL PUMPING COEFFICIENT COMPARISON

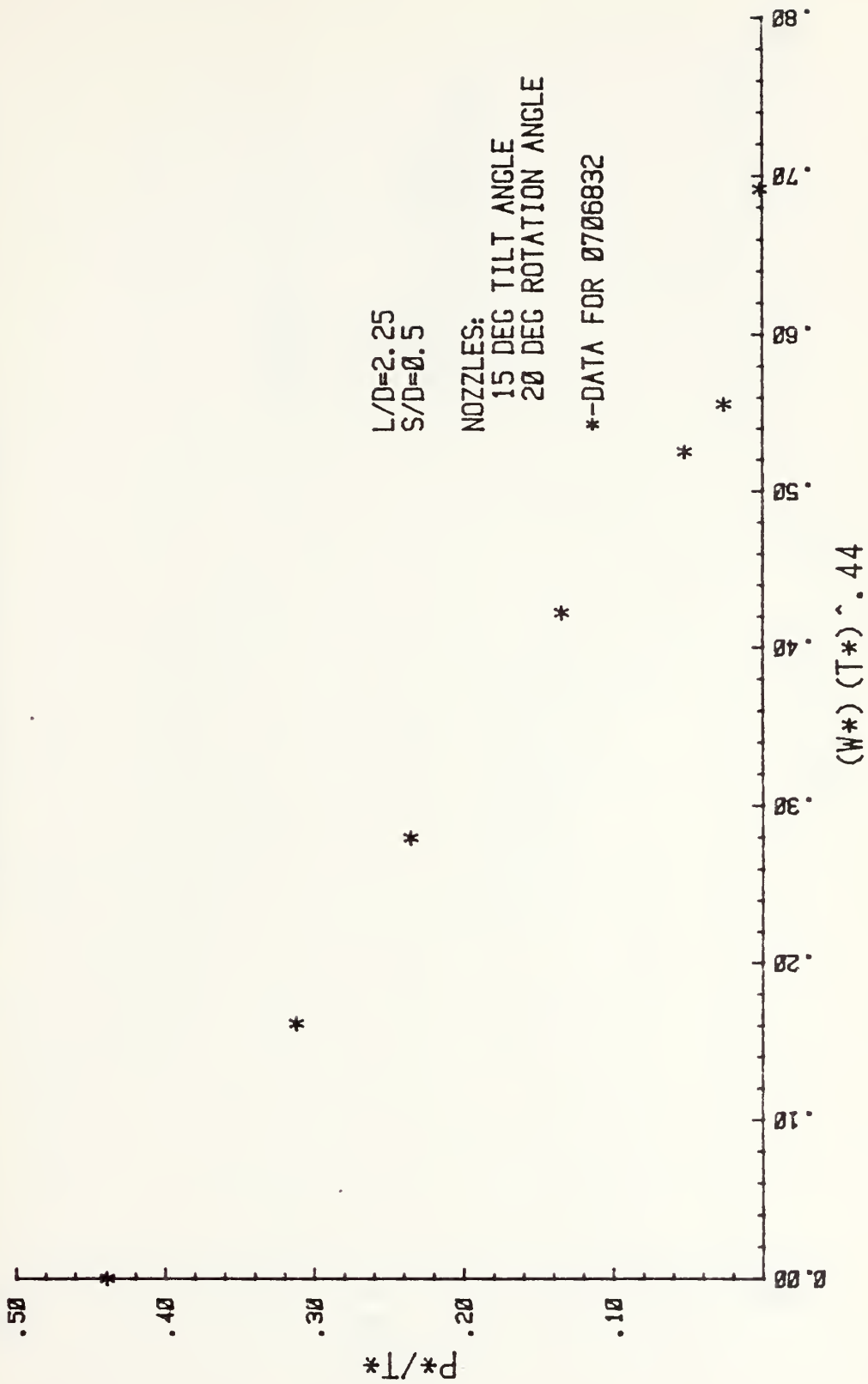


FIGURE 35 - PERFORMANCE PLOTS FOR $L/D = 2.25$ 15/20 NOZZLES, PCD (SECONDARY)

EXPERIMENTAL PUMPING COEFFICIENT COMPARISON

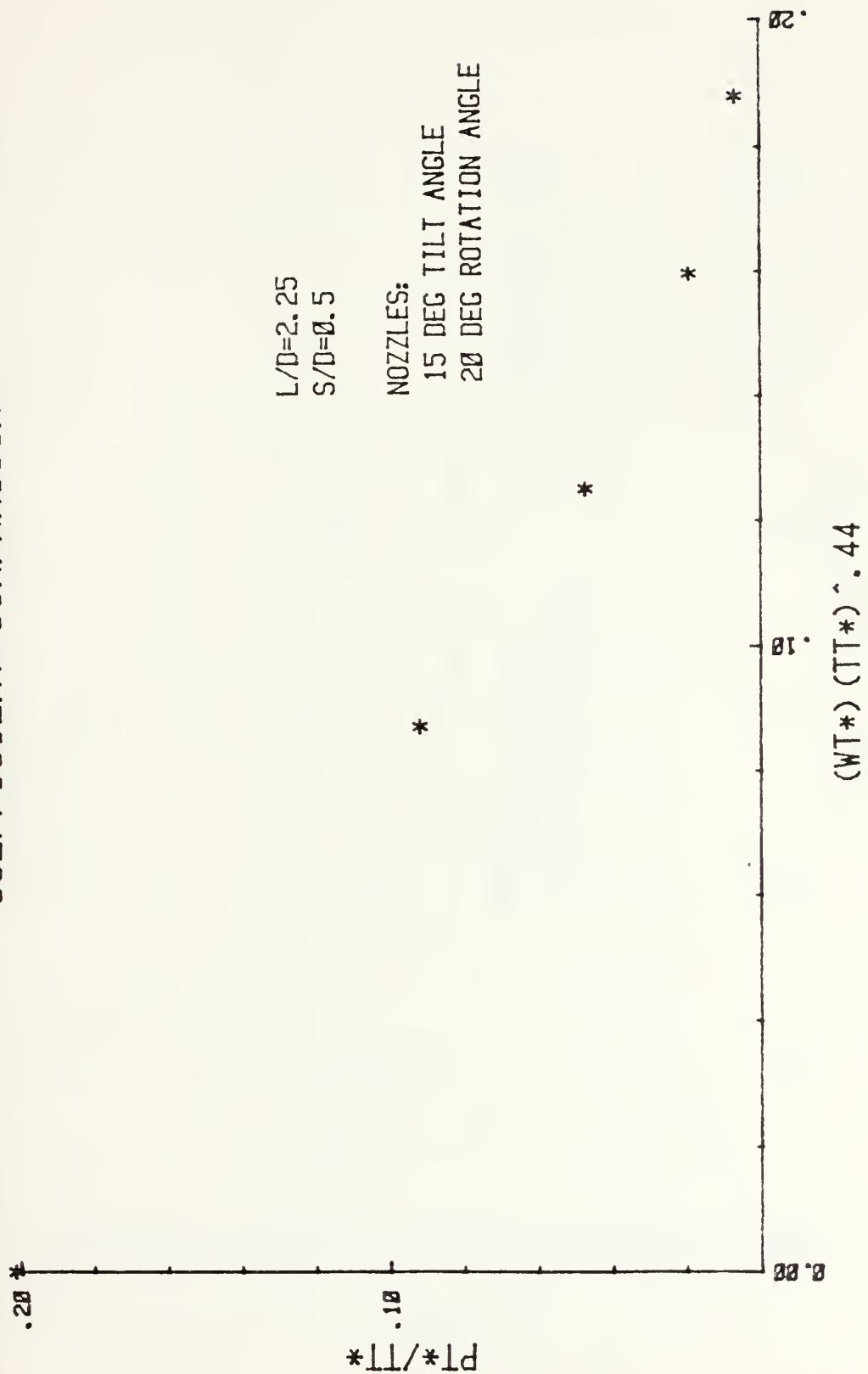


FIGURE 36 - PERFORMANCE PLOTS FOR L/D = 2.25 15/20 NOZZLES, PCD (TERTIARY)

AXIAL PRESSURE DISTRIBUTION COMPARISON

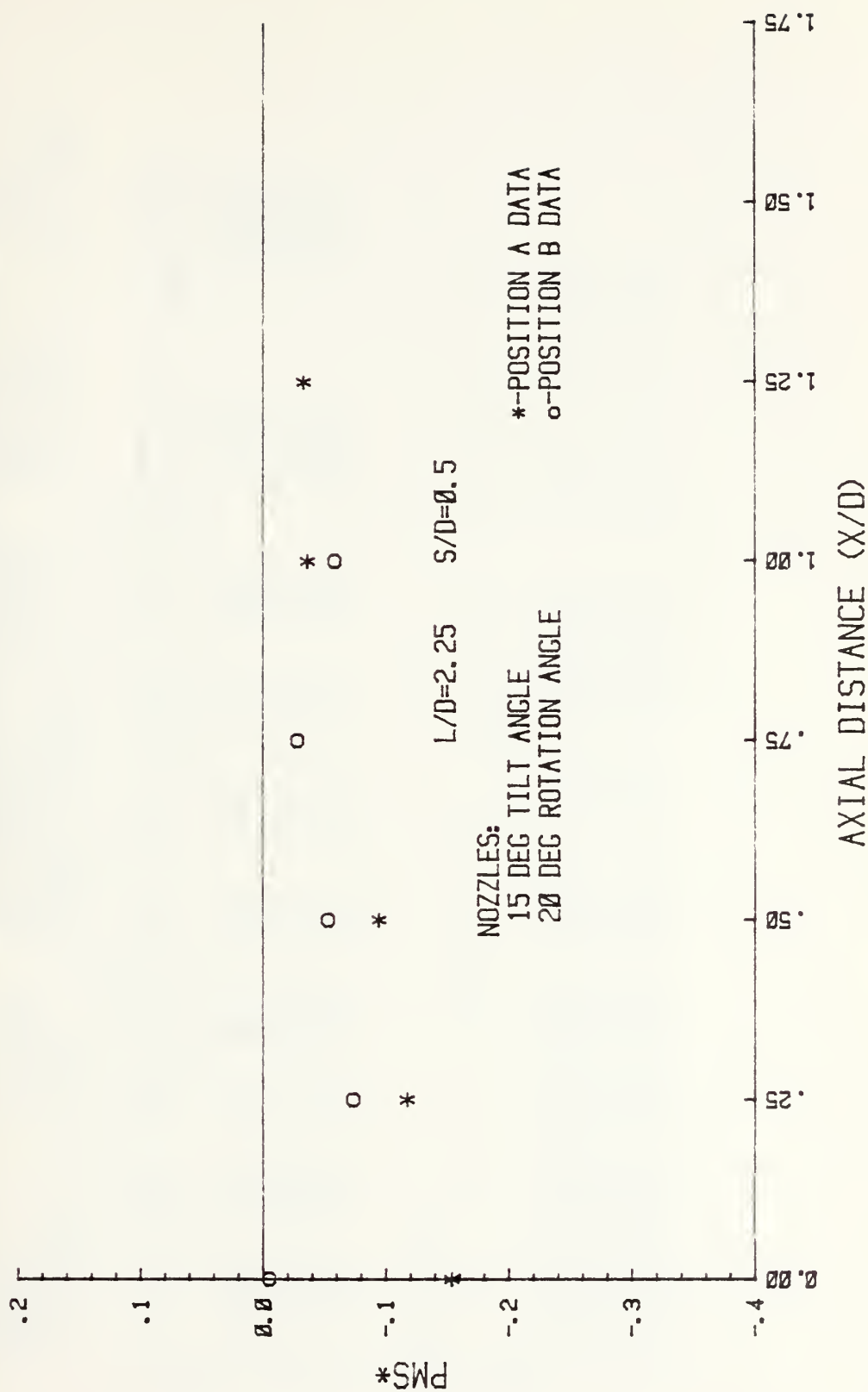


FIGURE 37 - PERFORMANCE PLOTS FOR L/D = 2.25 15/20 NOZZLES, MSD

DATA TAKEN ON: 05 MAY 83
 DATA TAKEN BY: N O PRITCHARD
 NOZZLE AM/AP AREA RATIO: 2.50
 COMMENTS:
 MIXING STACK INFORMATION:
 LENGTH: 17.55 [IN]
 DIAMETER: 11.70 [IN]
 L/D RATIO: 1.50
 S/D RATIO: 0.50
 PRIMARY NOZZLE INFORMATION:
 TILT ANGLE: 0.0 [DEG]
 ROTATION ANGLE: 0 [DEG]
 AREA PER NOZZLE: 10.752 [IN2]
 NUMBER OF NOZZLES: 4
 MISCELLANEOUS INFORMATION:
 ORIFICE DIAMETER: 6.902 [IN]
 ORIFICE BETA: 0.497
 UPTAKE AREA: 107.510 [IN2]
 ATM. PRESSURE: 30.18 [INHG]

N	POR	DPOR	TOR	TUPT	TAMB	PUPT	PSEC	PTER	SECONDARY AREA	TERTIARY AREA
RUN	IN OF H2O		DEGREES	F		IN OF H2O	SQUARE INCHES	SQUARE INCHES		
1	0.655	22.0	50.6	104.6	63.8	3.40	2.91	0.00	0.000	*****
2	0.655	22.0	51.2	105.0	64.0	4.50	1.79	0.00	12.566	*****
3	0.655	22.0	51.0	105.0	64.0	5.10	1.17	0.00	25.133	*****
4	0.655	22.0	51.0	105.0	64.8	5.60	0.59	0.00	50.265	*****
5	0.655	22.0	51.0	105.2	65.0	5.90	0.21	0.00	100.531	*****
6	0.655	22.0	51.0	105.2	65.2	6.00	0.11	0.00	150.796	*****
7	0.655	22.0	50.8	105.0	65.2	6.15	0.01	0.00	*****	*****

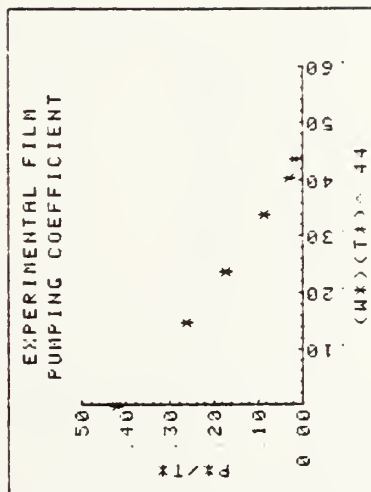
SECONDARY BOX

N	W#	P*	T*	P**T*	W**T*	44	W*	UP	UN	UUP	UPT	NACH
RUN							LBH/SEC	LBH/SEC	FT/SEC	FT/SEC	FT/SEC	
1	0.0000	0.3932	0.9277	0.4238	0.0000	3.7858	0.0000	180.01	72.01	72.01	0.062	
2	0.1529	0.2432	0.9274	0.2623	0.1479	3.7836	0.5787	179.54	81.96	71.82	0.062	
3	0.2473	0.1594	0.9274	0.1719	0.2392	3.7843	0.9357	179.30	88.13	71.73	0.062	
4	0.3509	0.0807	0.9288	0.0869	0.3397	3.7843	1.3279	179.05	94.93	71.63	0.061	
5	0.4186	0.0288	0.9288	0.0310	0.4052	3.7843	1.5841	178.95	99.40	71.59	0.061	
6	0.4544	0.0151	0.9292	0.0162	0.4399	3.7843	1.7195	178.90	101.77	71.57	0.061	
7	*****	0.0014	0.9295	0.0015	*****	3.7851	2.6988	178.83	*****	71.54	0.061	

TABLE 1. Shrouded Stack L/D = 1.5: Straight Nozzles

TERTIARY BOX

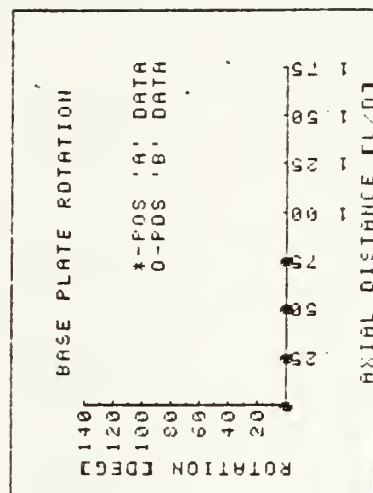
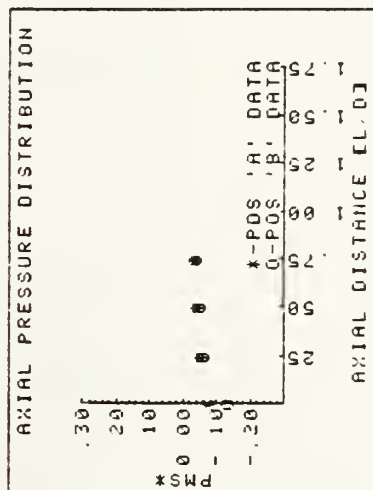
N	WT*	PT*	TT*	PT*/TT*	WT*TT^ 44	UM	WT	UE
RUN						LBM/SEC	LBM/SEC	FT/SEC
1	*****	0.0000	0.9277	0.0000	*****	3.786	*****	*****
2	*****	0.0000	0.9274	0.0000	*****	4.362	*****	*****
3	*****	0.0000	0.9274	0.0000	*****	4.720	*****	*****
4	*****	0.0000	0.9288	0.0000	*****	5.112	*****	*****
5	*****	0.0000	0.9288	0.0000	*****	5.368	*****	*****
6	*****	0.0000	0.9292	0.0000	*****	5.504	*****	*****
7	*****	0.0000	0.9295	0.0000	*****	*****	*****	*****



PCD

MIXING STACK DATA FOR RUN 7

TOP (POSITION 'A') DATA				DIAGONAL (POSITION 'B') DATA			
X/D	PRESSURE [IN H2O]	ROTATION [DEG]	PMS*	X/D	PRESSURE [IN H2O]	ROTATION [DEG]	PMS*
0.00	-0.545	0	-0.075	0.00	-0.950	0	-0.130
0.25	-0.395	0	-0.054	0.25	-0.420	0	-0.058
0.50	-0.321	0	-0.044	0.50	-0.328	0	-0.045
0.75	-0.280	0	-0.038	0.75	-0.275	0	-0.038



MSD

DATA TAKEN ON: 7 MAY 83
 DATA TAKEN BY: N O PRITCHARD

NOZZLE AM/AP AREA RATIO: 2.50

COMMENTS:

MIXING STACK INFORMATION:
 LENGTH: 17.55 [IN]
 DIAMETER: 11.70 [IN]
 L/D RATIO: 1.50
 S/D RATIO: 0.50

PRIMARY NOZZLE INFORMATION:
 TILT ANGLE: 0.0 [DEG]
 ROTATION ANGLE: 0 [DEG]
 AREA PER NOZZLE: 10.752 [IN2]
 NUMBER OF NOZZLES: 4

MISCELLANEOUS INFORMATION:
 ORIFICE DIAMETER: 6.902 [IN]
 ORIFICE BETA: 0.497
 UPTAKE AREA: 107.510 [IN2]
 ATM. PRESSURE: 30.08 [INHG]

N	POR	DPOR	TOR	TUPT	TAMB	PUP	PSEC	PTER	SECONDARY AREA	TERTIARY AREA
RUN	IN OF H2O	DEGREES	F	IN OF H2O	SQUARE INCHES	SQUARE INCHES				
1	0.675	22.0	54.2	107.4	70.0	6.10	0.01	0.23	785.000	0.000
2	0.675	22.0	54.2	107.5	70.0	6.10	0.01	0.16	785.000	12.566
3	0.675	22.0	54.2	107.8	70.8	6.10	0.01	0.10	785.000	25.133
4	0.675	22.0	54.2	108.0	71.0	6.10	0.01	0.06	785.000	50.265
5	0.675	22.0	54.2	108.3	71.6	6.10	0.01	0.02	785.000	100.531
6	0.675	22.0	55.4	108.6	72.2	6.10	0.01	0.02	785.000	100.531

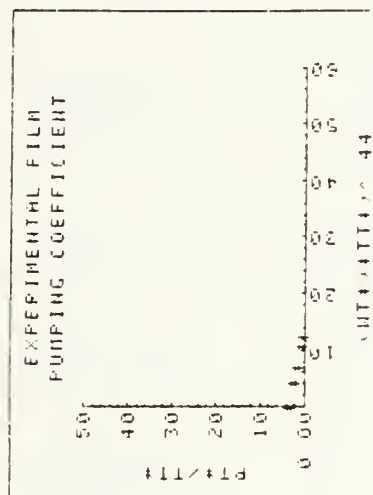
SECONDARY BOX

N	W*	P*	T*	P*/T*	W*/T*	44	UP	NS	UP	UM	UUP	UPT	MACH
RUN	LBM/SEC	LBM/SEC	FT/SEC	FT/SEC	FT/SEC	FT/SEC	FT/SEC	FT/SEC	FT/SEC	FT/SEC	FT/SEC	FT/SEC	FT/SEC
1	0.0014	0.0014	0.9340	0.0015	0.0015	3.7662	2.6821	179.29	0.061	71.72	0.061	0.061	
2	0.0014	0.0014	0.9353	0.0015	0.0015	3.7662	2.6801	179.32	0.061	71.73	0.061	0.061	
3	0.0014	0.0014	0.9348	0.0015	0.0015	3.7662	2.6801	179.41	0.061	71.77	0.061	0.061	
4	0.0014	0.0014	0.9348	0.0015	0.0015	3.7662	2.6796	179.48	0.061	71.80	0.061	0.061	
5	0.0014	0.0014	0.9354	0.0015	0.0015	3.7662	2.6781	179.57	0.061	71.84	0.061	0.061	
6	0.0014	0.0014	0.9359	0.0015	0.0015	3.7613	2.6766	179.46	0.061	71.79	0.061	0.061	

Tertiary

TERTIARY BOX

W	WT#	PT#	YT#	PT#	YT#	WT	UE
RUN							
						LBW/SEC	LBW/SEC FT/SEC
1	0	0000	0	0318	0	9340	0 0341
2	0	0456	0	0222	0	9353	0 0237
3	0	0720	0	0138	0	9348	0 0148
4	0	1116	0	0083	0	9348	0 0089
5	0	1288	0	0028	0	9354	0 0030
6	0	0000	0	0028	0	9359	0 0030



Tertiary

DATA TAKEN ON 02 MAY 83
DATA TAKEN BY: N D PRITCHARD

MIXING STACK INFORMATION:

LENGTH: 17.55 [IN]
DIAMETER: 11.70 [IN]
L/D RATIO: 1.50
S/D RATIO: 0.50

NOZZLE ANGLE 2.50

PRIMARY NOZZLE INFORMATION

TILT ANGLE: 15.0 [DEG]
ROTATION ANGLE: 20 [DEG]
AREA PER NOZZLE: 10.752 [IN2]
NUMBER OF NOZZLES: 4

MISCELLANEOUS INFORMATION
ORIFICE DIAMETER: 6.902 [IN]
ORIFICE BETA: 0.497
UPTAKE AREA: 107.510 [IN2]
ATM. PRESSURE: 30.20 [INHG]

RUH	N	FOR	IN OF H2O	TOR	TUFT	TAMB	PUPT	PSEC	PTER	SECONDARY AREA		TERTIARY AREA	
										SQUARE INCHES	SQUARE INCHES	SQUARE INCHES	SQUARE INCHES
1	0	655	22.0	53.6	108.2	69.8	4.15	2.45	0.00	0.000	0.000	0.000	0.000
2	0	665	22.0	54.4	108.2	69.4	4.75	1.71	0.00	12.566	12.566	12.566	12.566
3	0	665	22.0	54.8	108.2	69.0	5.10	1.26	0.00	25.133	25.133	25.133	25.133
4	0	665	22.0	54.8	108.2	68.6	5.50	0.74	0.00	50.265	50.265	50.265	50.265
5	0	660	22.0	54.6	108.4	68.6	5.90	0.29	0.00	100.531	100.531	100.531	100.531
6	0	660	22.0	55.0	108.4	68.6	6.00	0.15	0.00	150.796	150.796	150.796	150.796
7	0	660	22.0	54.8	108.6	68.6	6.05	0.01	0.00	0.000	0.000	0.000	0.000

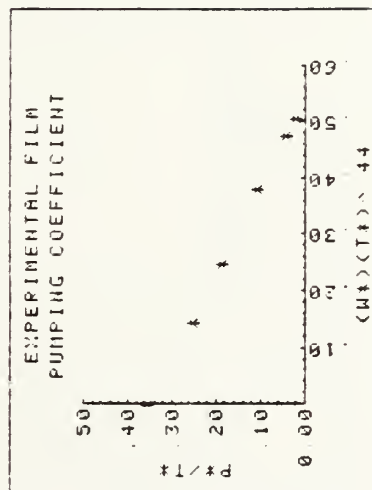
SECONDARY BOX

N	W*	P*	T*	P*/T*	W*/T*	HP	WS	UP	UM		UPT	
									LBN/SEC	FT/SEC	FT/SEC	FT/SEC
1	0 0000	0 3333	0 9324	0 3575	0 0000	3 7760	0 0000	180 37	72 15	72 15	0 062	
2	0 1490	0 2330	0 9317	0 2501	0 1444	3 7730	0 5621	179 89	81 91	71 96	0 062	
3	0 2563	0 1726	0 9310	0 1854	0 2484	3 7715	0 9667	179 63	89 95	71 86	0 062	
4	0 3922	0 1011	0 9303	0 1087	0 3793	3 7723	1 4793	179 40	97 90	71 77	0 061	
5	0 4928	0 0400	0 9299	0 0430	0 4773	3 7723	1 8591	179 30	104 57	71 73	0 061	
6	0 5220	0 0199	0 9299	0 0214	0 5056	3 7708	1 9684	179 17	106 45	71 68	0 061	
7	*****	0 0016	0 9296	0 0018	*****	3 7716	2 9479	179 21	*****	71 69	0 061	

Table 2. Shrouded Stack L/D = 1.5: 15-20 Nozzles

TERTIARY BOX

RUN	N	WT	PT	TT	TT	WTATT	44	WM	WT	UE
								LBN/SEC	LBN/SEC	FT. SEC
1	*****	0.0000	0.9324	0.0000	*****	3.776	*****	*****	*****	*****
2	*****	0.0000	0.9317	0.0000	*****	4.335	*****	*****	*****	*****
3	*****	0.0000	0.9310	0.0000	*****	4.738	*****	*****	*****	*****
4	*****	0.0000	0.9303	0.0000	*****	5.251	*****	*****	*****	*****
5	*****	0.0000	0.9299	0.0000	*****	5.631	*****	*****	*****	*****
6	*****	0.0000	0.9299	0.0000	*****	5.739	*****	*****	*****	*****
7	*****	0.0000	0.9296	0.0000	*****	*****	*****	*****	*****	*****



PCD

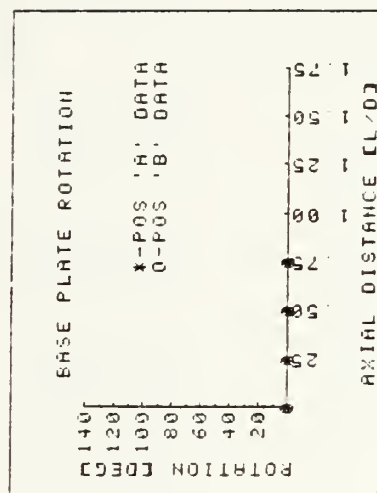
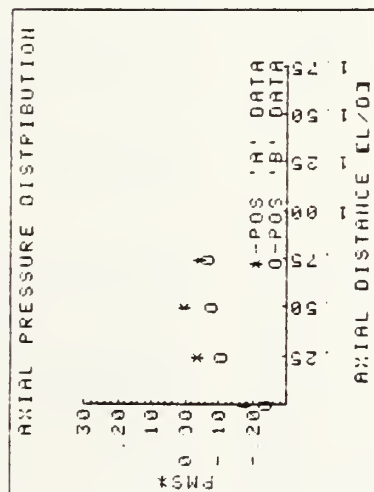
MINING STACK DATA FOR RUN 7

TOP (POSITION 'A') DATA

X/D	PRESSURE [IN H2O]	ROTATION [DEG]	PMS*
0.00	-1.250	0	-0.172
0.25	-0.265	0	-0.036
0.50	0.010	0	0.001
0.75	-0.290	0	-0.040

DIAGONAL (POSITION 'B') DATA

X/D	PRESSURE [IN H2O]	ROTATION [DEG]	PMS*
0.00	-1.720	0	-0.236
0.25	-0.760	0	-0.104
0.50	-0.560	0	-0.077
0.75	-0.480	0	-0.066



MSD

DATA TAKEN ON 03 MAY 83
 DATA TAKEN BY: N O PRITCHARD

NOZZLE AN/AP AREA RATIO 2 50

COMMENTS:

MIXING STAGE INFORMATION
 LENGTH: 17 55 [IN]
 DIAMETER: 11 70 [IN]
 L/D RATIO: 1 50
 S/D RATIO: 0 50

PRIMARY NOZZLE INFORMATION
 TILT ANGLE 15 0 [DEG]
 ROTATION ANGLE 20 [DEG]
 AREA PER NOZZLE: 10 752 [IN2]
 NUMBER OF NOZZLES: 4

MISCELLANEOUS INFORMATION
 ORIFICE DIAMETER 6 902 [IN]
 ORIFICE BETA 0 497
 UPTAKE AREA: 107 510 [IN2]
 ATM PRESSURE: 30 28 [INHG]

N	FOR	DFOR	TOR	TUPT	TAMB	PUPT	PSEC	PTER	SECONDARY AREA SQUARE INCHES	TERTIARY AREA SQUARE INCHES
RUN	IN OF H2O	DEGREES F					IN OF H2O			
1	0 660	22 0	63 0	114 8	78 8	5 90	0 01	0 95	785 000	0 000
2	0 660	22 0	61 2	114 6	79 4	5 92	0 01	0 53	785 000	12 566
3	0 660	22 0	60 0	114 0	79 8	5 98	0 01	0 32	785 000	25 133
4	0 660	22 0	61 6	114 4	80 2	6 00	0 01	0 14	795 000	50 265
5	0 660	22 0	63 0	115 0	80 4	5 98	0 01	0 04	785 000	100 531
6	0 660	22 0	63 2	116 0	81 0	6 00	0 01	0 03	*****	*****

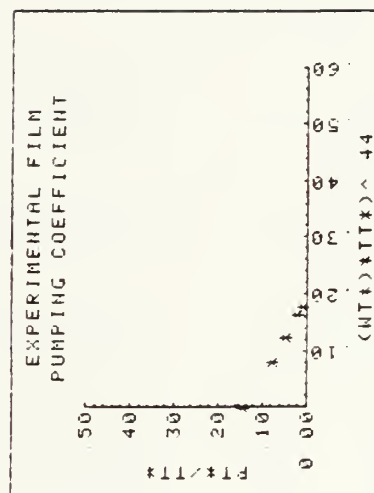
SECONDARY BOX

N	W*	P*	T*	P*/T*	WKT*	44	UP	WS	UP	UM	UUPT	UPT	NACH
RUN					LBM/SEC	LBM/SEC	FT/SEC	LBM/SEC	FT/SEC	FT/SEC	FT/SEC		
1	*****	0 0014	0 9373	0 0015	*****	3 7468	2 6689	179 50	*****	71 81	0 061		
2	*****	0 0014	0 9387	0 0015	*****	3 7533	2 6674	179 75	*****	71 91	0 061		
3	*****	0 0014	0 9404	0 0015	*****	3 7576	2 6665	179 77	*****	71 91	0 061		
4	*****	0 0014	0 9404	0 0015	*****	3 7519	2 6655	179 62	*****	71 85	0 061		
5	*****	0 0014	0 9398	0 0015	*****	3 7468	2 6650	179 56	*****	71 83	0 061		
6	*****	0 0014	0 9392	0 0015	*****	3 7461	2 6635	179 84	*****	71 94	0 061		

Tertiary

TERTIARY BOX

RUN	N	WT*	PT*	TT*	PT*	TT*	WT*TT^44	WM	NT	UE
								LBM/SEC	LBM SEC	FT/SEC
1	0	0000	0	1324	0	9373	0	1412	0	0000
2	0	0828	0	0732	0	9382	0	0785	0	0905
3	0	1285	0	0445	0	9404	0	0474	0	1251
4	0	1702	0	0135	0	9404	0	0208	0	1657
5	0	1822	0	0056	0	9398	0	0059	0	1773
6	+	+	+	+	+	+	+	+	+	+



Tertiary

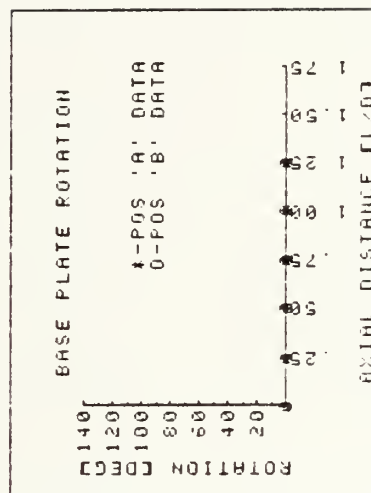
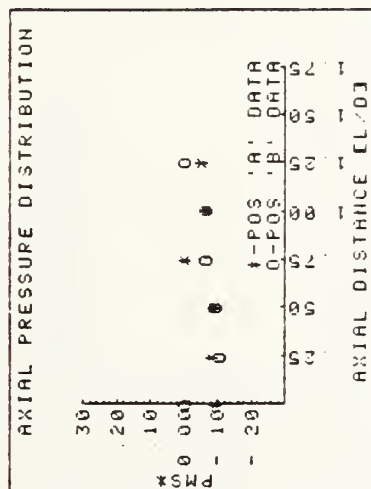
MIXING STACK DATA FOR RUN 7

TOP (POSITION 'A') DATA

X/D	PRESSURE [IN H2O]	ROTATION [DEG]	PMS*
0.00	-0.669	0	-0.091
0.25	-0.609	0	-0.083
0.50	-0.649	0	-0.089
0.75	0.000	0	0.000
1.00	-0.480	0	-0.066
1.25	-0.379	0	-0.052

DIAGONAL (POSITION 'B') DATA

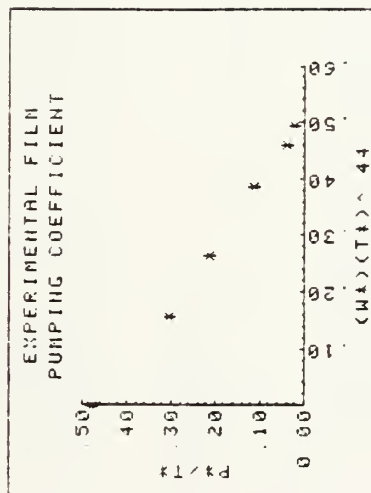
X/D	PRESSURE [IN H2O]	ROTATION [DEG]	PMS*
0.00	0.000	0	0.000
0.25	-0.781	0	-0.107
0.50	-0.659	0	-0.090
0.75	-0.468	0	-0.064
1.00	-0.460	0	-0.063
1.25	0.000	0	0.000



PCD

TERTIARY BOX

H	WT*	PT*	TT*	PT*/TT*	WT*TT* 44	WM	WT	UE
RUN						LBM/SEC	LBM/SEC	FT/SEC
1	*****	0 0000	0 9218	0 0000	*****	3 689	*****	*****
2	*****	0 0000	0 9225	0 0000	*****	4 298	*****	*****
3	*****	0 0000	0 9226	0 0000	*****	4 700	*****	*****
4	*****	0 0000	0 9227	0 0000	*****	5 153	*****	*****
5	*****	0 0000	0 9233	0 0000	*****	5 447	*****	*****
6	*****	0 0000	0 9234	0 0000	*****	5 575	*****	*****
7	*****	0 0000	0 9241	0 0000	*****	*****	*****	*****



MSD

DATA TAKEN ON 07 JUNE 83
 DATA TAKEN BY N D PRITCHARD

MIXING STACK INFORMATION
 LENGTH 26.25 [IN]
 DIAMETER 11.70 [IN]
 L/D RATIO 1.75
 S/D RATIO 0.50

HOZZLE AN HP AREA RATIO 2.50

PRIMARY NOZZLE INFORMATION
 TILT ANGLE 0.0 [DEG]
 ROTATION ANGLE 0.0 [DEG]
 AREA PER NOZZLE 10.752 [IN2]
 NUMBER OF NOZZLES 4

MISCELLANEOUS INFORMATION
 ORIFICE DIAMETER 6.902 [IN]
 ORIFICE BETA 0.497
 UPTAKE AREA 107.510 [IN2]
 ATM PRESSURE 30.02 [INHG]

COMMENTS

N	POR	DPOR	TOR	TUFT	TAMB	PAPT	PSEC	PTER	SECONDARY AREA	TERTIARY AREA
RUN	IN OF H2O			DEGREES F		IN OF H2O			SQAREA INCHES	SQAREA INCHES
1	0.665	22.0	55.2	109.0	67.6	5.90	0.01	0.70	785.000	0.000
2	0.663	22.0	55.6	109.0	67.8	6.00	0.01	0.36	785.000	12.566
3	0.660	22.0	55.2	109.0	68.0	6.09	0.01	0.20	785.000	25.133
4	0.663	22.0	55.4	109.2	68.4	6.05	0.01	0.10	785.000	50.265
5	0.662	22.0	55.4	109.2	68.4	6.05	0.01	0.03	785.000	100.531
6	0.660	22.0	55.4	109.2	68.6	6.07	0.01	0.02	785.000	785.000

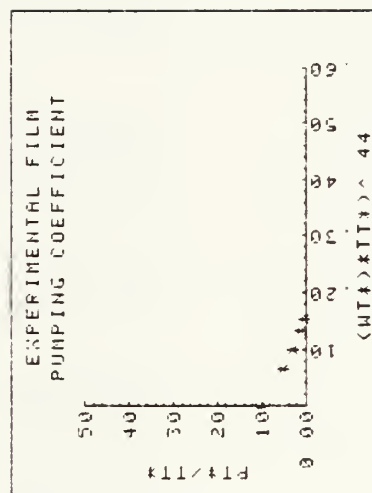
SECONDARY BOX

N	WT	F#	T#	P#T#	WT#	44	WP	WS	UP	UM	UUP	UPT	MACH
RUN							LBM/SEC	LBM/SEC	FT/SEC	FT/SEC	FT/SEC		
1	0.0016	0.0016	0.9272	0.0018	0.0018	0.0018	3.7588	2.9413	179.80	71.93	71.93	0.062	
2	0.0016	0.0016	0.9276	0.0018	0.0018	0.0018	3.7574	2.9413	179.73	71.90	71.90	0.062	
3	0.0016	0.0016	0.9279	0.0018	0.0018	0.0018	3.7588	2.9407	179.80	71.93	71.93	0.062	
4	0.0016	0.0016	0.9283	0.0018	0.0018	0.0018	3.7581	2.9396	179.83	71.94	71.94	0.062	
5	0.0016	0.0016	0.9283	0.0018	0.0018	0.0018	3.7581	2.9396	179.83	71.94	71.94	0.062	
6	0.0016	0.0016	0.9286	0.0018	0.0018	0.0018	3.7581	2.9391	179.83	71.94	71.94	0.062	

Tertiary

TERTIARY BOX

U	NT*	PT*	IT*	PT*	IT*	WT*	WT*	WT	UE
LBM SEC LBM/SEC FT/SEC									
RUN									
1	0 0000	0 0953	0 9272	0 1028	0 0000	0 0000	0 0000	0 0000	0 0000
2	0 0688	0 0497	0 9276	0 0536	0 0688	0 0688	0 259	0 259	0 259
3	0 1028	0 0277	0 9279	0 0299	0 0934	0 0934	0 386	0 386	0 386
4	0 1409	0 0130	0 9283	0 0141	0 1364	0 1364	0 530	0 530	0 530
5	0 1610	0 0043	0 9283	0 0046	0 1558	0 1558	0 605	0 605	0 605
6	0 0000	0 0022	0 9286	0 0024	0 0000	0 0000	0 0000	0 0000	0 0000



Tertiary

DATA TAKEN ON 07 JUN 83
 DATA TAKEN BY N D PRITCHARD

NOZZLE AM AP AREA RATIO 2 50

COMMENTS

MIXING STACK INFORMATION
 LENGTH 26.25 [IN]
 DIAMETER 11.70 [IN]
 L/D RATIO 2.25
 S/D RATIO 0.50

PRIMARY NOZZLE INFORMATION
 TILT ANGLE 15.0 [DEG]
 ROTATION ANGLE 20 [DEG]
 AREA PER NOZZLE 10.752 [IN2]
 NUMBER OF NOZZLES 4

MISCELLANEOUS INFORMATION
 ORIFICE DIAMETER 6.902 [IN]
 ORIFICE BETA 0.497
 UFTAKE AREA 107.510 [IN2]
 ATM PRESSURE 29.30 [INHG]

N	FOR	OPOR	TOR	TUPT	TAMB	PUPPT	FSEC	PTER	SECONDARY AREA	TERTIARY AREA
PUH	IN OF H2O	DEGREES F	IN OF H2O	IN OF H2O	IN OF H2O	IN OF H2O	IN OF H2O	IN OF H2O	SQAUPE INCHES	SQAUPE INCHES
1	0.655	22.0	56.0	109.4	66.6	3.95	3.01	0.00	0.000	*****
2	0.664	22.0	56.2	109.8	67.2	4.20	2.13	0.00	12.566	*****
3	0.664	22.0	56.8	110.4	67.8	4.80	1.60	0.00	25.133	*****
4	0.663	22.0	57.0	110.6	68.4	5.40	0.91	0.00	50.265	*****
5	0.663	22.0	57.2	110.6	68.4	5.93	0.35	0.00	100.531	*****
6	0.662	22.0	57.2	110.6	68.6	6.02	0.18	0.00	150.796	*****
7	0.660	22.0	57.2	110.6	69.0	6.15	0.01	0.00	*****	*****

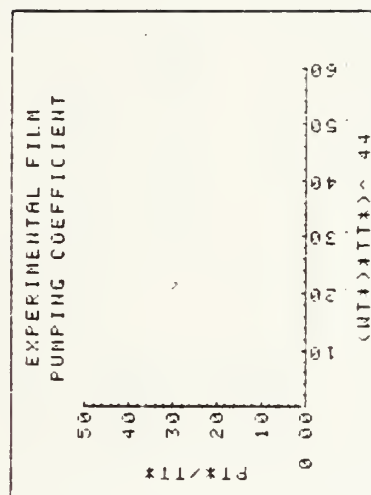
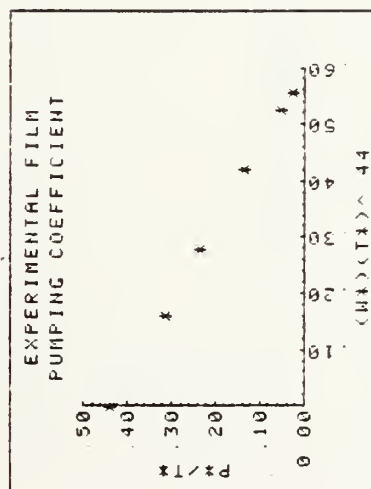
SECONDARY BOX

N	UH	P*	TA	P*/T*	WAT*	44	WP	HS	UP	UM	UUPT	UPT MACH
RUH												
1	0.0000	0.4059	0.9248	0.4389	0.0000	3.7105	0.0000	183.35	73.35	73.35	0.063	
2	0.1671	0.2886	0.9252	0.3119	0.1615	3.7098	0.6201	193.05	84.49	73.23	0.063	
3	0.2897	0.2174	0.9253	0.2349	0.2800	3.7076	1.0743	182.89	92.69	73.16	0.063	
4	0.4368	0.1242	0.9260	0.1341	0.4223	3.7069	1.6194	182.60	102.53	73.05	0.062	
5	0.5435	0.0482	0.9260	0.0520	0.5254	3.7062	2.0143	182.31	109.60	72.93	0.062	
6	0.5747	0.0240	0.9264	0.0259	0.5557	3.7062	2.1300	182.23	111.69	72.90	0.062	
7	*****	0.0014	0.9271	0.0015	*****	3.7062	2.6496	182.15	*****	72.87	0.062	

Table 4. Shrouded Stack L/D = 2.25: 15-20 Nozzles

TERTIARY BOX

N	WT*	PT*	TT*	PT*/TT*	NT*TT^-.44	UM	WT	UE
RUN								
1	*****	0.0000	0.9248	0.0000	*****	3.711	*****	*****
2	*****	0.0000	0.9252	0.0000	*****	4.330	*****	*****
3	*****	0.0000	0.9253	0.0000	*****	4.782	*****	*****
4	*****	0.0000	0.9260	0.0000	*****	5.326	*****	*****
5	*****	0.0000	0.9260	0.0000	*****	5.721	*****	*****
6	*****	0.0000	0.9264	0.0000	*****	5.836	*****	*****
7	*****	0.0000	0.9271	0.0000	*****	*****	*****	*****



PCD

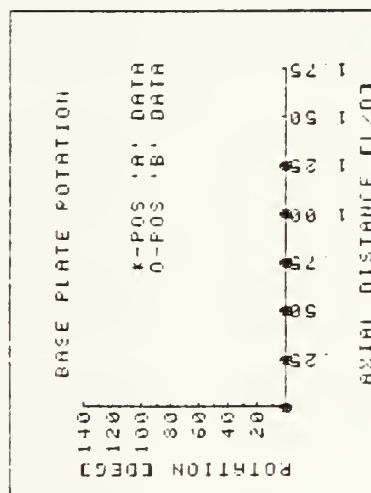
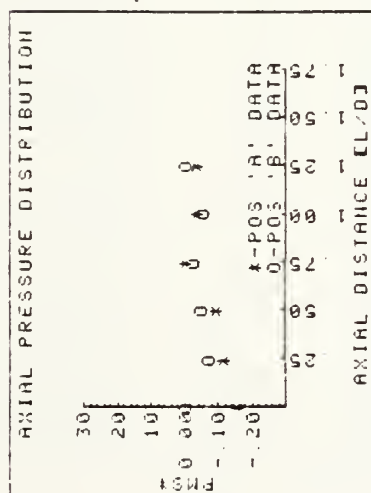
MISSING STACK DATA FOR RUN 2

TOP (POSITION 'A') DATA

X/D	PRESSURE [IN H2O]	ROTATION [DEG]	PMS*
0.00	-1.120	0	-0.154
0.25	-0.855	0	-0.117
0.50	-0.690	0	-0.095
0.75	0.000	0	0.000
1.00	-0.265	0	-0.036
1.25	-0.241	0	-0.033

DIAGONAL (POSITION 'B') DATA

X/D	PRESSURE [IN H2O]	ROTATION [DEG]	PMS*
0.00	0.000	0	0.000
0.25	-0.500	0	-0.059
0.50	-0.351	0	-0.048
0.75	-0.168	0	-0.023
1.00	-0.389	0	-0.053
1.25	0.000	0	0.000



MSD

DATA TAKEN ON 8 JUN 83
 DATA TAKEN BY N O PRITCHARD
 NOZZLE AM. HP AREA RATIO 2 50
 MIXING STACK INFORMATION
 LENGTH 26 25 [IN]
 DIAMETER 11.70 [IN]
 L O RATIO 2 25
 S O RATIO 0 50
 PRIMARY NOZZLE INFORMATION
 TILT ANGLE 15 0 [DEG]
 ROTATION ANGLE 20 [DEG]
 AREA PER NOZZLE 10 752 [IN2]
 NUMBER OF NOZZLES 4
 COMMENTS
 TER DATA
 MISCELLANEOUS INFORMATION
 ORIFICE DIAMETER 6 902 [IN]
 ORIFICE BETA 0 497
 UPTAKE AREA 107 510 [IN2]
 ATN. PRESSURE 30 02 [INHG]

N	POR	DPOP	TOR	TUPT	TAMB	PUPT	PSEC	PTER	SECONDARY AREA	TERTIARY AREA
PUN	IN OF H2O						IN OF H2O		SQUARE INCHES	SQUARE INCHES
1	0 665	22 0	55 6	108 6	65 2	6 05	0 02	1 35	785 000	0 000
2	0 666	22 0	55 4	108 6	66 0	6 05	0 02	0 62	785 000	12 566
3	0 665	22 0	55 6	108 6	66 0	6 10	0 02	0 32	785 000	25 133
4	0 665	22 0	55 6	108 6	66 4	6 05	0 02	0 13	785 000	50 265
5	0 665	22 0	55 4	108 6	66 6	6 08	0 02	0 05	785 000	100 531
6	0 665	22 0	55 8	108 8	67 0	6 08	0 02	0 02	+++++	+++++

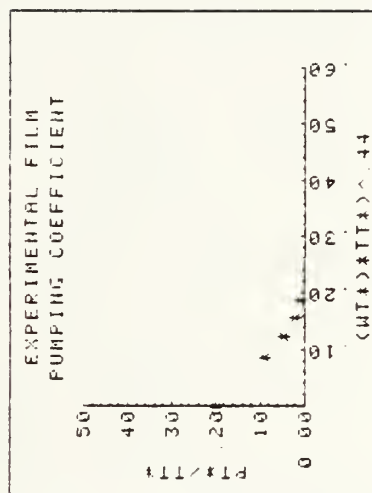
SECONDARY BOX

N	W#	P#	T#	P#	T#	UPT	44	WF	WS	UP	UM	UUPT	UPT	MACH
RUN									LBN/SEC	LBN/SEC	FT/SEC	FT/SEC		
1	+++++	0 0029	0 9236	0 0031	+++++	+++++	+++++	3 7573	3 9066	179 61	+++++	71 85	0 061	
2	+++++	0 0029	0 9250	0 0031	+++++	+++++	+++++	3 7581	3 8976	179 64	+++++	71 86	0 062	
3	+++++	0 0029	0 9250	0 0031	+++++	+++++	+++++	3 7573	3 8976	179 61	+++++	71 85	0 061	
4	+++++	0 0029	0 9257	0 0031	+++++	+++++	+++++	3 7573	3 8961	179 61	+++++	71 85	0 061	
5	+++++	0 0029	0 9261	0 0031	+++++	+++++	+++++	3 7581	3 8954	179 64	+++++	71 86	0 062	
6	+++++	0 0029	0 9265	0 0031	+++++	+++++	+++++	3 7566	3 8939	179 64	+++++	71 86	0 061	

Tertiary

TERTIARY BOX

N	WT#	PT#	TT#	PT#	TT#	WT#	TT#	WT	UE
LBM/SEC LBM/SEC FT/SEC									
1	0 0000	0 1859	0 9236	0 3013	0 0000	0 0000	0 000	0 000	0 000
2	0 0902	0 0849	0 9250	0 0918	0 0872	0 0872	0 339	0 339	0 339
3	0 1294	0 0437	0 9250	0 0473	0 1251	0 1251	0 486	0 486	0 486
4	0 1652	0 0178	0 9257	0 0193	0 1597	0 1597	0 621	0 621	0 621
5	0 1943	0 0062	0 9261	0 0067	0 1879	0 1879	0 730	0 730	0 730
6	0 0000	0 0030	0 9265	0 0033	0 0000	0 0000	0 000	0 000	0 000



Tertiary

	Straight Nozzles		15-20 Nozzles	
	Straight Shroud	Slant Shroud	Straight Shroud	Slant Shroud
L/D = 1.5	* .51	.43	+ .59	.58
L/D = 2.25	o .49	---	---	---
L/D = 2.5	---	.49	---	.60

* Data by Davis (Note: No Shroud)
+ Data by Drucker
o Data by Lemke & Staehli

Table 5. Secondary Pumping Coefficient Comparison
(Open to Environment)

	Straight Nozzles		15-20 Nozzles	
	Straight Shroud	Slant Shroud	Straight Shroud	Slant Shroud
L/D = 1.5	---	.17	.135 ⁺	.190
L/D = 2.25	.12 ^o	---	----	----
L/D = 2.5	---	.155	----	.180

⁺ Data by Drucker
^o Data by Lemke and Staehli
 Table 6. Tertiary Pumping Coefficient Comparison
 (Open to Environment)

APPENDIX A: FORMULAE

Presented here are the formulas used to obtain the primary and secondary mass flow rates. According to the ASME primary Test Code {Ref.10}, the general equation for mass flow rate appearing in equation (a)

$$W(\text{lbm/sec}) = 0.12705 K A Y F_a (\rho \Delta P)^{0.5} \quad (a)$$

may be used with flow nozzles and square edge orifices provided the flow is subsonic. In the above equation, K (dimensionless) represents the flow coefficient for the metering device and is defined as $K = C(1-\beta^4)^{-0.5}$ where C is the coefficient of discharge and β is the ratio of throat to inlet diameters; $A(\text{in}^2)$ is the total cross sectional area of the metering device; Y (dimensionless) is the expansion factor for the flow; F_a (dimensionless) is the area thermal expansion factor; $\rho (\text{lbm/ft}^3)$ is the flow mass density; and ΔP (inches H_2O) is the differential pressure across the metering device. Each of these quantities are evaluated, according to the guidelines set forth in Reference {10} for the specific type of flow measuring device used.

Using a square edge orifice for measurement of the primary mass flow rate, the quantities in equation (a) are defined as follows:

1. The flow coefficient K is 0.62 based on a β of 0.502 and a constant coefficient of discharge over the range of flows considered of 0.60.

2. The orifice area is 37.4145 in^2 .

3. Corresponding to the range of pressure ratios encountered across the orifice, the expansion Y is 0.98.

4. Since the temperature of the metered air is nearly ambient temperature, thermal expansion factor is essentially 1.0.

5. The primary air mass density ρ_{or} is calculated using the perfect gas relationship with pressure and temperature evaluated upstream of the orifice.

Substituting these values into equation (a) yields

$$W_p \text{ (lbm/sec)} = (2.88455) (\rho_{or} \Delta P_{or})^{0.5} \quad (b)$$

The secondary mass flow rate is measured using long radius flow nozzles for which case the quantities in equation (a) becomes:

1. For a flow nozzle installed in a plenum, β is approximately zero in which case the flow coefficient is approximately equal to the coefficient of discharge. For the range of secondary flows encountered, the flow coefficient becomes 0.98.

2. A is the sum of the throat areas of the flow nozzles in use (in^2).

3. Since the pressure ratios across the flow nozzles are very close to unity, the expansion coefficient Y is 1.0.

4. Since the temperature of the metered air is nearly ambient temperature, the thermal expansion factor is essentially 1.0.

5. The secondary air mass density ρ_s is evaluated using the perfect gas relationship at ambient conditions. Substituting these values into equation (a) yields the equation for the secondary mass flow rate measured using long radius flow nozzles.

$$W_s \text{ (lbm/sec)} = (0.12451) A (\rho_s \Delta P_s)^{0.5} \quad (c)$$

APPENDIX B: UNCERTAINTY ANALYSIS

The determination of the uncertainties in the experimentally determined pressure coefficients, pumping coefficients, and velocity profiles was made using the methods described by Kline and McClintock {Ref. 13}. The basic uncertainty analysis for the cold flow eductor model test facility was conducted by Ellin {Ref. 1}. The uncertainties obtained by Ellin using the second order equation suggested by Kline and McClintock were applicable to the experimental work conducted during the present research and are listed in the following table.

UNCERTAINTY IN MEASURED VALUES

T_s	$\pm 1 \text{ R}$
T_p	$\pm 1 \text{ R}$
P_a	$\pm 0.01 \text{ psia}$
ΔP	$\pm 0.01 \text{ in. H}_2\text{O}$
P_V	$\pm 0.01 \text{ in. H}_2\text{O}$
P_u	$\pm 0.05 \text{ in. H}_2\text{O}$
$\Delta P_s(+)$	$\pm 0.01 \text{ in. H}_2\text{O}$
$\Delta P_t(**)$	$\pm 0.01 \text{ in. H}_2\text{O}$
P_{or}	$\pm 0.01 \text{ in. H}_2\text{O}$
ΔP_{or}	$\pm 0.20 \text{ in. H}_2\text{O}$

T_a

$\pm 1 \text{ R}$

$PT(***)$

$\pm 0.1 \text{ in. H}_2\text{O}$

UNCERTAINTY IN CALCULATED VALUES

$\frac{P^*}{T^*}$

1.9%

$W^*T^{*0.44}$

1.4%

V/V_{avg}

2.5%

(+)

The pressure differential across the secondary flow nozzles, P_s , is the major source of uncertainty in the pumping coefficient.

(++)

The pressure differential across the tertiary flow nozzles, P_t , is the major source of uncertainty in the pumping coefficient.

(+++)

The measurement of the total pressure for the velocity profile is the major source of uncertainty in the velocity calculation.

LIST OF REFERENCES

1. Ellin, C.R., Model Test of Multiple Nozzle Exhaust Gas Eductor Systems for Gas Turbine Powered Ships, Engineer's Thesis, Naval Postgraduate School, June 1977.
2. Moss, C.M., Effects of Several Geometric Parameters on the Performance of a Multiple Nozzle Eductor System, Master's Thesis, Naval Postgraduate School, September 1977.
3. Lemke, R.J. and Staehli, C.P., Performance of Multiple Nozzle Eductor Systems with Several Geometric Configurations, Master's Thesis, Naval Postgraduate School, September 1978.
4. Shaw, R.S., Performance of a Multiple Nozzle Exhaust Gas Eductor System for Gas Turbine Powered Ships, Master's Thesis, Naval Postgraduate School, December 1980.
5. Ryan, D.L., Flow Characteristics of a Multiple Nozzle Exhaust Gas Eductor System, Master's Thesis, Naval Postgraduate School, March 1981.
6. Davis, C.C., Performance of Multiple, Angled Nozzles with Short Mixing Stack Eductor Systems, Master's Thesis, Naval Postgraduate School, September 1981.
7. Drucker, C.J., Characteristics of a Four-Nozzle, Slotted Short Mixing Stack with Shroud, Gas Eductor System, Master's Thesis, Naval Postgraduate School, March 1982.
8. Boykin, J.W., Characteristics of a Fluted Nozzle Gas Eductor System, Master's Thesis, Naval Postgraduate School, March 1983.
9. Pucci, P.F., Simple Eductor Design Parameters, Ph.D. Thesis, Stanford University, September 1954.
10. American Society of Mechanical Engineers Interim Supplement 19.5 of Instrumentation and Apparatus, Fluid Meters, Sixth Edition, 1971.
11. Hill, J.A., Hot Flow Testing of Multiple Nozzle Exhaust Eductor Systems, Master's Thesis, Naval Postgraduate School, September 1979.

12. Harrel, J.P., Jr., Experimentally Determined Effects of Eductor Geometry on the Performance of Exhaust Gas Eductors for Gas Turbine Powered Ships, Engineer's Thesis, Naval Postgraduate School, September 1977.
13. Kline, S.J. and McClintock, F.A., "Describing Uncertainties in Single-Sample Experiments", Mechanical Engineering, pp. 3-8, January 1953.

INITIAL DISTRIBUTION LIST

	No. Copies
1. Defense Technical Information Center Cameron Station Alexandria, Virginia 22314	2
2. Library, Code 0142 Naval Postgraduate School Monterey, CA 93943	2
3. Chairman, Code 69 Department of Mechanical Engineering Naval Postgraduate School Monterey, CA 93943	1
4. Professor Paul F. Pucci, Code 69Pc Department of Mechanical Engineering Naval Postgraduate School Monterey, CA 93943	5
5. Dean of Research, Code 012 Naval Postgraduate School Monterey, CA 93943	1
6. Commander Attn: NAVSEA Code 0331 Naval Sea Systems Command Washington, DC 20362	1
7. Mr. Olin M. Pearcy NSRDC Code 2833 Naval Ship Research and Development Center Annapolis, MD 21402	1
8. LT Jerry W. Boykin 1717 Moon Valley Drive Virginia Beach, VA 23456	1
9. Mr. Mark Goldberg NSRDC Code 2833 Naval Ship Research and Development Center Annapolis, MD 21402	1
10. Mr. Eugene P. Weinert Head, Combined Power and Gas Turbine Branch Naval Ship Engineering Center Philadelphia, PA 19112	1

11. Mr. Donald N. McCallum 1
NAVSEC Code 6136
Naval Ship Engineering Center
Washington, DC 21362
12. LT Carl Drucker, USN 1
1032 Marlborough Street
Philadelphia, PA 19155
13. LCDR C. M. Moss, USN 1
625 Midway Road
Powder Springs, GA 30073
14. LCDR J. A. Hill, USN 1
RFD 2, Box 116B
Elizabeth Lane
York, ME 03909
15. LCDR J. P. Harrel, Jr., USNR 1
1600 Stanley
Ardmore, OK 73401
16. LCDR R. J. Lemke, USN 1
2902 No. Cheyenne
Tacoma, WA 98407
17. LCDR C. P. Staehli, USN 1
2808 39th St., N.W.
Gig Harbor, WA 98335
18. LT R.S. Shaw, USN 1
147 Wampee Curve
Summerville, SC 29483
19. LCDR D. L. Ryan, USN 1
6393 Caminito Luisito
San Diego, CA 92111
20. LCDR C. C. Davis, USN 1
1608 Linden Drive
Florence, SC 29501
21. LCDR D. Welch, USN 1
1036 Brestwick Commons
Virginia Beach, VA 23464
22. CDR P. D. Ross, Jr., USN 1
6050 Henderson Drive, No. 8
La Mesa, CA 92041

- | | | |
|-----|---|---|
| 23. | CAPT F. S. Hering
NAVSEA Systems Command (SEA 55X)
Washington, D.C. 20362 | 1 |
| 24. | LCDR N. D. Pritchard
Main Street
St. Remy, N.Y. 12401 | 1 |
| 25. | Mr. Joseph Londino
NAVSEA Code 56X11
Washington, DC 20362 | 1 |

202554

Thesis

P944165 Pritchard

c.1

Characteristics of
a four nozzle, slott-
ed mixing stack with
slanted shroud, gas
eductor system.

202554

Thesis

P944165 Pritchard

c.1

Characteristics of
a four nozzle, slott-
ed mixing stack with
slanted shroud, gas
eductor system.

thesP944165

Characteristics of a four nozzle, slotte



3 2768 001 93210 6

DUDLEY KNOX LIBRARY